

Mechanism of Photosolvolytic Rearrangement of *p*-Hydroxyphenacyl Esters: Evidence for Excited State Intramolecular Proton Transfer as the Primary Photochemical Step

by



Kai Zhang
B.Sc., Nanjing University, 1989
M.Sc., Peking University, 1995

A Thesis Submitted in Partial Fulfillment of the
Requirements for the Degree of

MASTER OF SCIENCE

in the Department of Chemistry

We accept this thesis as conforming
to the required standard




Dr. P. C. Wan, Supervisor (Department of Chemistry)


Dr. T. E. Gough, Department Member (Department of Chemistry)


Dr. R. H. Mitchell, Department Member (Department of Chemistry)



Dr. L. A. Hobson, Outside Member (Department of Biology)


Dr. R. Boch, External Examiner (Quadra Logic Technologies)

© Kai Zhang, 1998

University of Victoria

All right reserved. This thesis may not be reproduced in whole or in part, by
photocopy or other means, without the permission of the author.

QD275

745

U.S. Department of Agriculture

Forest Service

1945

Supervisor: Dr. P. C. Wan


ABSTRACT

The photosolvolytic rearrangement of *p*-hydroxyphenacyl alcohols **56**, **57**, *p*-hydroxyphenacyl esters **58a-d**, **59a-d**, and *p*-methoxyphenacyl derivative **60** has been studied in aqueous solution using product studies and nanosecond laser flash photolysis. The *p*-hydroxyphenacyl moiety has recently been proposed as a new and efficient photoactivated protecting group in aqueous solution. However, although their practical applications have been amply demonstrated, much less is known about the mechanism of photoreaction. Our data support a novel mechanism in which the primary photochemical step from the singlet excited state is intramolecular proton transfer from the phenolic proton to the carbonyl oxygen of the distal ketone, to generate the corresponding *p*-quinone methide phototautomer, which subsequently expels the ester group with concerted rearrangement to a spiroketone intermediate leading to the final observed product, *p*-hydroxyphenylacetic acid.

Irradiation of these *p*-hydroxyphenacyl derivatives in 1:1 (v/v) H₂O-CH₃CN produced the corresponding *p*-hydroxyphenyl acetic acid (**31**) or its di-*tert*-butyl derivative **61** as the only photoproduct. Conversion to **31** or **61** can be taken to quantitative yield upon prolonged photolysis for all of these compounds without the formation of significant by-products. These results rule out the involvement of C-OCOR bond homolysis in the mechanism. All of these *p*-hydroxyphenacyl derivatives were unreactive in neat CH₃CN indicating that H₂O is necessary for the reaction. *p*-

Methoxyphenacyl acetate (**60**) failed to give any observable reaction under the same conditions, which shows that the phenol HO group is required. Quantum yield measurements showed that neither acid nor base catalyzed the reaction. All of the above results are indicative of the involvement of excited state intramolecular proton transfer (ESIP) in the mechanism. Such a mechanism would be expected to generate p-quinone methide (p-QM) intermediates. Direct evidence was provided by laser flash photolysis (LFP), which gave observable transients at 330 and 360 nm assignable to p-QM **67a** and **67b**, respectively.

Examiners:


Dr. P. C. Wan, Supervisor (Department of Chemistry)


Dr. T. E. Gough, Department Member (Department of Chemistry)


Dr. R. H. Mitchell, Department Member (Department of Chemistry)


Dr. L. A. Hobson, Outside Member (Department of Biology)



Dr. R. Boch, External Examiner (Quadra Logic Technologies)

TABLE OF CONTENTS**Preliminary Pages**

Abstract	(ii)
Table of Contents	(iv)
List of Figures	(vii)
List of Tables	(ix)
Abbreviations	(x)
Acknowledgments	(xi)
Dedication	(xii)

Chapter 1

Introduction	1
1.1 Photochemically-Removable Protecting Groups	1
1.1.1 2-Nitrobenzyl (2NB) and Related Groups	4
1.1.2 Benzoin	9
1.1.3 Phenacyl Derivatives	15
1.1.4 Miscellaneous Systems	22
1.2 Photoprototropic Behavior of Hydroxyarenes	26
1.2.1 Excited State Intermolecular Proton Transfer (ESIerPT)	28
1.2.2 Excited State Intramolecular Proton Transfer (ESIraPT)	28
1.3 Proposed Research	32

Chapter 2	
Results & Discussion	35
2.1 Product Studies	
2.1.1 Photolysis of p-Hydroxyphenacyl Alcohol 56 , 57 , p-Hydroxyphenacyl Acetates 58a , 59a , and p-Methoxyphenacyl Acetate (60)	35
2.1.2 Photolysis of p-Hydroxyphenacyl Esters 58b-d and 59b-d	41
2.2 Quantum Yield Measurements	44
2.3 Solvent Isotope Effect	51
2.4 Triplet Quenching	53
2.5 Laser Flash Photolysis (LFP)	56
2.5.1 p-Hydroxyphenacyl Acetate (58a)	56
2.5.2 Di- <i>tert</i> -Butyl-p-Hydroxyphenacyl Acetate (59) and p-Hydroxyacetophenone (69)	65
2.6 Mechanism	69
2.7 Summary	71
Chapter 3	
Experimental	74
3.1 General Instrumentation	74
3.2 Common Laboratory Reagents	74
3.3 Materials	75

3.4	Product Studies	75
3.5	Quantum Yield Measurements	81
3.6	Solvent Isotope Effect	84
3.7	Triplet Quenching Experiments	84
3.8	Laser Flash Photolysis	85
	References	92

List of Figures

Figure 2.1	UV-Vis traces for the conversion of 58a to 31 on photolysis at 300 nm (in 1:1 H ₂ O-CH ₃ CN); argon purged. Each trace represents about 1 min photolysis time.	45
Figure 2.2	pH Effect on the quantum yields (Φ_p) for formation of 31 from 58a (triangles) and 61 from 59a (circles) photolyzed in 1:1 H ₂ O-CH ₃ CN, measured by ¹ H NMR.	47
Figure 2.3	Dependence of Φ_p on H ₂ O (circles)/ CH ₃ OH (squares) concentration on the conversion of 58a to 31 or 65 in mixture with CH ₃ CN measured by UV-Vis spectrophotometry.	50
Figure 2.4	Energy level diagram for triplet-triplet energy transfer	54
Figure 2.5	Transient absorption observed on LFP of flowing, neat CH ₃ CN solutions of 58a purged by N ₂ (circles) and O ₂ (squares).	57
Figure 2.6	Transient absorption observed on LFP of flowing, O ₂ purged 1:1 H ₂ O-CH ₃ CN solution of 58a . Decay trace taken at 400 ns intervals [The first trace (■) was centered at ~ 50 ns, the second one (●) was centered at ~ 100 ns, the third one (▲) was centered at 250 ns, and the last one (▼) was centered at ~ 3 μs]. [Inset: biexponential decay of transients at 330 nm with $k_d = 6.3 \times 10^6 \text{ s}^{-1}$ and $k_d = 1.8 \times 10^5 \text{ s}^{-1}$.]	58
Figure 2.7	Spectrum observed on LFP of hydroxybenzyl alcohol 76 in 1:1 H ₂ O-CH ₃ CN (taken from reference 79).	62
Figure 2.8	ΔA at 330 nm vs pH observed on LFP of 58a in 1:1 H ₂ O-CH ₃ CN.	64
Figure 2.9	ΔA at 360 nm vs pH observed on LFP of 59a in 1:1 H ₂ O-CH ₃ CN.	68
Figure 2.10	ΔA at 340 nm vs pH observed on LFP of 69 in 1:1 H ₂ O-CH ₃ CN.	69

Figure 3.1 Decay trace of the 330 nm transient from **58a** in 1:1
H₂O-CH₃CN at pH 6.8 fitted to biexponential decay with R = 0.997. 88

List of Tables

Table 2.1	Data for UV spectra of some <i>p</i> -QMs (73)	61
Table 3.1	Data for the fitting of decay traces of the 330 nm transient obtained by LFP of 58a in 1:1 H ₂ O-CH ₃ CN at various pHs.	89
Table 3.2	Data for the fitting of decay traces of the 360 nm transient obtained by LFP of 59a in 1:1 H ₂ O-CH ₃ CN at various pHs.	90
Table 3.3	Data for the fitting of decay traces of the 340 nm transient obtained by LFP of 69 in 1:1 H ₂ O-CH ₃ CN at various pHs.	91

Abbreviations

K_a	Acid dissociation constant
CI	Chemical ionization
EI	Electron impact
ESPT	Excited state proton transfer
ESIerPT	Excited state intermolecular proton transfer
ESIrPT	Excited state intramolecular proton transfer
HRMS	High resolution mass spectrum
KSIE	Kinetic solvent isotope effect
LFP	Laser flash photolysis
TLC	Thin layer chromatography
PT	Proton transfer
Φ_p	Product quantum yield
QM	Quinone methide

ACKNOWLEDGMENTS

I would like to thank my supervisor Dr. Peter Wan for giving me the opportunity to work on this project. I am very grateful for everything that I learned from him. I would also like to thank members and past-members of Dr. Wan's group: Yijian Shi, Li Diao, Maiké Fischer, Zihui Chen, and Darryl Brousmiche. Many thanks to Dr. Cornelia Bohne's group for help with laser flash photolysis experiments. Finally, I would like to thank NSERC and the University of Victoria for their support of this research.

Dedication

To Jie HUANG, with love

Chapter 1

Introduction

1.1 Photochemically-Removable Protecting Groups

Research into photochemically-removable protecting groups was first performed in the field of organic synthesis.¹ This is because specifically removable blocking groups are of importance in many phases of organic synthesis, particularly in synthesis involving polyfunctional molecules. In conventional methodology, activation of the blocked functional group is generally performed either by oxidation, reduction, elimination, acid or base hydrolytic methods, or a combination of these methods. Sometimes, the substrate may be sensitive to these conditions which can create complications. Therefore, the use of a protecting group for which the regeneration of the blocked function can be accomplished by photochemical means - under non-destructive, neutral conditions, avoiding the need for rigorous chemical treatment of the substrates - is an attractive alternative.

A photochemically-removable protecting group contains a chromophore which is sensitive to light, but relatively stable to most of the wide variety of chemical reagents commonly encountered in the ground state manifold. The wavelength of the light to be used must be such that it will be absorbed only by the protecting group and will not affect other parts of the molecule. The photochemical reaction of the protecting group chromophore should in no way affect the substrate molecule and the protecting group's photoproduct should be readily separable from the deprotected compound.² The

protecting group should also be capable of being introduced and cleaved from the functional group in essentially quantitative yields. The protecting group should neither possess nor introduce a chiral centre. Another important factor to be considered in the selection of a photochemically-removable protecting group is the lifetime of the excited species that is responsible for the particular photoreaction. Thus, if the protected substrate has a long excited state lifetime before cleavage occurs, the chances for undesirable quenching processes to reduce the efficiency of the cleavage reaction are greater.³ Such energy dissipation processes might result in some undesired changes in the substrate. Therefore, it would be a distinct advantage to design a protecting group with a chromophore characterized by a short-lived excited state.

Photochemical reactions provide a convenient means for activating important functional groups like carboxyl, hydroxyl and carbonyl under mild, neutral conditions. In the photochemical activation approach, the functional group is protected by a light-sensitive chromophore, which can serve as a latent activator of the functional group. On irradiation with light of suitable wavelength, the functional group is converted to an active form and the light-sensitive chromophore is removed. Such mild and neutral photochemical activation approaches have been found to offer effective protection for peptides, nucleotides, and polysaccharides.

The field of photochemically-removable protecting groups started in the 1960's. The first report of a successful development of a photoremovable protecting group is that of Barltrop *et al.*⁴ in 1962, who observed that benzyloxycarbonylglycine is readily

converted to the free amino acid by irradiation with UV light. Since then, a large number of photochemically-removable protecting groups have been developed for various functional groups, and their usage has also progressed from simple protection of reactive functional groups in synthetic organic chemistry⁵ to such fields as: light-directed protein and DNA syntheses,^{6,7} photogenerating organic bases,⁸ and the photorelease of biologically-relevant compounds,⁹ the later being very useful in biochemistry, biology, and physiology.

Biologically-inert photocleavable derivatives of effectors or reporter species have been widely exploited in modern research, because it can be used in the technique of "caging",¹⁰ wherein a biological molecule is rendered both inactive and membrane-permeable by the photosensitive protecting ("cage") group followed by the addition of the "caged" compound to a biological preparation such as a muscle fibre or tissue slice, which is then left for a period of time to allow uniform diffusion of the photocleavable reagent. Once located inside a cell or an enzyme active site, the protecting group can be released by irradiation with a pulse of near-UV light on a time scale much faster than that of the biological or enzymatic process, permitting the study of the time evolution of the phenomena without diffusion artifacts.¹¹ In this case, photosensitive protecting groups permit a greater range of application because illumination can be so easily controlled in timing, location, and amplitude,^{12,13} which provide control of spatial and temporal distribution of substrate concentration. This capability is particularly valuable when rapid mechanical mixing is impractical, for example inside a more-or-less intact cell, tissue, or

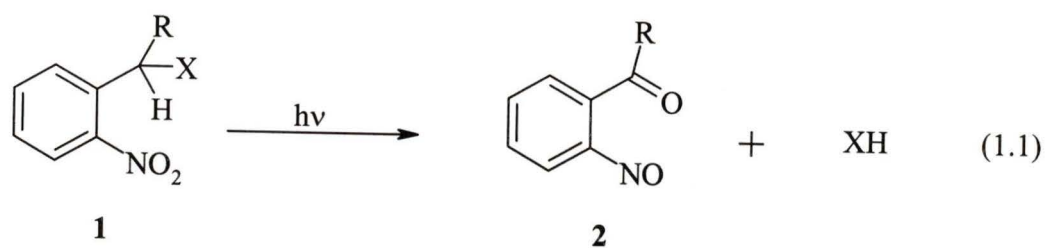
protein crystal, or when microscopic spatial gradients are desired.

Caged groups are most commonly designed by modifying the desired biomolecule with a suitable photoremovable protecting group or caging group. According to Lester,¹⁴ the ideal caging group should possess the following five properties: (1) good solubility in water at high ionic strength; (2) rapid and efficient photoreactivity; (3) good thermal and solvolytic stability; (4) high absorptivity at wavelengths greater than 310 nm; and (5) biological stability (inertness) of the released protecting group. Since the introduction of caged compounds in 1977,¹⁵ several different kinds of caging groups have been described, the most important of which are discussed below.

1.1.1 2-Nitrobenzyl (2NB) and Related Groups

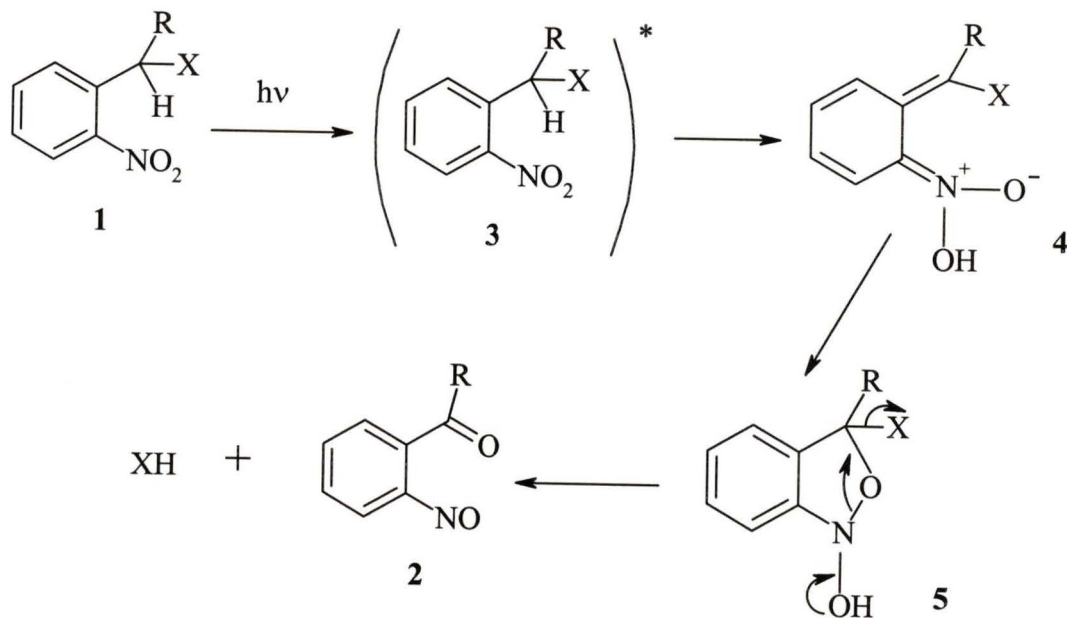
1.1.1.1 Mechanism

The use of the 2NB photoremovable group is shown by the general reaction of eq. 1.1. On photolysis, **1** undergoes an overall intramolecular redox reaction, giving rise to 2-nitrosobenzaldehyde-related by-product **2**, and the photoreleased molecule XH. The primary photochemical process is an intramolecular hydrogen abstraction of the benzylic hydrogen by the n,π^* excited nitro group, to give the aci-nitro intermediate **4** within picoseconds (Scheme 1.1).^{1,16} This is followed by oxygen attack at the benzylic position to produce the cyclic intermediate **5**, from which the nitroso product **2** is produced.



R= H, CH₃

X= OPO₃²⁻, OR, OCONHR, OCOR, etc.

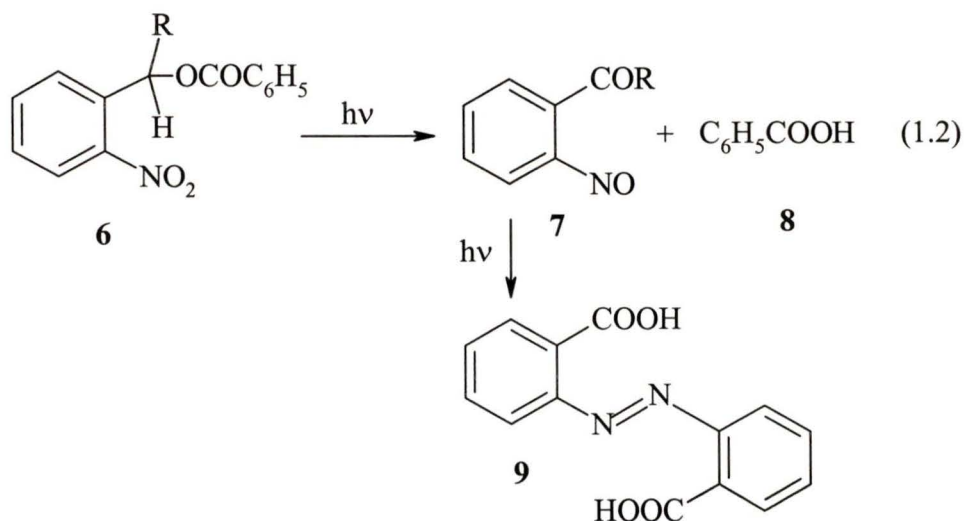


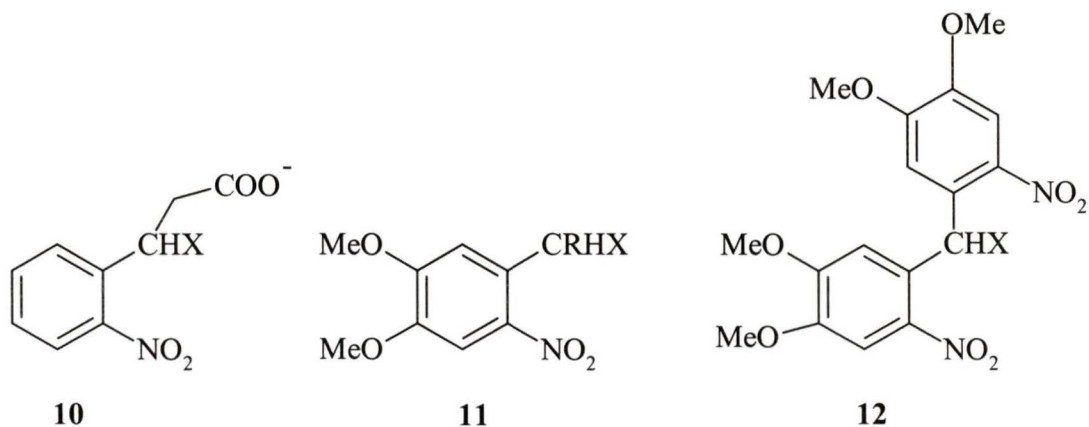
Scheme 1.1

Ciamician and Silber²⁰ originally discovered this kind of redox reaction in 1901. Since then, these types of light induced intramolecular redox reactions of aromatic nitro

compounds containing a carbon-hydrogen bond *ortho* to the nitro group have been the subject of much investigation,^{17,18,19} and are by far the best studied.

The photochemical removal of the 2NB group was first observed in the irradiation of 2NB benzoate (**6**, R = H, eq. 1.2) by Barltrop *et al.*²¹ in 1966. In this case, benzoic acid (**8**) was formed in only 17% yield, since 2-nitrosobenzaldehyde (**7**, R = H) was further transformed into azobenzene-2,2'-dicarboxylic acid (**9**) which acted as an internal light filter. This side-reaction was eliminated by using α -substituted 2NB esters. The yields were increased to 75-95% for α -phenyl-substituted 2NB groups (**6**, R = C₆H₅) for different carboxylic acids. The yield was ~100% for the same kind of carboxylic acids by using α -2-nitrophenyl-substituted 2NB groups (**6**, R = *o*-NO₂-C₆H₄).²² The increased cleavage efficiency of the later group might be due to the presence of one more 2-nitrobenzyl moiety, which can further enhance the cleavage of the ester bond. Other 2NB derivatives, such as **10**, **11**, and **12**, have also been studied.



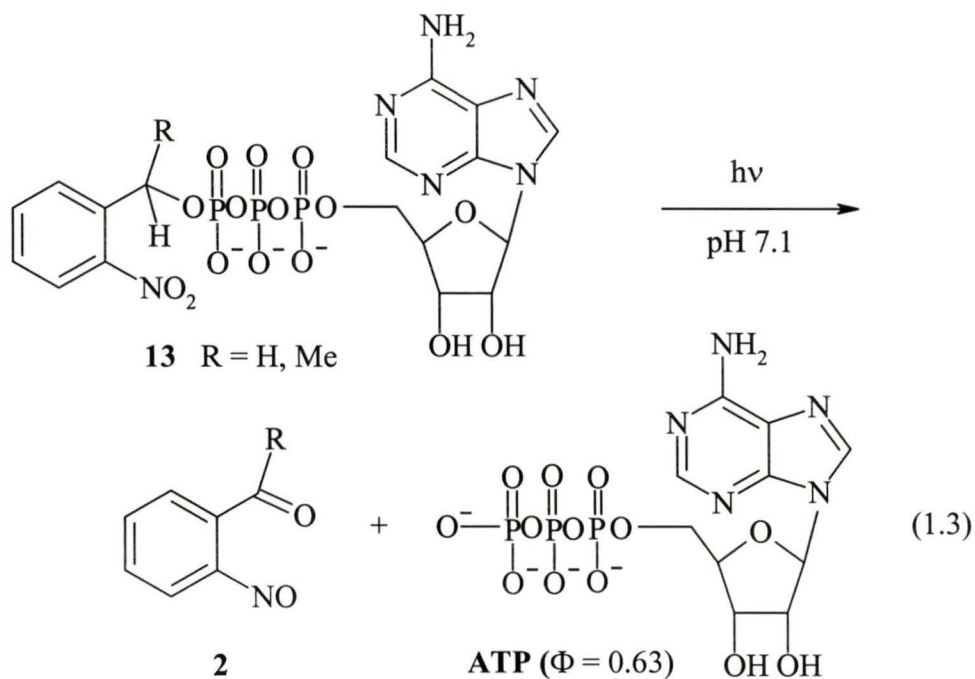


X = OPO_3^{2-} , OCONHR , OR , etc.

1.1.1.2 Applications

Research in the photochemistry of *o*-nitrobenzyl derivatives has focussed on the mechanism of photolysis, with a view towards improving the rate, efficiency, and action spectrum of the reaction. Most photochemists find the time scale of the reactions ($\sim 10^{-3}$ s and longer) of little interest, and therefore the development work has taken place primarily in the fields of biochemistry, biology, and physiology.

Engels and Schlaeger¹⁵ first reported in 1977 that the 2NB ester of cAMP released free cAMP upon photolysis. Subsequently, Kaplan, Forbush, and Hoffman²³ reported the efficient photorelease of ATP and inorganic phosphate (Pi) from the corresponding 2NB and the *o*-nitrophenethyl (1-(2-nitrophenyl)ethyl or 2NPE) esters (**13**, eq. 1.3). The release of biochemical substrates from 2NB esters of nucleotides, oligopeptides, proteins, and amino acids has since rapidly gained wide use in biochemistry and physiology.²⁴⁻³²



Caging groups based on the photochemistry of 2NB derivatives are by far the most prevalent in presently used caged compounds.³³ Their advantages include compatibility with a wide variety of functional groups, ease of synthesis, and reasonable light sensitivity and kinetics. The reactions are generally unaffected by modest changes in temperature and media, occur with high quantum efficiencies ($\Phi = 0.1 \sim 0.6$), and are activated by wavelengths greater than 300 nm. All of these facts make 2NB derivatives as ideal cages. However there are several disadvantages which limit the application of the nitrobenzyl chromophore. A well-known shortcoming is the slow release of the protected moiety from a relatively long-lived aci-nitro intermediate. Typically, the photoactivated release of a substrate from 2NB cages is limited to the millisecond to second time regime ($k_r =$

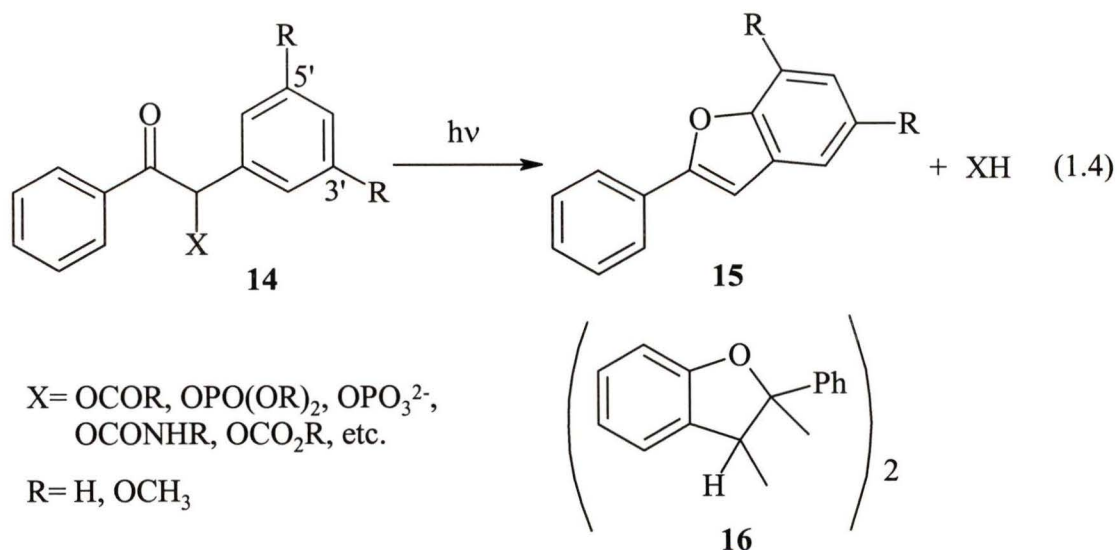
$1 \sim 10^3 \text{ s}^{-1}$), which makes it unsuitable for some rapid biochemical events. A second major disadvantage derives from the highly absorbing products that often interfere with spectroscopic analysis of the reactions of the released molecule and the extent of the conversion of the caged molecule. The third limitation is that the photoproduct is not biochemically benign because of the reactivity of the nitroso functional group with primary amines which may interfere with the normal biochemical functions under investigation. Finally, the instability of the caged derivative and the competing pathway for energy migration and electron transfer prior to C-O bond cleavage also cause some concerns.

Efforts to optimize photolysis quantum efficiencies and rates by substitution at the benzylic position or on the aromatic nucleus of the *o*-nitrobenzyl group have been made.¹² However, these efforts usually result in unpredictable and undesirable changes in the photochemistry and the bioavailability of the substrate. Moreover, the release rates tend to be highly sensitive to the nature of the leaving group. For these reasons, attention has been drawn to the design and study of new, potentially faster, and less damaging cage groups. An emerging class that shows promise is the α -keto cage derivatives, of which the benzoin group is a leading candidate.³⁴

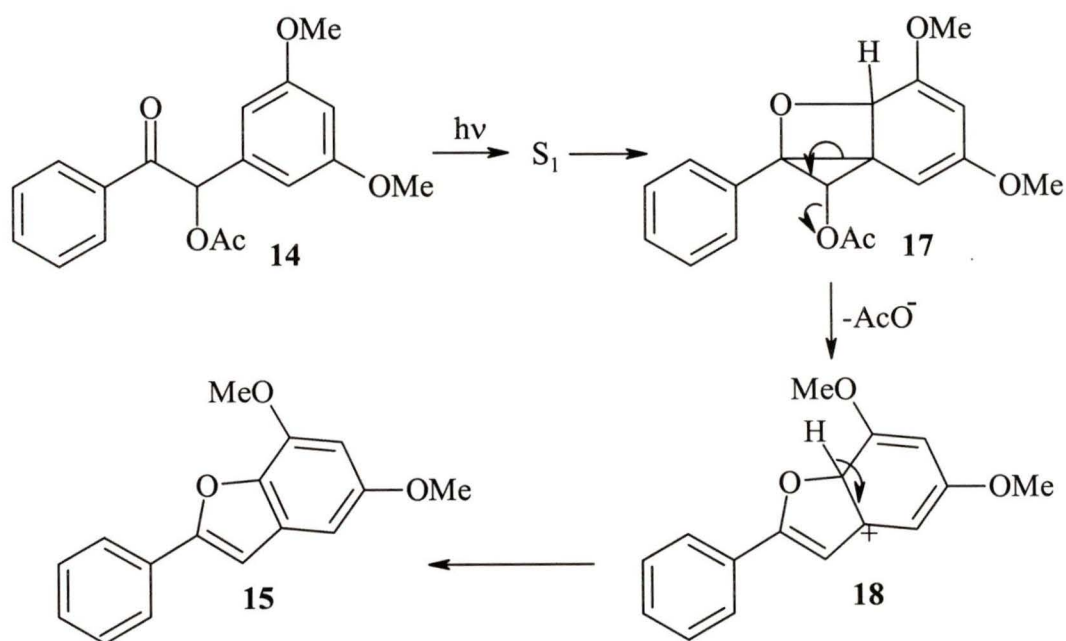
1.1.2 Benzoin

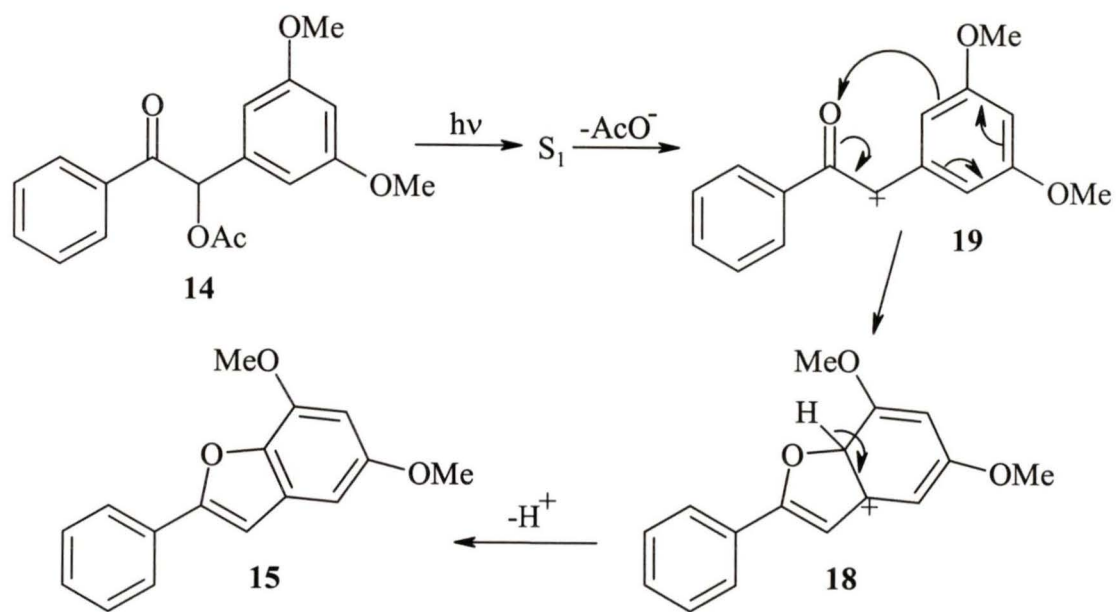
The benzoin chromophore was first investigated as a possible photoprotecting group for carboxylic acids by Sheehan and Wilson in 1964.^{35a} They found that benzoin

esters **14** ($X = \text{OAc}$) undergo a photocyclization to yield 2-phenylbenzofuran (**15**) and free carboxylic acid XH upon irradiation with light of wavelength 366 nm (eq. 1.4). The benzofuran is photostable and highly fluorescent. The efficiency for the formation of the furan ring and release of XH was shown to be highly dependent on the nature of the substituents on the benzyl aromatic ring, with the methoxy substituent greatly enhancing the reactivity and 3',5'-dimethoxy substituents (3',5'-dimethoxybenzoin, (3',5'-DMB)) giving the highest yield of the benzofuran and release of XH . The reactions for the unsubstituted benzoin esters tend to produce photodimers of benzofuran (**16**) and therefore are generally less clean than that for the 3',5'-DMB system. The suggested mechanism for the formation of benzofuran involves n,π^* excitation of the ketone followed by intramolecular cyclization. Photolysis of 3',5'-DMB esters is unaffected by triplet quenchers,^{35,36} whereas unsubstituted benzoin esters are quenched.³⁷ However, details of the mechanism are not clear.

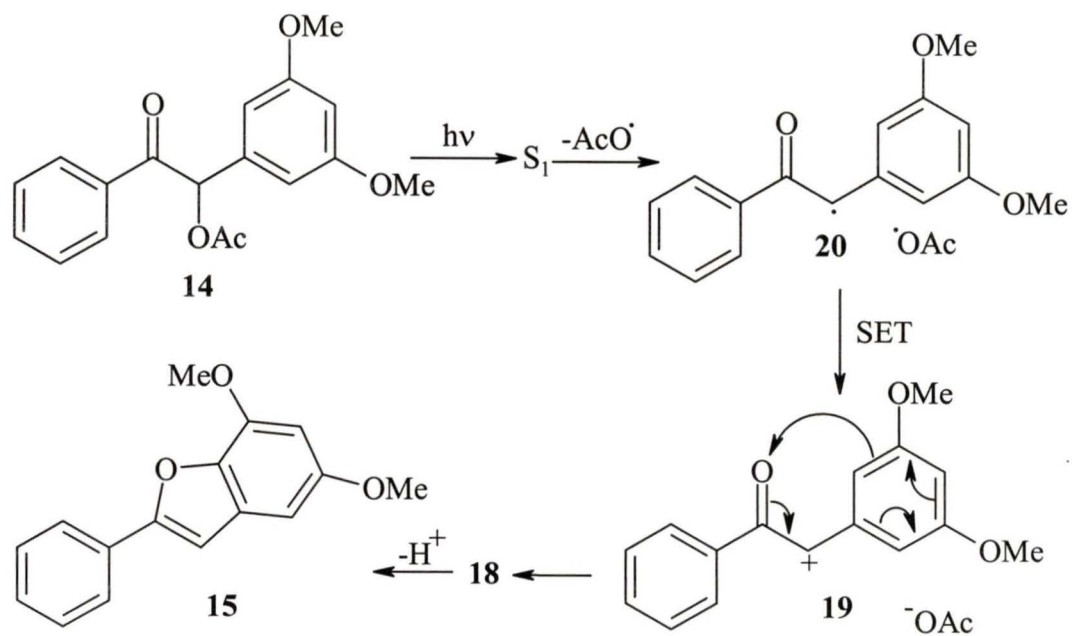


Sheehan *et al.*³⁵ postulated a rather unlikely mechanism involving Paterno-Buchi addition of the singlet n,π^* photoexcited carbonyl group to the substituted aromatic ring, resulting in the formation of a strained bicyclic intermediate **17** (Scheme 1.2). Ring opening with the loss of the acetate ion was suggested to give the dimethoxycyclohexadienyl cation **18**, followed by the benzofuran product upon deprotonation. Later, Pirrung *et al.*³⁶ suggested a mechanism based on a hypothesis that the reaction proceeds by photosolvolysis (Scheme 1.3), in which the C-X bond undergoes direct heterolysis to generate cation **19**. Another mechanism was proposed by Cameron *et al.*³⁸. They believed that the C-X bond was initially homolyzed followed by single electron transfer (SET) as illustrated in Scheme 1.4. Givens *et al.*³⁷ also preferred this mechanism where phosphate esters are used in place of the carboxylates.



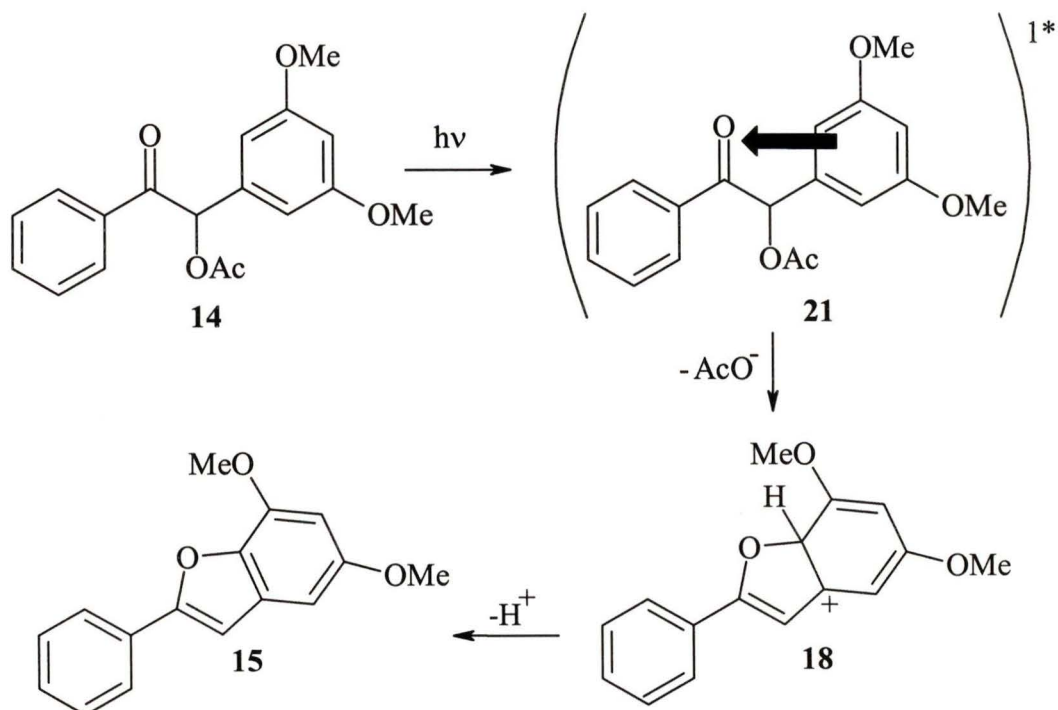


Scheme 1.3



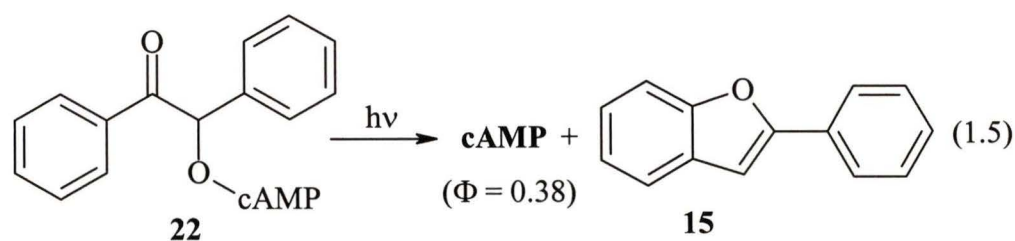
Scheme 1.4

With the growing importance of the DMB systems in applied photochemistry, members of our group³⁹ have also contributed to the mechanism. The photorelease of several carboxylic acids of 3',5'-DMB esters were studied by laser flash photolysis and product characterization. All the esters reacted cleanly and efficiently to give the expected benzofuran and the corresponding carboxylic acid, with no detectable radical-derived products. Evidence was presented to show that the primary photochemical event is electronic interaction between the electron rich dimethoxybenzene ring and the singlet n,π^* excited carbonyl group of the acetophenone moiety, as shown in Scheme 1.5, to give the cyclohexadienyl cation **18** in the primary step. Neither transient spectroscopy on the ns time scale nor product studies gave evidence for formation of α -keto cation **19**.



Many examples have been reported on the application of the benzoin group during the past decades. Studies by Givens *et al.*,³⁷ Corrie *et al.*,⁴⁰ Baldwin *et al.*,⁴¹ Pirrung *et al.*,³⁶ Futura *et al.*,⁴² and Cameron *et al.*⁴³ have demonstrated the utility of the benzoin for the release of phosphates, nucleotides, carbamates, and amino acids.

The initial studies on phosphate photorelease by Givens *et al.*³⁷ provided the first example of a new α -keto phototrigger as an alternative to 2-NB. Benzoin phosphate and other α -keto phosphate derivatives have subsequently been shown to release the phosphate efficiently with a rate constant of 10^5 s^{-1} or higher. Of particular importance is that cAMP, as its caged ester **22** (eq. 1.5), was released by irradiation at 350 nm with a rate constant of $7.2 \times 10^8 \text{ s}^{-1}$, and quantum yield of 0.38.³⁷ This represented a remarkable increase by 3 orders of magnitude in the rate constant for a phototrigger while maintaining a reasonably high efficiency relative to the best nitrobenzyl analogues. Others, especially the group of Corrie and Trentham⁴⁰, have also reported the development of caged phosphates, *e.g.*, 3',5'-dimethoxybenzoin ATP, as an alternative to the 2NB and 2NPE, further substantiating the potential of benzoin derivatives.

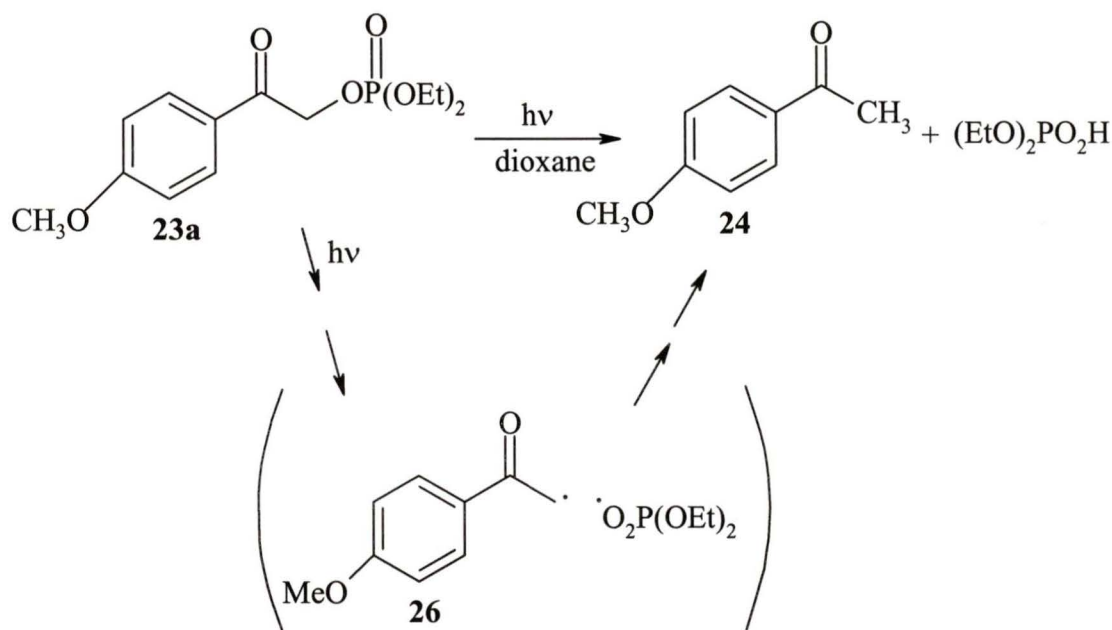


All of these reports demonstrate the advantages of benzoin. The rates of C-O cleavage for the benzoin phosphates are at least 3-6 orders of magnitude faster than those reported for irradiations of *o*-nitrobenzyl derivatives. The reaction efficiencies for the benzoin phosphates are uniformly good and appear to be independent of the nature of the solvent or the structure of the phosphate, but are pH dependent. A second major advantage of the benzoin is that the benzofuran product is relatively unreactive, and appears to be biochemically benign, a feature that is not true for the photoproducts of *o*-nitrobenzyl derivatives. Besides, the benzofuran is nonpolar and inert and therefore readily separable. An important consideration in the development of the benzoin group as a useful cage is also the ease of synthesis of mixed esters containing the benzoin ligand. While at the present time, these studies show that the benzoin group is severely limited because of its poor aqueous solubility of its derivatives and hydrolytic instability. Problems may arise when used for the protection of chiral compounds, since the benzylic carbon constitutes another chiral centre and it might be difficult to separate the individual diastereomers. As a result, research into the use of phenacyl derivatives, members of another family of α -keto cage groups, has been active.

1.1.3 Phenacyl Derivatives

In 1961, Anderson and Reese⁴⁴ reported that phenacyl chlorides (**23b**, eq. 1.6) containing electron-donating substituents at the *para* and *ortho* positions (*e.g.*, 4-OH, 4-OCH₃, and 2-OCH₃), upon irradiation, primarily rearranged to esters **25**, whereas electron-

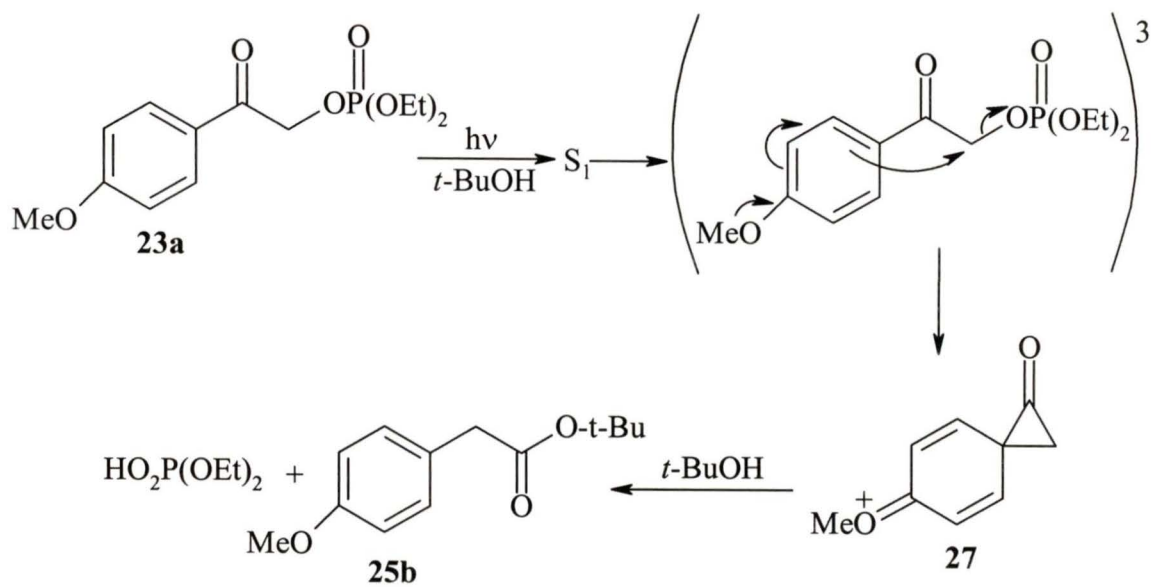
phosphate bond followed by hydrogen abstraction from the solvent by the α -keto radical **26** (Scheme 1.6). They further suggested that the 4-methoxyphenacyl group might serve as a photoprotecting group for nucleotides. Baldwin and coworkers' study⁴¹ in 1990 on the photolysis of *p*-methoxyphenacyl dihydrogen phosphate (**23d**) also confirmed the report by Epstein *et al.*⁴⁷ that *p*-methoxyacetophenone (**24**) was the only product.



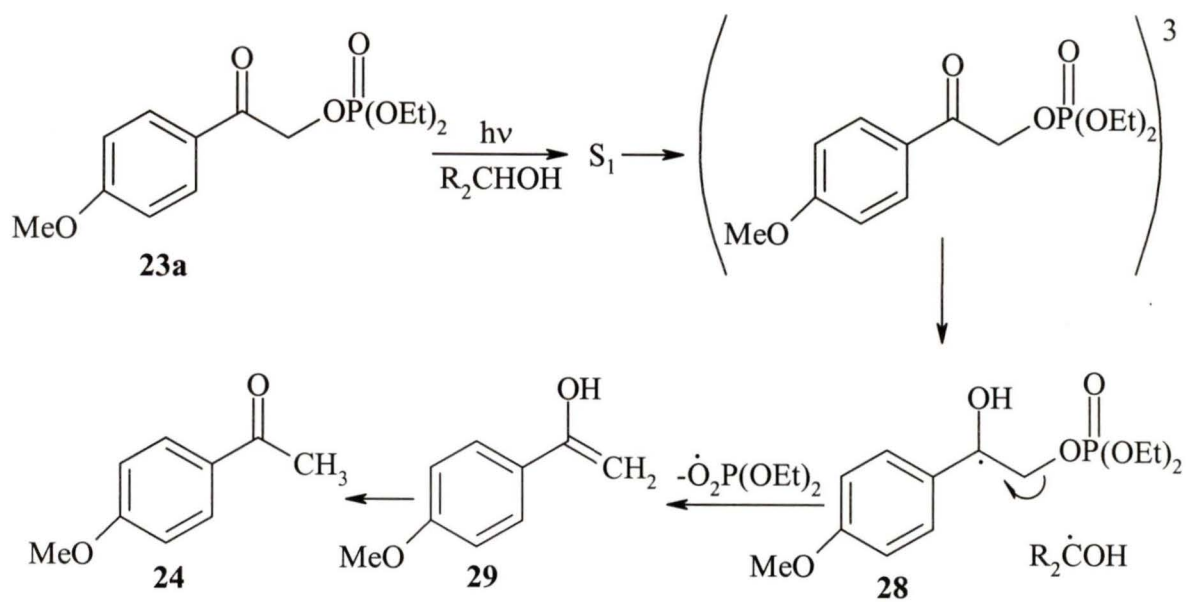
Scheme 1.6

Givens and coworkers⁴⁸ have reinvestigated the photochemistry of *p*-methoxyphenacyl diethyl phosphate (**23a**) in more polar solvents, methanol and *tert*-butyl alcohol. They found that, in addition to the products of the type reported by

Epstein *et al.*⁴⁷ and Baldwin *et al.*⁴¹, the rearranged *tert*-butyl *p*-methoxyphenacyl acetate (**25b**) was the major product in *tert*-butyl alcohol, a solvent known to be poor hydrogen-atom donor. Likewise, even in methanol, which is a better hydrogen-atom donor, the yield of the rearrangement product was appreciable, i.e., 38%. In both solvents, rearrangement dominated over reduction. The change in the nature of the products as a function of solvent and structure of the phosphate is reminiscent of an earlier study on the corresponding phenacyl halides by Anderson and Reese.⁴⁴ Furthermore, they also found that the reaction could be quenched by triplet quenchers. Based on all this information, it was proposed⁴⁹ that the intermediates generated from α -keto halides, phosphates, and related nucleofuge groups tend to favour heterolysis when a neighbouring group or direct conjugation can participate effectively at the reaction centre. Homolysis dominates when no special stabilization of the α -keto carbocation is possible and when the nucleofugacity of the α -substituent is not strong. Thus formation of the rearranged ester **25b** can best be rationalized by a conventional neighbouring *p*-anisyl group participation at the developing electron-deficient α -ketocarbocation-like centre (Scheme 1.7). The origin of the reduction product **24** in methanol and dioxane was thought to arise via initial hydrogen abstraction from the solvent by the carbonyl n,π^* triplet, followed by homolysis of the carbon-oxygen bond of the phosphate (Scheme 1.8).

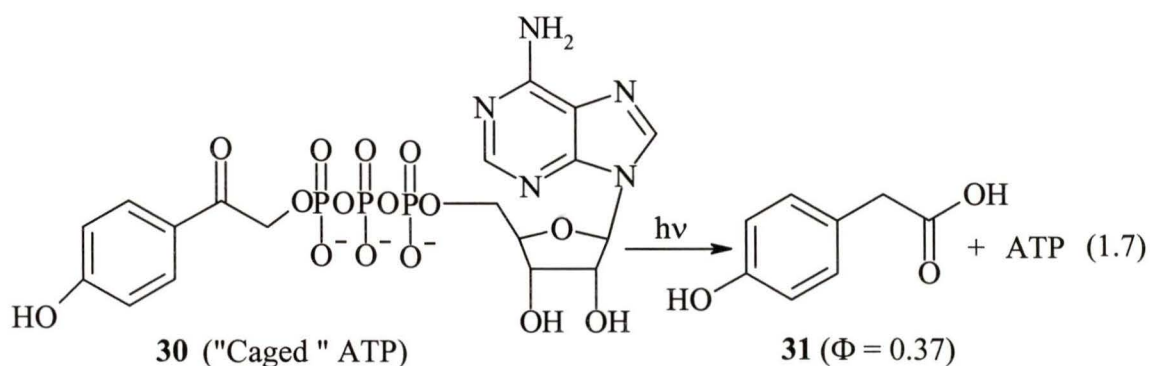


Scheme 1.7



Scheme 1.8

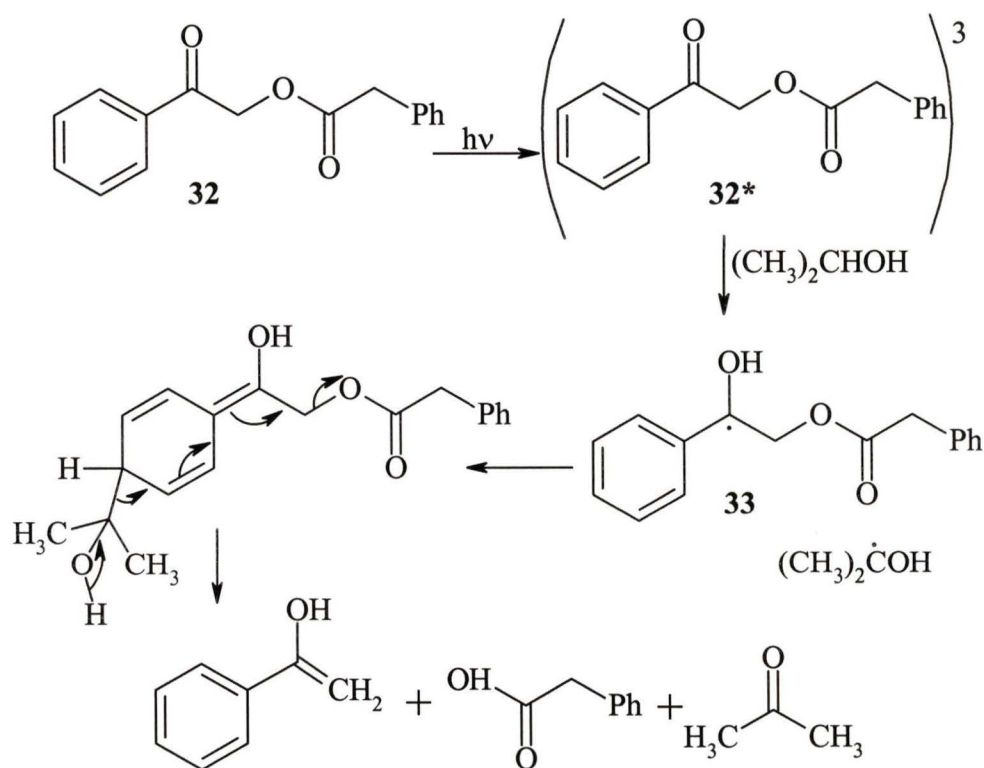
Recently, based on work on the *p*-hydroxyphenacyl group, Givens *et al.*⁵⁰ showed that the rearrangement is the exclusive pathway for *p*-hydroxyphenacyl phosphate and ATP (**30**) in aqueous media (eq. 1.7). The mechanism they suggested is the same as that proposed for the *p*-methoxyphenacyl group, but also suggested that it is also possible another mechanism might be operative.



Bannerjee and Falvey⁶⁹ have recently studied the mechanism of phenacyl esters lacking the *p*-hydroxy group (*i.e.*, phenacyl phenylacetate (**32**), Scheme 1.9) and concluded that in H-atom donating solvents, the mechanism of photorelease of the carboxylic acid is not via C-OCOR homolysis, but via initial hydrogen abstraction by the acetophenone carbonyl, to generate a ketyl radical (**33**) which can further react thereby releasing the carboxylate.

These kinds of α -keto cages, (the *p*-methoxy and *p*-hydroxyphenacyl groups), alleviates major limitations that accompany the benzoin group while at the same time

preserving the high efficiency and rapid photorelease of the coupled substrate and also maintaining the ready synthetic accessibility realized with the benzoin group. An additional beneficial feature of this group is the absence of the added chiral center. The *p*-hydroxyphenacyl group is even better than the *p*-methoxy analogue because of its excellent aqueous solubility, the simplified photoproducts, and the hypochromic shift of the UV absorption upon rearrangement of the cage to the *p*-hydroxyphenylacetic acid (**31**) product. All of these results warrant further elaboration of the *p*-hydroxyphenacyl group for uncaging of biological compounds.

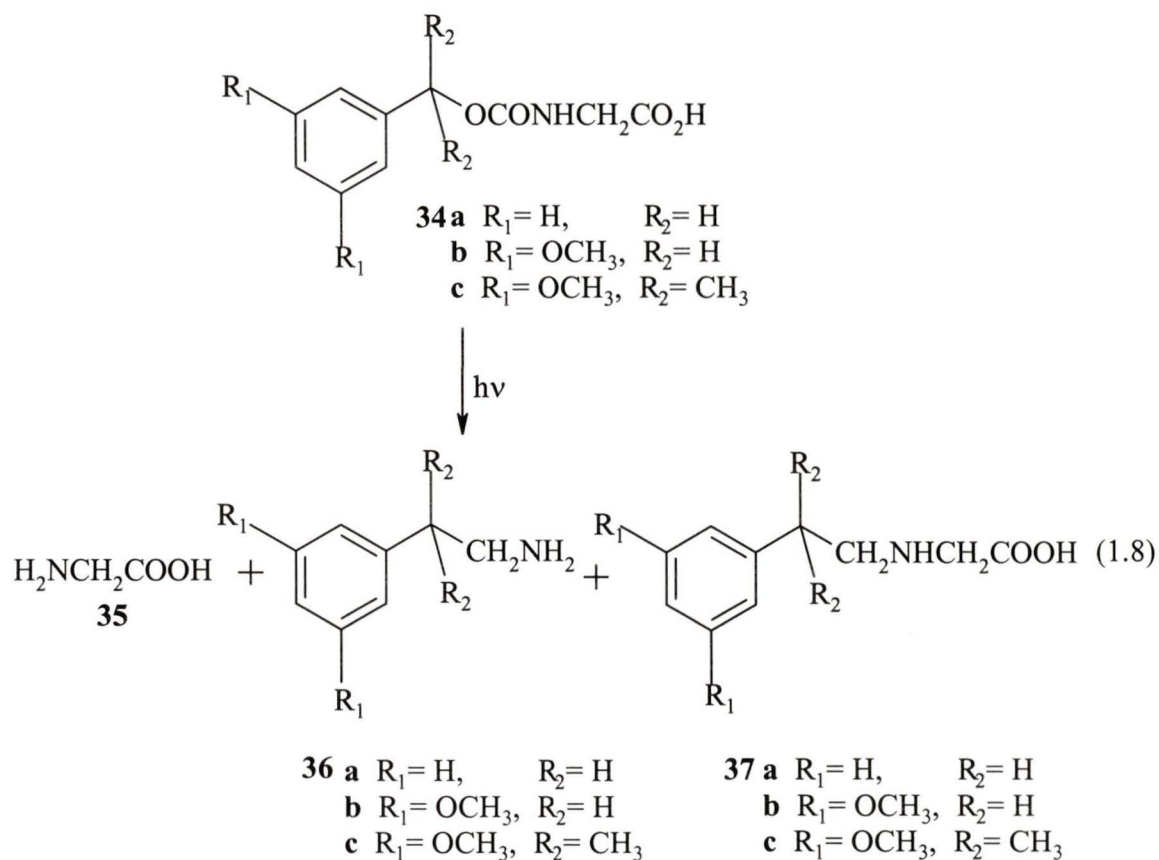


Scheme 1.9

1.1.4 Miscellaneous Systems

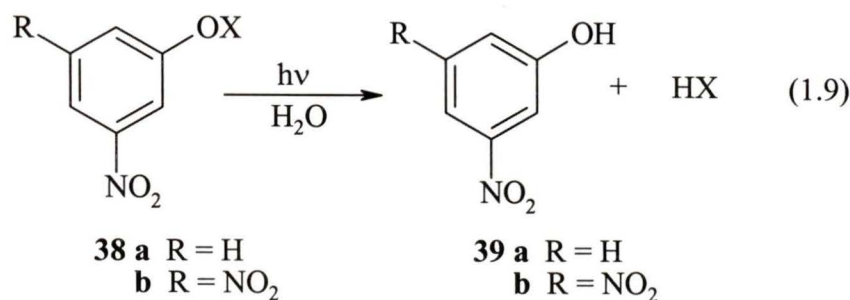
1.1.4.1 Benzyloxycarbonyl and Related Groups

The benzyloxycarbonyl group was the first one used successfully in the photochemical removal of a blocking group.^{1b,4} Under irradiation, benzyloxycarbonyl glycine (**34a**, eq. 1.8) is readily converted to the free amino acid **35**, along with the side products, phenylethylamine (**36a**), and N-benzylglycine (**37a**). The formation of **36** and **37** is rationalised in terms of intramolecular N- and C-alkylation mechanisms. Zimmerman and coworkers⁵¹ studied the photochemical solvolysis of substituted benzyl acetates and found that *m*-methoxy substitution enhanced the reactivity. Chamberlin⁵² used this reaction to develop the 3,5-dimethoxybenzyloxycarbonyl group (**34b**) as a selective N-protecting group. That 3,5-dimethoxybenzyloxycarbonyl amino acids and peptides are deprotected by photolysis in ethanol containing water. The requirement of water restricts the application of this cage. Besides, the activated carboxyl groups are hydrolysable by water thermally. Later, Birr *et al.*⁵³ developed a very efficient protecting group, the α,α -dimethyl-3,5-dimethoxybenzyloxycarbonyl group (Ddz) (**34c**), which is six times more reactive than the 3,5-dimethoxybenzyloxycarbonyl group. Also water is not necessary in the photochemical reaction.



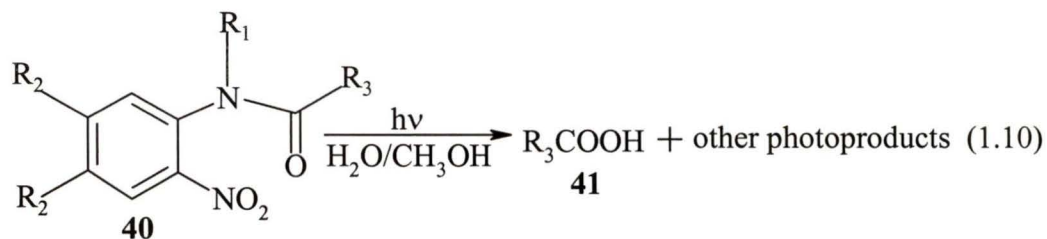
1.1.4.2 3-Nitrophenyl and Derivatives

The 3-nitrophenyl phosphate esters (**38a**, eq. 1.9) are stable in aqueous solution over a wide range of pH. However they undergo efficient photohydrolysis to the nitrophenol (**39a**), and the phosphate, HX, on irradiation that is absorbed by the aromatic system. The 3,5-dinitrophenyl (DNP) group (**38b**) is more efficient than the parent compound. This kind of protecting group can also be used for protecting amino functions. Potential problems include the danger of other nucleophiles competing in the photosolvolysis.



1.1.4.3 2-Nitroanilides

The photorearrangement of N-substituted 2-nitroanilides (**40**) to give the free carboxylic acids (**41**) in good yield (70% ~ 80%) is a reaction quite analogous to the photo-redox reaction of 2-NB derivatives.¹ On account of their mild cleavage and stability under hydrolytic conditions, the corresponding N-substituted 2-nitroanilides have been suggested to be potential photosensitive protecting groups for the carboxyl function in polyfunctional molecules. These groups are removed by irradiation with light of wavelength longer than 350 nm in aqueous methanol solution. The carboxylic hydrogen is derived from a process involving hydrogen-abstraction by the excited nitro group from the solvent. Their application needs more investigation.



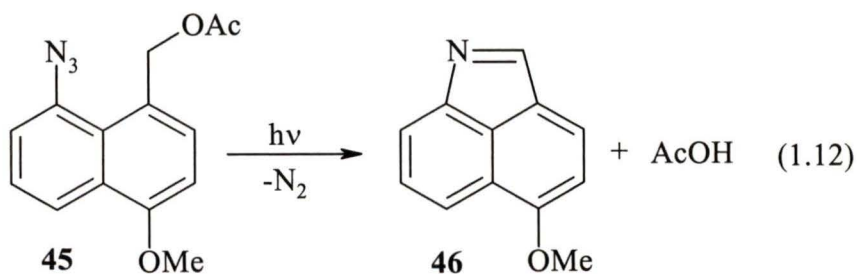
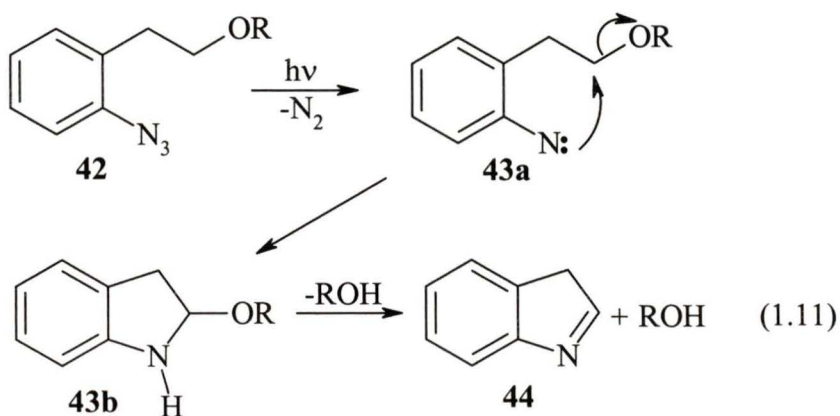
R₁ = Me, n-butyl, cyclohexyl, benzyl

R₂ = H, OMe

R₃ = Me, phenyl, o-chlorophenyl, 3,4-dichlorophenyl, 2-naphthyl

1.1.4.4 Aromatic Azides

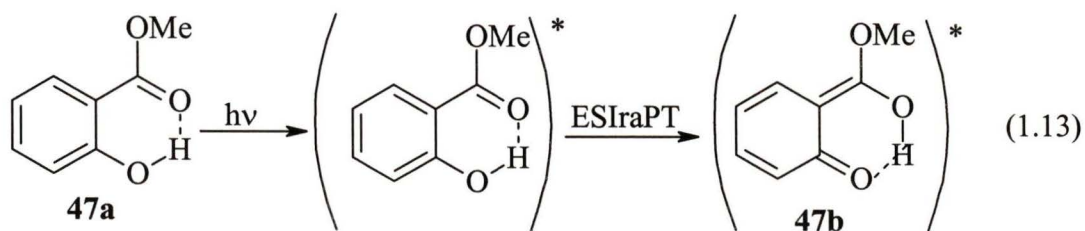
The use of certain light-sensitive aromatic azides as protecting groups has also been explored. Photolysis of alkyl or aryl derivatives **42** of β -(2-azidophenyl)ethyl alcohol yields isoindole **44**, and the corresponding alcohol or acid, through the intermediate, nitrene **43a**, which inserts into a peri-methylene group to give **43b** which then triggers elimination of the molecule being caged. The yields of the regenerated alcohols or acids are low. Derivatives of 5-azido-4-hydroxymethyl-1-methoxynaphthalene, such as **45**, were found to be better photocleavable protecting groups for the carboxylic function. One problem with this group is the danger of nitrene insertion at other sites, which would result in no release.



1.2 Photoprototropic Behaviour of Hydroxyarenes

Proton transfer (PT) is a common reaction in chemistry and biochemistry, which involves the acidic and/or basic groups of the solute.⁵⁴ The acidity/basicity of these groups is subject to change upon excitation since the electronic configuration of the molecule changes, making these groups either more or less electron rich. Therefore, the excited state dissociation constants pK_a^* often differs greatly from the ground state pK_a , leading to protonation or deprotonation of the excited species. If the pK_a of a group decreases upon excitation, the solute will dissociate, *i.e.*, undergo PT more readily in the excited state than in the ground state. In the case of excited state intramolecular proton transfer (ESIraPT), PT occurs most readily for those molecules whose acidic and basic groups both increase in acidity and basicity upon excitation, respectively.⁵⁵ PT can be initiated by a pre-existing intramolecular hydrogen bond or along hydrogen-bonded solvent molecules between the acidic and basic groups of the same or different species. In the latter case, usually the proton is transferred in a concerted manner from one site to another along a hydrogen-bonded solvent array. Excited state proton transfer (ESPT) reactions are ubiquitous in the photobehaviour of aromatic compounds, especially among hydroxyarenes.

Methyl Salicylate (**47a**) was the first compound shown to undergo ESPT for a hydroxyarene as well as being the first example reported to undergo ESIraPT.⁵⁶ Facilitated by an intramolecular hydrogen bond, PT led to the characteristic large Stokes shift for the emission from tautomer **47b**.



Since then, considerable study of ESPTs has been performed and the different types of such reactions have been divided into several classes.⁵⁷ There are two kinds of ESPTs, excited state intermolecular proton transfer (ESIerPT) and ESIraPT. ESIerPT involves intermolecular ionization PT, whereas ESIraPT results either from direct intramolecular hydrogen bonding interactions within the molecule (intrinsic intramolecular PT) or from solvent-solute complexes (proton-relay PT). Previous studies have involved a transfer of a hydroxyl or amino proton to a carbonyl oxygen or nitrogen acceptor. ESIraPT can lead to adiabatic tautomer formation which can result in a large Stokes-shifted emission due to the large electronic and structural rearrangements generally associated with PT.⁵⁵ Proton-relay ESIraPT mechanisms tend to require solvent reorganization in the excited state and this can lead to nonadiabatic tautomer formation. ESPTs can be probed by quenching studies of the normal emission, by monitoring of the tautomer fluorescence rise time, or by detection of the tautomer absorption via laser techniques.

1.2.1 Excited State Intermolecular Proton Transfer (ESierPT)

ESierPT involves transferring a proton between substrates, *i.e.*, the solvent either accepts or donates a proton, in the excited state. Therefore the rate of proton transfer depends on both the acidity of the proton donor and the basicity of the acceptor. ESierPT in polar solvents proceeds via charge transfer type of transition state with formation of solvated ions as the products. Naphthols⁵⁸, phenylphenols⁵⁹ and their derivatives have been studied in detail.

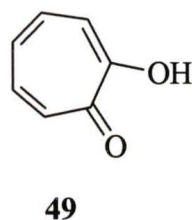
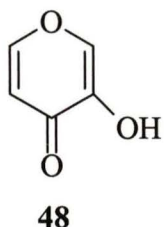
1.2.2 Excited State Intramolecular Proton Transfer (ESiraPT)

The term ESiraPT applies when both the proton donor and acceptor reside on the same molecule.⁵⁷ Reactions of this type usually involve transferring an acidic proton from an oxygen atom to a more basic oxygen or nitrogen acceptor, to give a tautomer of the substrate. From this point of view, ESiraPT is a tautomerization reaction on the S_1 state. There are several different kinds of ESiraPTs.

1.2.2.1 Intrinsic ESiraPT

This is an ultra-rapid process (ps, fs) where the proton is transferred across an internal hydrogen bond between the H atom being transferred and the acceptor. Numerous molecules with an internal hydrogen bond can undergo this kind of PT, *e.g.*, 3-hydroxy-4-pyrone (**48**), and methyl salicylate (**47a**). Those PTs giving rise to a tautomer identical to the normal form, *e.g.*, 2-hydroxytropolone (**49**), are termed symmetrical intramolecular PT. The intrinsic ESiraPT is inhibited if the intramolecular

hydrogen bond is broken by external hydrogen bonding interaction with solvent. A slow PT involving solvent may then occur.

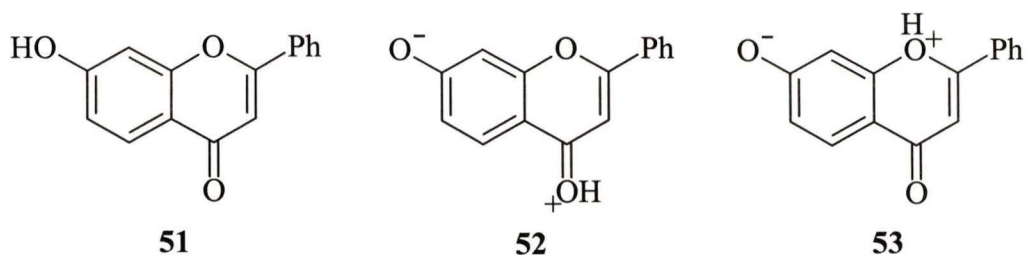
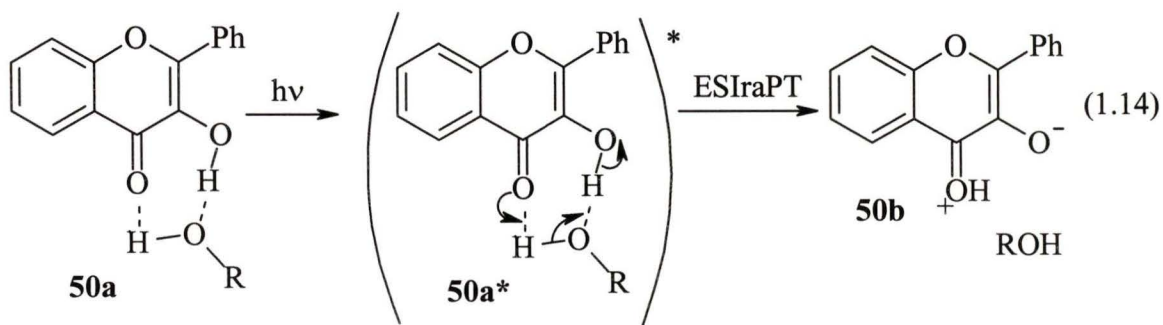


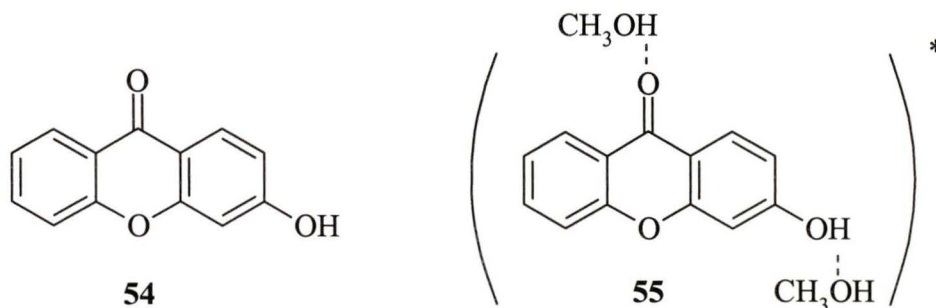
1.2.2.2 Proton-Relay ESIRA_{PT}

This type of PT involves one or several hydrogen-bonded solvent bridges forming a hydrogen-bonded cyclic complex with distant proton donor and acceptor sites.⁵⁷ In this class, the proton donor and the proton acceptor are so far apart that it is impossible to form an internal H-bond. Therefore a mediator is required to transport the proton. This mediator can be either the substrate itself (via a dimer or oligomer) or other component (containing an OH group) in the solution. Concerted biprotonic transfer, a subclass of it, involves a cooperative double proton transfer within a cyclic complex or dimer. This cyclical complex consists either of a doubly-bonded solute dimer or a solute doubly-hydrogen-bonded to a solvent molecule. 3-Hydroxyflavone (**50a**) was shown to undergo this kind of reaction.⁶⁰

7-Hydroxyflavone (**51**) was studied by Itoh and Adachi.⁶¹ They found that a 1:2 complex between **51** and methanol led to PT in the mixture of methanol and tetrahydrofuran. Two tautomers, **52** and **53**, were thought to exist. More recently, Itoh

*et al.*⁶² reinvestigated the ESPT of both 3-hydroxyxanthone (**54**) and **51** in methanol. They both behaved similarly. It was suggested that the anion and tautomer were formed adiabatically, contrary to the previous claim of two different tautomers being produced. The precursors for the tautomer and anion were thought to be different: a monosolvate (1:1 solute: methanol) led to the anion and a disolvate (1:2 solute: methanol) led to the tautomer. Possibly tautomer formation occurs via a methanol dimer in a cyclic transition state, although these authors represent its precursor as **55**.





The role of solvents has also been investigated because of its importance in ESIRaPT. It was found that the PT rate correlated with the solvent's donating ability as well as with $E_T(30)$ (a microscopic measurement of polarity within the cybotactic region which reflects mostly the hydrogen-bonding ability of the solvent).^{63,64} The stronger the hydrogen bond between the solute and solvent, the faster the PT rate. It was proposed that solvent motion was required since PT was slower than in the dimer substrate complex and also a dependence on temperature and solvent viscosity was observed. Generally speaking, this solvent reorientation would be required to form a cyclic complex within the excited state lifetime due to the increase in the basicity and/or acidity of related groups. In their studies, Varma and coworkers⁶⁴ found that if alcohols were used as solvent, the larger alcohol molecules have a lesser probability of being involved in hydrogen bonding with other alcohols, i.e., larger solvent clusters are less likely to form. Furthermore, bulkier solvents need more time for solvent reorganization.

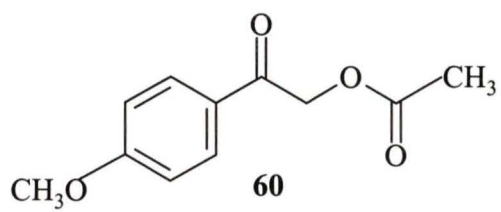
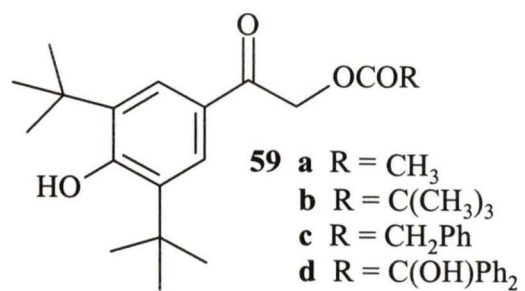
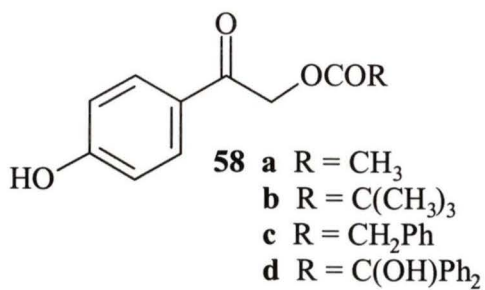
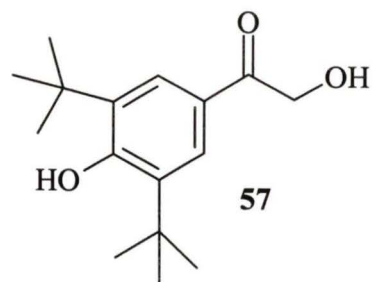
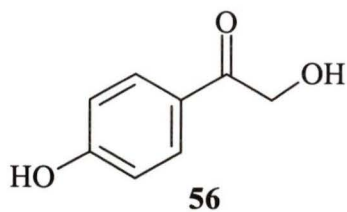
1.3 Proposed Research

As discussed in Section 1.1, photochemically-removable protecting groups play important roles in biochemistry, biology, and physiology. The *p*-hydroxyphenacyl group is a new, promising phototrigger to release a variety of caged biologicals (ATP, amino acids, etc.) in aqueous solution. In view of the current interest in the mechanism and potential applications of these reactions as well as our group's recent investigations⁷⁰ of the mechanistic photochemistry of a variety of hydroxyaromatic compounds in aqueous solution (where it is observed that proton transfer from the hydroxy group (either to solvent or intramolecularly to another basic site of the molecule) from the singlet state is the primary photochemical step which is ultimately responsible for chemistry), the present study has been undertaken. It is concerned about the possibility that a proton transfer mechanism might be operative for the reaction shown in eq. 1.7 for these *p*-hydroxyphenacyl esters. The aim of this Thesis is to explore the mechanistic photochemistry of a variety of *p*-hydroxyphenacyl derivatives **56-60** with anticipation that its reaction mechanism can be elucidated.

Studies reported by Givens and coworkers⁵⁰ were restricted to the photoreactivity of *p*-hydroxyphenacyl phosphates and relatively simple esters. In this mechanistic investigation, the photosolvolytic rearrangements of a variety of *p*-hydroxyphenacyl derivatives **56-60** will be studied, which includes the parent *p*-hydroxyphenacyl alcohol **56**, the di-*tert*-butyl-*p*-hydroxyphenacyl alcohol **57**, *p*-methoxy derivative **60**, and a variety of esters (**58** and **59**) which differ greatly in the propensity of the corresponding

acyloxy radical (if generated in the reaction mechanism) to decarboxylate. Pincock and coworkers⁷¹ have shown a dramatic dependence of the ratio of products derived from ionic versus radical intermediates resulting from different rates of decarboxylation of the acyloxy radical. Pivalate esters gave the highest yield of radical-derived products consistent with a very fast rate of decarboxylation for the pivaloyloxy radical $[(\text{CH}_3)_3\text{CO}_2\cdot, k_d = 1.1 \times 10^{10} \text{ s}^{-1}]$.⁷¹ The reported rate for decarboxylation of the benziloyloxy radical $[(\text{Ph})_2\text{C}(\text{OH})\text{CO}_2\cdot, k_d = (2-8) \times 10^{11} \text{ s}^{-1}]$ ⁷² is an order of magnitude faster. Thus, if the reaction mechanism involved initial C-OCOR bond homolysis followed by electron transfer (in **58** and **59**), one should see dramatic effects on the observed product distribution in these substrates, as shown by Pincock and coworkers.⁷¹

Indirect evidence for intermediate will be obtained via product studies if the expected acid is produced from trapping the spiroketone with water. Direct detection of the intermediate will be attempted by monitoring the absorption spectrum and decay of the produced transient via LFP. Solvent isotope effects will be studied to determine the role of water in the reaction. Also the effect of the water concentration on the yield of product will be monitored. A similar experiment with methanol instead of water will be performed in order to further verify the role of water. A triplet quenching study will reveal whether the reactive excited state is singlet or triplet. pH Effects on product formation will be measured as well as the pH effects on transient absorption by LFP, to explore whether the reaction is acid or base catalysed to further confirm the involvement of proton transfer.



Chapter 2

Results & Discussion

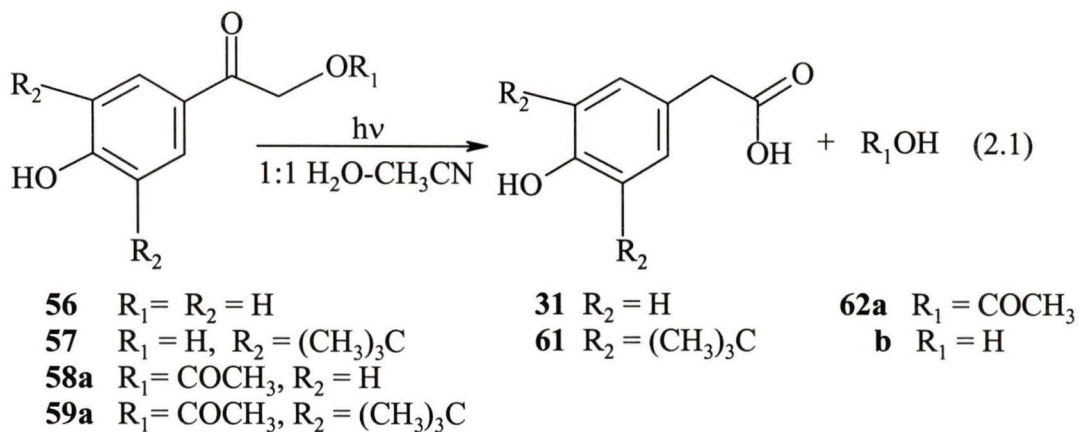
2.1 Product Studies

The photochemical reactions of the parent *p*-hydroxyphenacyl acetate (**58a**), its di-*tert*-butyl derivative **59a**, and the parent alcohol **56** and its di-*tert*-butyl derivative **57** were initially studied in 1:1 (v/v) H₂O-CH₃CN. For comparison, the photochemical behavior of a series of *p*-hydroxyphenacyl esters **58b-d**, **59b-d**, and the *p*-methoxy derivative **60** under identical conditions were also studied. All of these compounds were prepared by Dr. J. E. T. Corrie and coworkers at the National Institute for Medical Research, UK, who are our collaborators on this research project.

2.1.1 Photolysis of *p*-Hydroxyphenacyl Alcohols **56**, **57**, *p*-Hydroxyphenacyl Acetates **58a**, **59a**, and *p*-Methoxyphenacyl Acetate (**60**)

Irradiation of an argon purged $\sim 10^{-3}$ M solution of *p*-hydroxyphenacyl acetate (**58a**) in 1 : 1 H₂O-CH₃CN (40 ml) in a Rayonet RPR 100 photochemical reactor (300 nm, 8 lamps) at approximately 15 °C for 3 min led to formation of *p*-hydroxyphenylacetic acid (**31**) and photorelease of the corresponding "protected" acetic acid (**62a**) (eq. 2.1). Product **31** was isolated by preparative TLC (silica gel, CH₂Cl₂) and characterized by comparing its MS and ¹H NMR (characteristic methylene δ 3.48) with a sample of authentic compound, which is commercially available. The product yield of **31** ($\sim 40\%$) was measured by ¹H NMR, and the remaining $\sim 60\%$ of the product mixture was starting

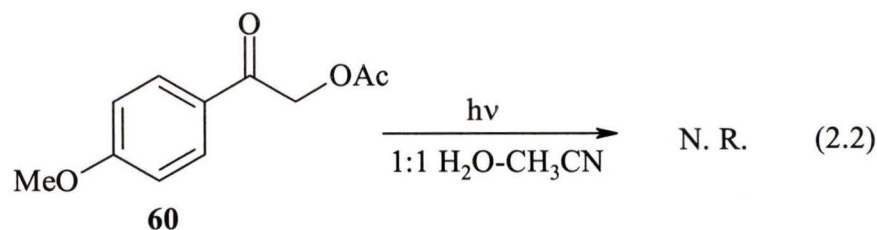
material. Under prolonged photolysis (~10 min), the yield of **31** was 100%. Only a trace (< 5%) of the photosolvolytic product **56** was observed even on quantitative conversion of substrate.



Photolysis of **59a** under identical conditions gave 4-hydroxy-3,5-di-*tert*-butylphenylacetic acid (**61**) and release of **62a** with a yield of 36%, which is almost the same as that observed for **58a**. Product **61** was also separated by preparative TLC and characterized by ¹H NMR (characteristic methylene δ3.48, and *tert*-butyl δ1.40) and MS. Photolysis of **56** and **57** in 1:1 H₂O-CH₃CN gave the corresponding acetic acids **31** and **61** with only about 20% yield (the remaining 80% was starting material) under much longer irradiation conditions (16 lamps, 30 min), which means that these *p*-hydroxyphenacyl alcohols are ≈ 40 fold less photosensitive than the corresponding *p*-hydroxyphenacyl acetates. This can be attributed to the much poorer leaving group ability of HO⁻ compared to that of CH₃COO⁻. All of the above reactions can be taken

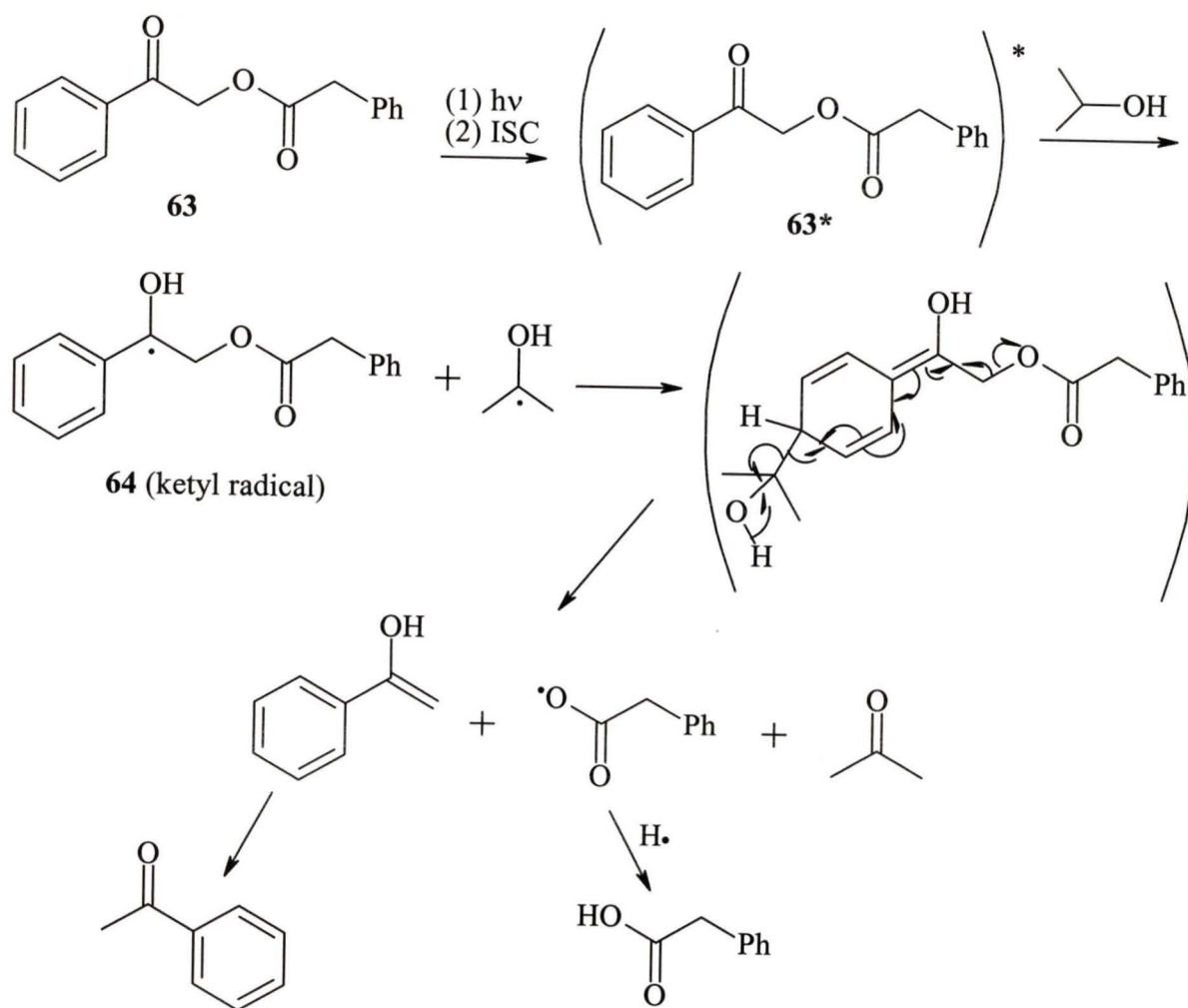
to essentially 100% conversion without any evidence for formation of radical-derived products which would be attributable to C-OR₁ bond homolysis.

Equally informative was the finding that under the conditions employed for the above compounds, substrate **60** failed to give any observed reaction (including simple photosolvolysis of the acetate group) (eq. 2.2) showing that the phenolic OH is required for the reaction. This observation also argues against a primary step involving simple C-OR₁ bond heterolysis (to form an α -acyl carbocation) as the hydroxyl and methoxy groups should have very similar electronic properties with regards to electron donation in ground and excited states.



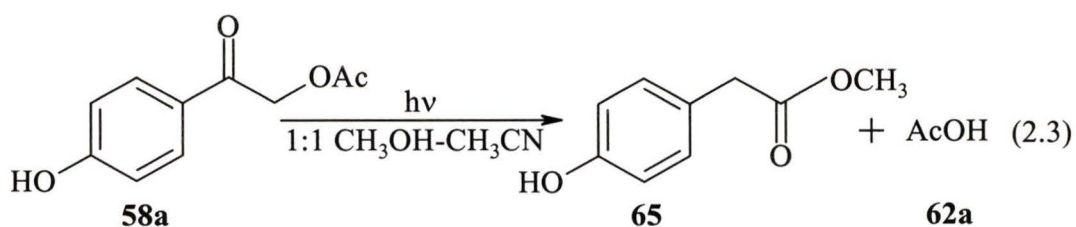
Interestingly, Sheehan and Umezawa⁷⁹ reported that a number of *p*-methoxyphenacyl esters including the benzoate (**63**) released the corresponding acid on photolysis in dioxane and ethanol. Notably, addition of water to these solutions decreased the yield of cleavage. The *p*-methoxyphenacyl fragment was reduced to *p*-methoxyacetophenone in the reaction. Although no quantum yields were measured, yields were as high as 96%. The proposed mechanism by the authors involves α -cleavage

from the triplet excited state, to generate the radical pair, followed by reduction by the solvent. However, the recent report from Bannerjee and Falvey⁶⁹ would suggest that the mechanism in the presence of H-atom donors probably involves initial hydrogen abstraction by the carbonyl oxygen, to generate a ketyl radical **64** which subsequently fragments to the enol of the acetophenone and the acyloxy radical, the latter reduced to give the corresponding carboxylic acid (Scheme 2.1).



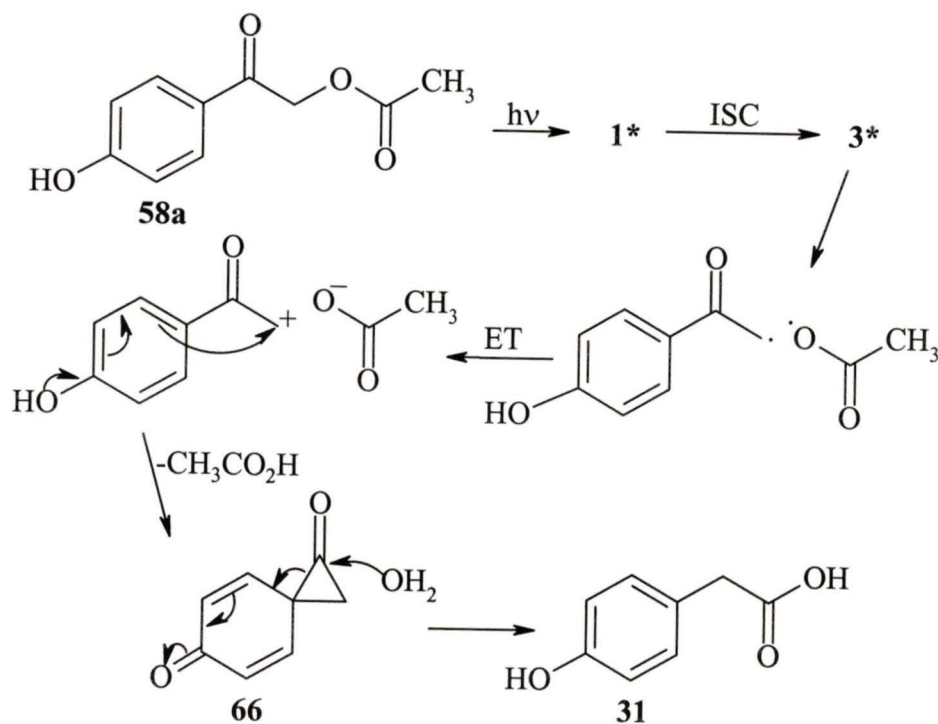
Scheme 2.1

Photolysis of **56** and **58a** in neat CH_3CN resulted in complete recovery of the substrates. Therefore water is necessary for this photosolvolytic-rearrangement reaction. For compound **58a**, photolysis in 1:1 $\text{CH}_3\text{OH}-\text{CH}_3\text{CN}$ and in neat CH_3OH was also carried out (eq. 2.3). Only the corresponding photoproduct methyl *p*-hydroxyphenyl acetate (**65**) and photoreleased acetic acid (**62a**) were detected by ^1H NMR. Ester **65** was collected by preparative TLC and characterized by ^1H NMR (characteristic methylene δ 3.48, and methoxy δ 3.61) and MS. It was found that the conversion from **58a** to **65** was about 5-fold lower than that observed from **58a** to **61** in 1:1 $\text{H}_2\text{O}-\text{CH}_3\text{CN}$ solution. It is known that CH_3OH is a better nucleophile than H_2O . Therefore the difference in observed yield must come from other factors, such as solvent polarity. In other words, the solvent itself probably plays some crucial role in the reaction mechanism besides acting as a nucleophile. Control experiments performed in the absence of light did not give any observable reaction for all of the above reactions.



All of the above reactions are very clean with the *p*-hydroxyphenyl acetic acid (**31**), its di-*tert*-butyl derivative **61**, or methyl *p*-hydroxyphenyl acetate (**65**) as the only photoproducts. Dimeric products, which may be formed via initial C-OR₁ bond homolysis, was not observed. These observations argue strongly against a mechanism involving initial C-OR₁ bond homolysis. A different primary step must be operative.

As discussed in Section 1.1.3, the published mechanism for several *p*-hydroxyphenacyl systems^{51c} states that this rearrangement reaction is via the triplet excited state with the spiroketone **66** as the intermediate (Scheme 2.2). However, photolysis of *p*-hydroxyphenacyl acetate (**58a**) purged by O₂ under identical conditions produced **31** with the same yield as that observed when purged by argon. This was also the case for **56**, **57**, and **59a**. Therefore, it is unlikely that the reaction goes via the triplet excited state because most of such reactions are significantly quenched by O₂, hence giving a much lower yield of photoproduct. This was not the case at all for the *p*-hydroxyphenacyl derivatives studied. Experiments involving triplet quenching experiments using triplet quenchers besides oxygen need to be carried out to verify this point further (*vide infra*).



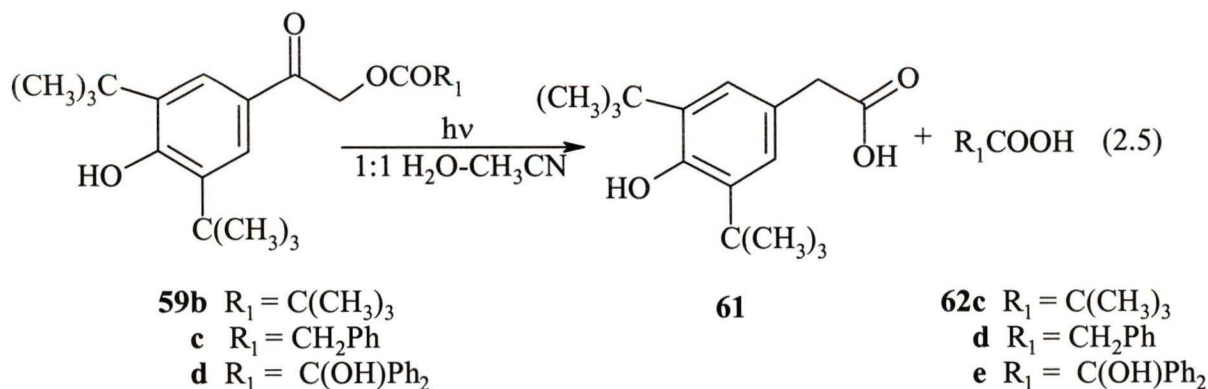
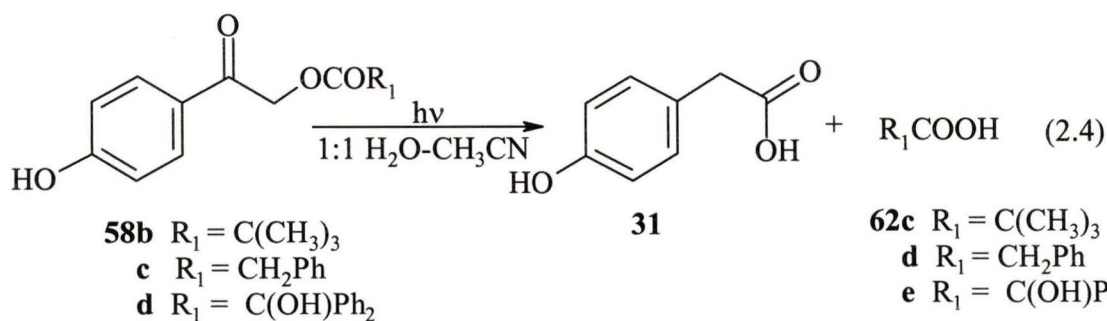
Scheme 2.2

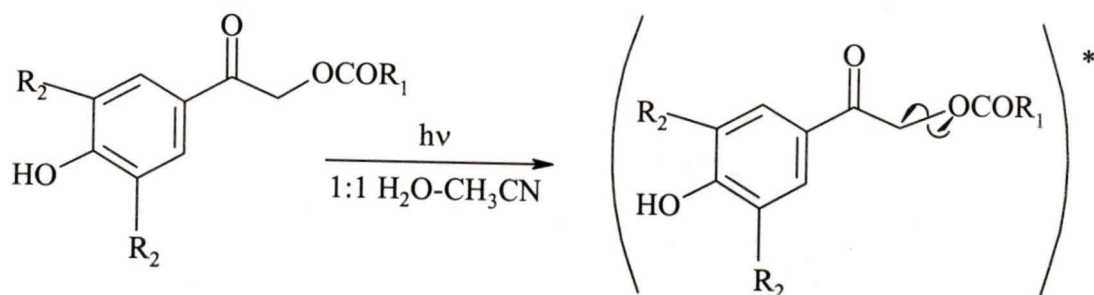
2.1.2 Photolysis of *p*-Hydroxyphenacyl Esters 58b-d and 59b-d

Results of product studies of a series of *p*-hydroxyphenacyl esters **58b-d** and **59b-d** also argue against a C-OCOR₁ bond homolysis mechanism. All of these esters gave the corresponding *p*-hydroxyphenylacetic acid (**31**) or its di-*tert*-butyl derivative **61** as the only photoproduct, and photoreleased **62c-e** (eqs. 2.4 and 2.5) with similar yields as that observed for the parent esters **58a** and **59a** when irradiated in 1:1 H₂O-CH₃CN under identical conditions. No side products were detected by ¹H NMR for any of them.

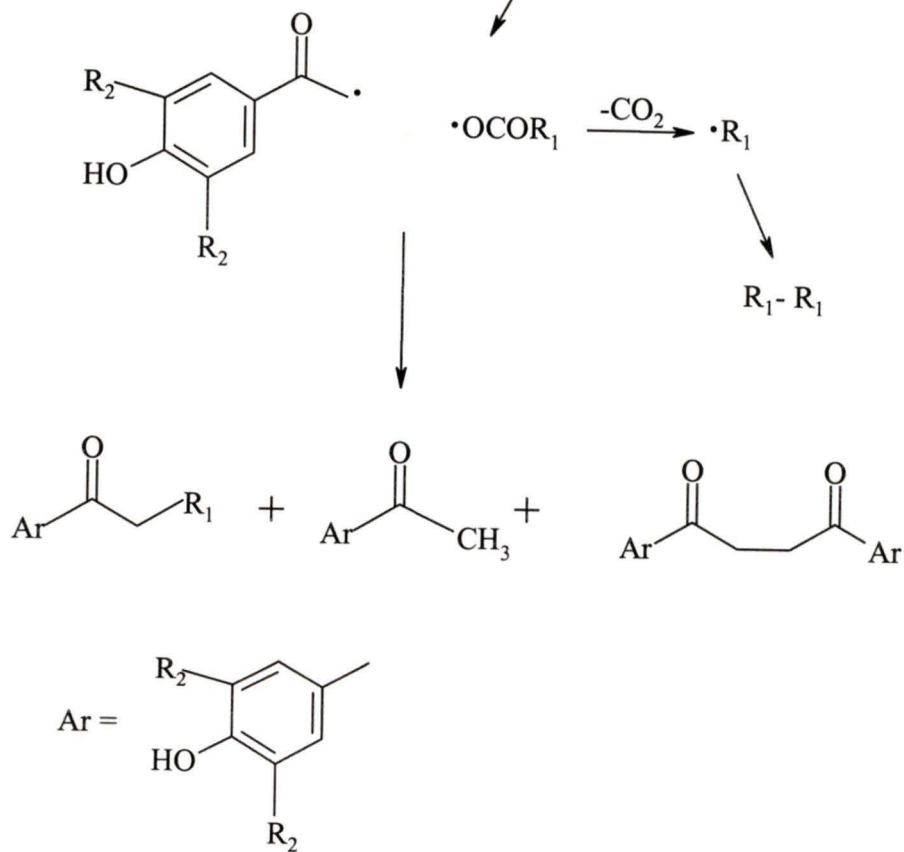
The series of *p*-hydroxyphenacyl esters **58** and **59** differ greatly in the propensity

of the corresponding acyloxy radical (if generated in the reaction mechanism) to decarboxylate. Pincock and coworkers⁷¹ have shown a dramatic dependence of the ratio of products derived from ionic versus radical intermediates resulting from different rates of decarboxylation of the acyloxy radical. Pivalate esters gave the highest yield of radical-derived products consistent with a very fast rate of decarboxylation for the pivaloyloxy radical $[(\text{CH}_3)_3\text{CO}_2^{\cdot}; k_d \approx 1.1 \times 10^{10} \text{ s}^{-1}]$.⁷¹ The reported rate for decarboxylation of the benziloyloxy radical $[(\text{Ph})_2\text{C}(\text{OH})\text{CO}_2^{\cdot}; k_d \approx (2-8) \times 10^{11} \text{ s}^{-1}]$ ⁷² is an order of magnitude faster. Thus, if the reaction mechanism involved initial C-OCOR₁ bond homolysis followed by fast electron transfer, one should see dramatic effects on the observed product distribution in these substrates, as illustrated by Scheme 2.3.





58a-d, 59a-d
 ($R_1 = \text{CH}_3, (\text{CH}_3)_3\text{C}, \text{CH}_2\text{Ph}, \text{C}(\text{OH})\text{Ph}_2$
 $R_2 = \text{H}, (\text{CH}_3)_3\text{C}$)



Scheme 2.3

2.2 Quantum Yield Measurements

Photochemical efficiencies may be quantified in terms of a product quantum yield (Φ_p), which, by definition, is the moles of photochemical product formed for each mole of photon absorbed (eq. 2.6).⁶⁵

$$\Phi_p = \frac{\text{Moles of Product formed}}{\text{Moles of Photon Absorbed}} \quad (2.6)$$

The light intensity was measured with the potassium ferrioxalate ($K_3[Fe(C_2O_4)_3] \cdot 3H_2O$) chemical actinometer.⁶⁶ The product yield was measured by UV-Vis spectrophotometry according to Beer's law (eq. 2.7).

$$\text{Moles of Products formed} = V \times C = V \times \Delta A / (\epsilon l) \quad (2.7)$$

Where V is the volume of the solution used (3.000 ml); C is the concentration of the product calculated by Beer's law; ΔA is the absorption change of the solution at the monitoring wavelength after irradiation; ϵ is the extinction coefficient at the monitoring wavelength; and l is the length of the light path (1.000 cm).

Because the reactions are very clean; that is, essentially only one photoproduct is observed for all of them (even on 100% conversion), quantum yields for product formation would be identical to quantum yields for disappearance of substrate. The latter can be conveniently measured by UV-Vis since traces for conversion of these compounds to **31** (or **61**) showed substantial loss of the optical density on reaction progress, as expected (Figure 2.1). Using this technique, the absolute quantum yields for product

formation (Φ_p) for **58a** and **59a** were measured at pH 7 (1:1 H₂O:CH₃CN; quoted pH is of the water portion) by using an optical bench utilizing a mercury arc lamp in conjunction with a monochromator to obtain an excitation wavelength of 254 nm. Substrate **58a** or **59a** ($\sim 10^{-4}$ M) was irradiated in a 3 ml quartz cuvette at ambient temperature while purged with argon. Conversion was kept low ($< 20\%$) to minimize the interference from the photoproduct **31** or **61**. These measurements gave $\Phi_p = 0.41 \pm 0.04$ and 0.36 ± 0.04 for **58a** and **59a**, respectively, indicating that these reactions are quite efficient.

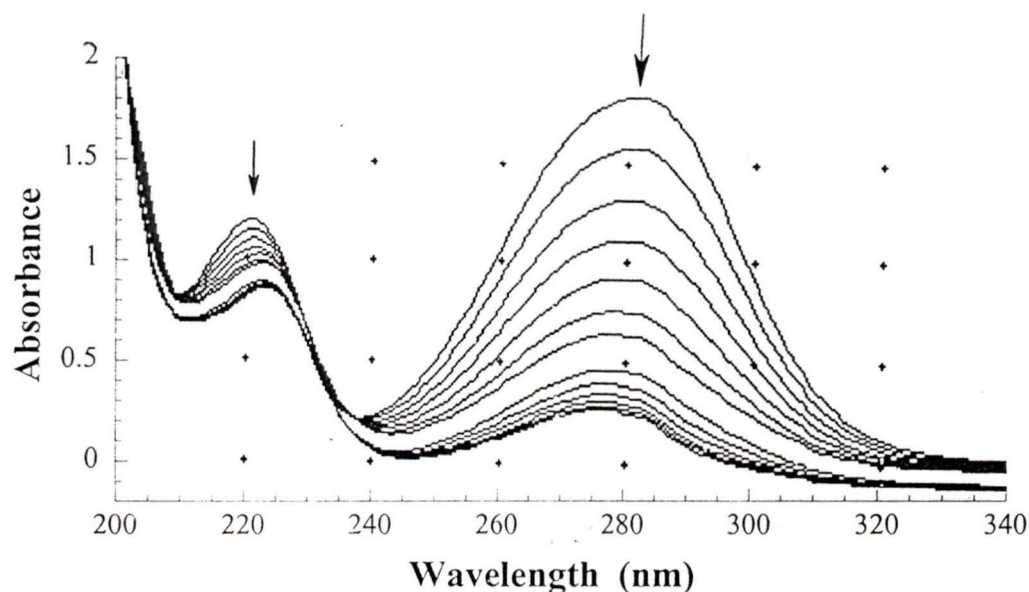


Figure 2.1 UV-Vis traces for the conversion of **58a** to **31** on photolysis at 300 nm (in 1:1 H₂O-CH₃CN); argon purged. Each trace represents about 1 min photolysis time.

Subsequently, quantum yields at other pHs (from pH 0 to pH 12) for the formation of photoproducts **31** or **61** from **58a** or **59a** in 1:1 H₂O-CH₃CN were measured by ¹H NMR under same conditions as that for products studies, using the value of Φ_p at pH 7 as a secondary reference (Figure 2.2). The UV-Vis technique was not used here due to complications arising from the formation of phenolate at high pHs. The plots show that these compounds are unreactive below pH ~ 0 and above pH ~ 12. Two "titration curves" are also apparent in this plot: one for the excited state ($pK(S_1) \sim 1$) and one for the ground state ($pK(S_0) \sim 10.5$), the latter in somewhat agreement with the known pK_a (8.5)⁶⁸ for ionization of the phenol of *p*-hydroxyacetophenone. The discrepancy is due to the substantial presence of CH₃CN in the solvent mixture, as confirmed by a UV-Vis titration of *p*-hydroxyacetophenone in 1:1 H₂O-CH₃CN, which gave an "apparent" $pK_a \sim 11$.

A number of control experiments were carried to ensure that the results of Figure 2.2 represented the true photochemical behavior of the compounds. For example, control runs showed that at the lower and higher pHs, no significant (< 5%) thermal hydrolysis was taking place during the time of the experiment (i.e., **58a** to **56**). Product studies for the reaction of **56** in 1:1 H₂O-CH₃CN (although 40-fold less reactive than **58a**) gave a pH plot that closely resembled that observed in Figure 2.2.

The results of Figure 2.2 strongly suggests that ESPT is involved in the reaction mechanism. This is consistent with the titration curve observed between pHs 0 and 2, a range of many known $pK_a(S_1)$ values for phenols.⁷³ The titration curve observed between pHs 10 and 12 indicate that excitation of the phenolate form does not result in reaction

(or that it is much less reactive). These results are consistent with the fact that **60** is not reactive (lacks phenol) and that an aqueous medium is optimum for reaction of **56-59**.

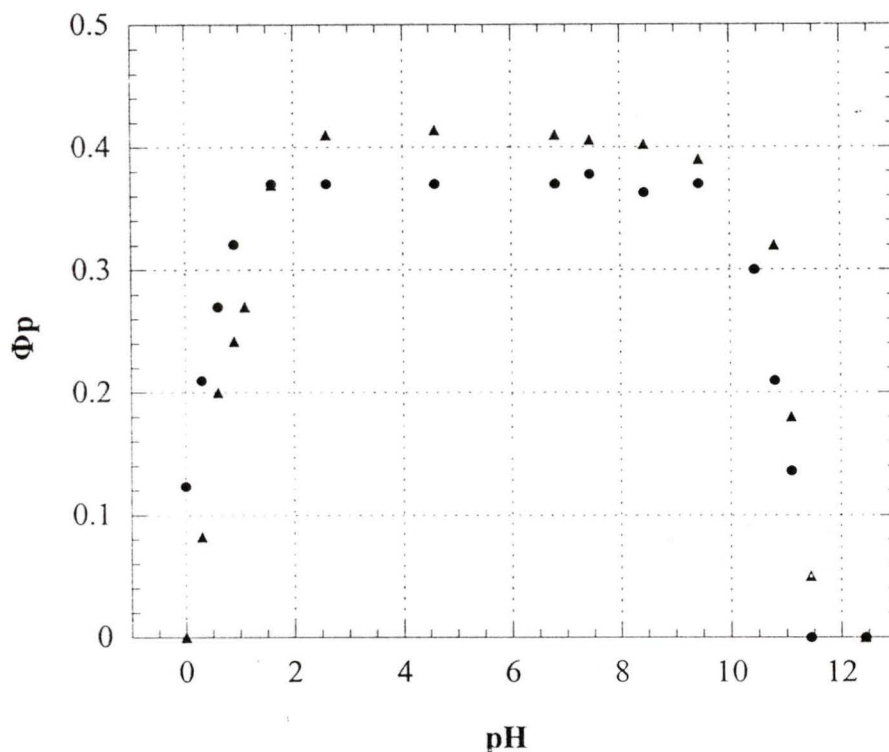


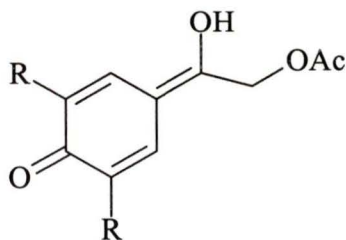
Figure 2.2 pH Effect on the quantum yields (Φ_p) for formation of **31** from **58a** (triangles) and **61** from **59a** (circles) photolyzed in 1:1 $\text{H}_2\text{O}-\text{CH}_3\text{CN}$, measured by ^1H NMR.

As discussed in Section 1.2, proton transfer is a widely developed area in chemistry and biochemistry. ESIRaPT mediated by solvent is common for hydroxyarenes. Reactions of this type usually involve transferring an acidic proton from an oxygen atom to a more basic oxygen or nitrogen acceptor, such as transferring a hydroxy proton to a carbonyl oxygen which are far apart, leading to the formation of a tautomer of the

substrate. In other words, ESIRaPT is a tautomerization reaction which is usually via the singlet excited state. In addition, the ESIRaPT is not catalyzed by acid or base (eq. 1.14).

Plots in Figure 2.2 show that the reactions do not involve direct photoprotonation because the quantum yields decrease at low pHs. The reactions do not involve the phenolate either. Direct photolysis of the phenolate resulted in no reaction. It is also known from product studies that the phenol is necessary for the reaction, and that an aqueous medium is optimum. All of these results are consistent with ESIRaPT in the reaction mechanism.

If ESIRaPT is involved in the mechanism for **58a** and **59a**, their tautomers, *p*-QM **67**, should be produced as an intermediate, by transferring the *p*-hydroxy proton to the carbonyl oxygen mediated by water. The highest quantum yield for formation of *p*-QM **67** should be in neutral solution because ESIRaPT cannot be accelerated by acid or base. If the existence of *p*-QM **67** could be directly shown, then the involvement of ESIRaPT would be strongly supported. Therefore laser flash photolysis will be employed (*vide infra*) to look for the existence of *p*-QM **67**.



67a R = H
b R = (CH₃)₃C

Aqueous media play a crucial role in ESIRaPT. In order to further explore the role of H₂O as solvent in the reaction, the effect of H₂O concentration in a H₂O-CH₃CN (pH 7) mixture on the quantum yield of reaction of **58a** was studied by UV-Vis spectrophotometry. Substrate **58a** has a strong absorption band (S₀ to S₁) at 279 nm ($\epsilon \approx 15,700 \text{ M}^{-1}\text{cm}^{-1}$). A UV-Vis spectrum recorded immediately after photolysis showed decrease in absorption at 279 nm indicating the loss of **58a**. The conversion was kept < 20% to avoid the interference of the photoproduct **31**. The S₀ to S₁ absorption of **31** is at 274 nm ($\epsilon \approx 1,600 \text{ M}^{-1}\text{cm}^{-1}$). The results (Figure 2.3) showed that there was no observable reaction in pure CH₃CN under these conditions. This was further confirmed by photolysis of **58a** in pure CH₃CN measured by ¹H NMR. However, upon addition of water (to CH₃CN), the quantum yield increased significantly, leveling off at about 40% H₂O (v/v). These results support the ESIRaPT mechanism. That is, the reaction can only take place when H₂O is present, and the product quantum yield increase when more and more H₂O is made available for this process. The quantum yield reaches a plateau when adding more H₂O fails to increase the rate of ESIRaPT.

The role of CH₃OH as a solvent was also explored under the same conditions as that for H₂O. It was found that the quantum efficiency for reactions of **58a** in CH₃OH-CH₃CN increased with the increasing concentration of CH₃OH, and reached a plateau at 70% CH₃OH-CH₃CN (Figure 2.3). However, the quantum yields in CH₃OH-CH₃CN are about 5-fold lower than that in H₂O-CH₃CN. This reduced quantum efficiency can be explained by solvent polarity difference. It is known that CH₃OH is much less polar than

H₂O, and a poorer proton donor. In addition, CH₃OH is a bulkier solvent. These effects decrease the rate of proton transfer in CH₃OH compared to H₂O and hence a decrease in quantum yield. As discussed in Section 1.2, the proton transfer rate is proportional to the proton donating ability of the solvent as well as E_T(30) (a microscopic measurement of polarity within the cybotactic region which reflects mostly the hydrogen-bonding ability of the solvent).^{63,64} The stronger the hydrogen bond of the solvent and solute, the faster the rate of proton transfer. These results are consistent with a mechanism involving proton transfer as it is well known that ESPT from phenols is optimum in aqueous media.⁷⁴

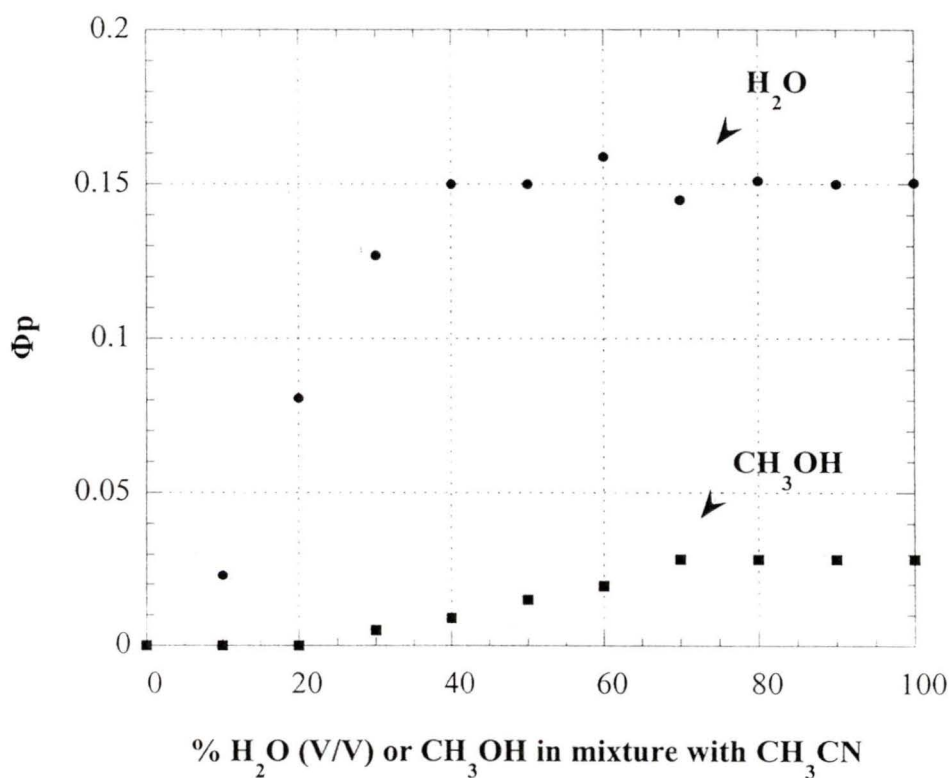


Figure 2.3 Dependence of Φ_p on H₂O (circles)/ CH₃OH (squares) concentration on the conversion of **58a** to **31** or **65** in mixture with CH₃CN measured by UV-Vis spectrophotometry.

2.3 Solvent Isotope Effect

A kinetic solvent isotope effect (KSIE) refers to the change of reaction rate constant due to isotope substitution (generally substitution of H with D) which is defined as the ratio of the rate constant of the unsubstituted molecule (k_H) to that of the substituted one (k_D), given by eq. 2.8,

$$\text{KSIE} = k_H / k_D \quad (2.8)$$

The primary KIE is generally classified where the bond containing the isotope is broken during the reaction. Since direct rate measurements are problematic in many photochemical reactions, an isotope effect on quantum yield is more readily accessible. In our experiments, a solvent isotope effect on quantum yield (QSIE) was measured (eq. 2.9). In certain circumstances, the QSIE data can be used to qualitatively rationalize the KSIE of the reaction.

$$\text{QSIE} = \Phi_H / \Phi_D \quad (2.9)$$

The strong possibility that the mechanism of photosolvolytic rearrangement of these compounds involves an ESPT step prompted the measurement of the solvent isotope effect on quantum yield for reaction of **58a**. Photolysis of **58a** in 1:1 H₂O-CH₃CN and 1:1 D₂O-CH₃CN was taken under identical conditions as that for product study. Essentially no difference was observed in the quantum yields ($\Phi(\text{H}_2\text{O})/\Phi(\text{D}_2\text{O}) = 0.95 \pm 0.05$). This value was confirmed by the disappearance quantum yields of **58a** (in 1:1 H₂O-CH₃CN and 1:1 D₂O-CH₃CN) measured by UV-Vis spectrophotometry described above. The value of $\Phi(\text{H}_2\text{O})/\Phi(\text{D}_2\text{O})$ was initially surprising since one would have

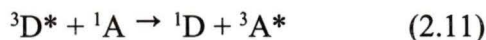
expected a substantial primary solvent isotope effect on the quantum yield if deprotonation is required in the reaction mechanism. However, it is known^{75a,b} that some very fast (on the femtosecond time scale) excited state intramolecular proton transfers (between oxygen and nitrogen,) exhibit no observable deuterium isotope effect on rates of transfer while others^{75c,74d} (intermolecular and solvent-mediated intramolecular cases) have observed rate differences of up to 3 (i.e., slower in D₂O). There appears to be no general expectation of what the solvent isotope effect should be in ESPT although Moog and Maroncelli^{75c} have offered a theory in which the proton transfer mechanism can be modeled by a two-step process: a solvent reorganization process and the actual proton transfer. Systems in which the proton transfer is very fast - whereby the rate determining step is solvent reorganization - would exhibit very small solvent isotope effects whereas systems in which proton transfer is much slower than solvent organization would exhibit substantial solvent isotope effects. Assuming that their theory applies to the ESPT which seems to be required for reaction of the p-hydroxyphenacyl systems studied in this work, the ESPT process of these compounds are all probably very fast such that the rate determining step will be solvent reorganization. In addition, proton transfers which have very early (or very late) transition states would also be expected to exhibit minimal isotope effect. Therefore, the lack of a primary solvent deuterium isotope effect in **58a** does not preclude ESPT in the reaction mechanism.

2.4 Triplet Quenching

Quenching and photosensitization play important roles in many aspects of organic photochemistry.⁶⁵ Quenching and photosensitization processes which involve energy transfer of the type shown in eq. 2.10 (D^* is excited state energy donor, A is ground state energy acceptor) may be used to control photochemical sequences and to study reaction mechanism, especially in the study of the excited state (S_1 or T_1) responsible for a photochemical reaction.



For example, singlet-singlet and triplet-triplet energy transfers may be used to indirectly populate A^* states or to quench D^* states. Of special importance is triplet-triplet energy transfer, which can be presented as eq. 2.11, because triplet-triplet energy transfer allows for the efficient indirect production of triplets which is difficult to be formed by direct excitation of the singlet ground state.



The most important single parameter in the selection of a triplet quencher or photosensitizer is the energy gap between ${}^3D^*$ and ${}^3A^*$, since only if the energy transfer is exothermic can it possess a maximal value of k_{ET} (the rate constant for energy transfer). The energetics of the transfer process are illustrated in Figure 2.4. Also important is that the quencher must not have a significant absorption in a region of the spectrum where the molecule is being excited.⁶⁵

Triplet quenching experiments involve selectively exciting the molecule in presence of an appropriate triplet quencher. It could be inferred that the reaction is from T_1 if the quencher inhibits the reaction. Otherwise, S_1 is the responsible excited state for reaction.

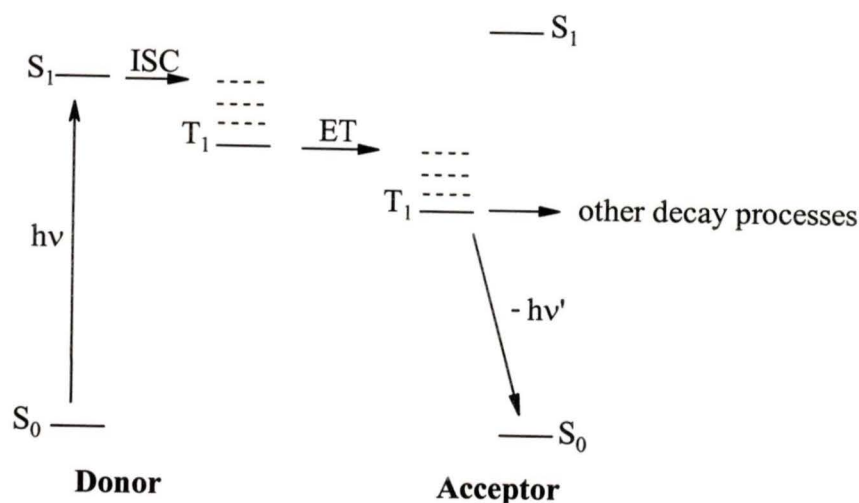
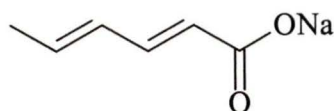


Figure 2.4 Energy level diagram for triplet-triplet energy transfer

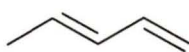
Givens and coworkers⁵⁰ reported that the triplet excited state is responsible for reaction in these *p*-hydroxyphenacyl systems based on triplet quenching experiments using sodium 2-naphthalenesulfonate. However, sodium 2-naphthalenesulfonate has considerable absorption out to 320 nm, very much like the *p*-hydroxyphenacyl chromophore itself. This indicates that its use as a triplet quencher is problematic. Triplet sensitization is even more difficult as few potential sensitizer that have the required triplet energy (i.e., significantly larger than that of acetophenone, which has $E_T \sim 70 - 74$ kcal

mol^{-1})⁶⁶ and absorb beyond 320 nm. Instead, sodium sorbate, trans-piperylene, and 1,3-cyclohexadiene were employed as triplet quenchers. These triplet quenchers do not absorb at all above 280 nm and therefore unencumbered with problems associated with competition for the exciting light in quenching studies. All of these quenchers are conjugated dienes and have triplet energies of around 50-55 kcal mol^{-1} ⁶⁶ and would be expected to quench the *p*-hydroxyphenacyl (acetophenone) triplets at diffusion controlled rates.

Irradiation of an argon-purged 1:1 $\text{H}_2\text{O}-\text{CH}_3\text{CN}$ solution of **58a** ($\sim 10^{-3}\text{M}$; 300 nm lamps) with 0.1 M sodium sorbate was carried out under identical condition as that for product studies. Results obtained by ^1H NMR showed only a marginal decrease in conversion yield compared to runs without quencher (i.e., from 40% to 35% conversion). Similar results were observed by using 0.1 M trans-piperylene, or 0.1 M 1,3-cyclohexadiene. The later quencher was used in 1:1 $\text{H}_2\text{O}-\text{THF}$ because of its poor solubility in 1:1 $\text{H}_2\text{O}-\text{CH}_3\text{CN}$. The marginal drop in conversion can be accounted for by the slight cloudiness of these solutions at such high quencher concentrations. These results indicate that the reactive state has a lifetime much less than 10 ns, which is highly incomparable with triplet state reactivity.



sodium sorbate



trans-piperylene



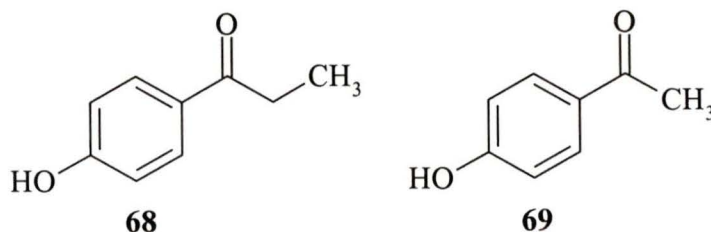
1,3-cyclohexadiene

2.5 Laser Flash Photolysis (LFP)

Results discussed up to this point strongly suggest the involvement of ESIRaPT in the mechanism, and therefore the existence of *p*-QM **67** as an intermediate. Direct evidence for the *p*-QM intermediate was provided by LFP (excimer laser, 308 nm, ~ 10 ns, < 30 mJ/pulse). To ensure uniform absorption upon excitation and to minimize self reaction, a low precursor concentration giving an initial absorption of ~ 0.3 at 308 nm was used. Flow cells were employed for measurement of spectra in order to ensure excitation of fresh sample and thus avoid interference from photolysis products and long-lived species.

2.5.1 *p*-Hydroxyphenacyl Acetate (**58a**)

Upon LFP of flowing solutions of **58a** in neat CH₃CN (~ 10⁻⁴ M, N₂ purged), a strong absorption with $\lambda_{\text{max}} = 380$ nm was observed, which was not observed when the solution was purged with O₂ (Figure 2.5). In N₂, the decay trace at 380 nm is single exponential decay with $\tau = (1.1 \pm 0.1)$ μs . This transient is assigned to the triplet excited state of **58a**. This assignment is consistent with studies by Banerjee and Falvey⁶⁹, and Scaiano and coworkers⁷⁶, as well as our control studies on *p*-hydroxyacetophenone (**69**).



Banerjee and Falvey⁶⁹ reported the triplet absorption for phenacyl phenylacetate (**64**) (which contains the parent acetophenone chromophore) in benzene with $\lambda_{\text{max}} = 340$ nm. Scaiano and coworkers⁷⁶ assigned a transient observed at $\lambda_{\text{max}} = 380$ nm to the triplet absorption of *p*-hydroxypropiophenone (**68**) (in wet acetonitrile). Our LFP studies of *p*-hydroxyacetophenone (**69**) in neat CH₃CN gave a transient at 360 nm also assignable to its triplet state.

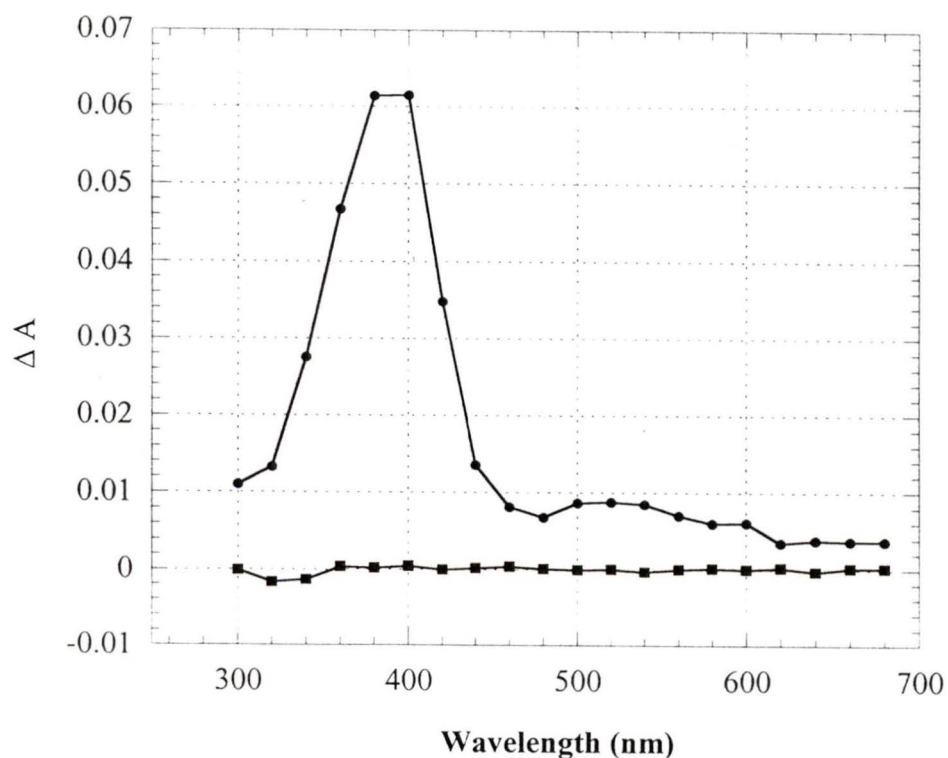


Figure 2.5 Transient absorption observed on LFP of flowing, neat CH₃CN solutions of **58a** purged by N₂ (circles) and O₂ (squares).

LFP studies of **58a** in 1:1 H₂O-CH₃CN (N₂ purged) gave a new and strong absorption at 330 nm, in addition to the 380 nm absorption, which was considerably weaker. The 380 nm transient is quenched by O₂, while the 330 nm transient is essentially insensitive to O₂ (Figure 2.6). This indicates that the 330 nm transient is not from the triplet state.

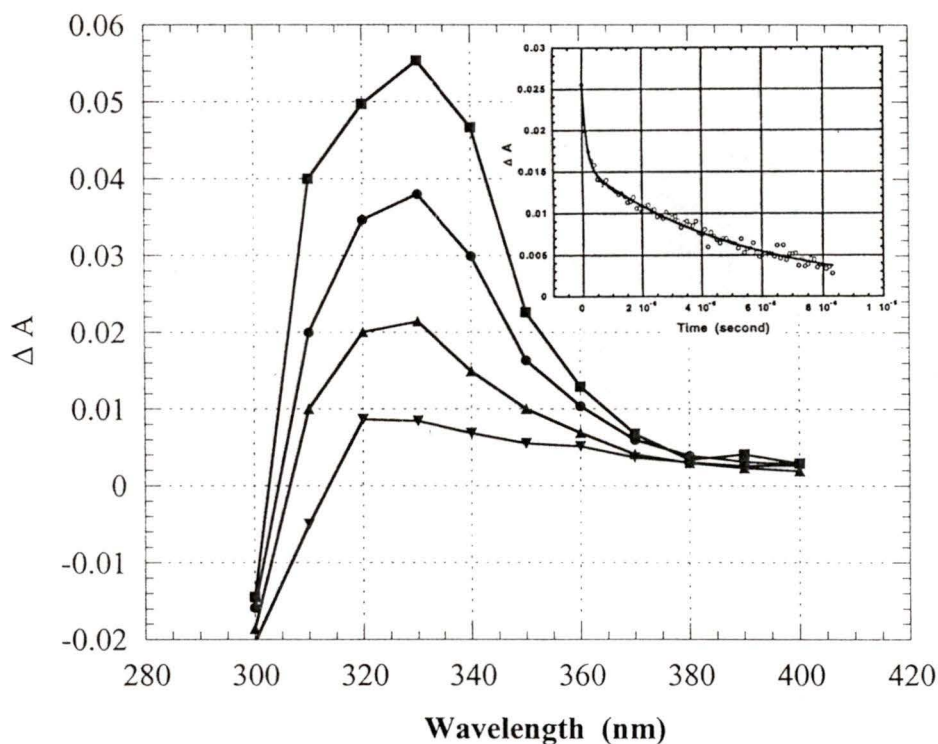
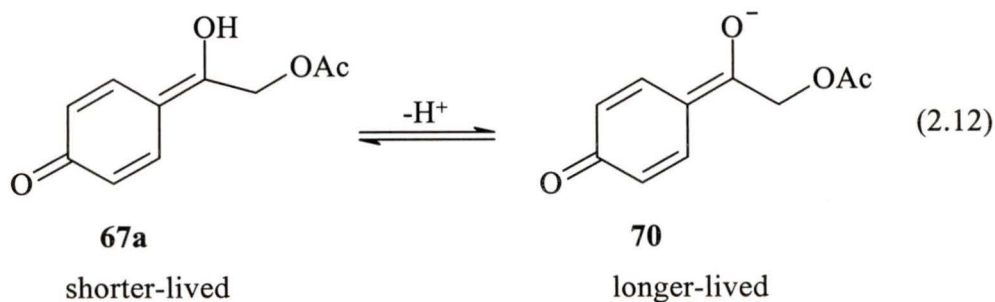


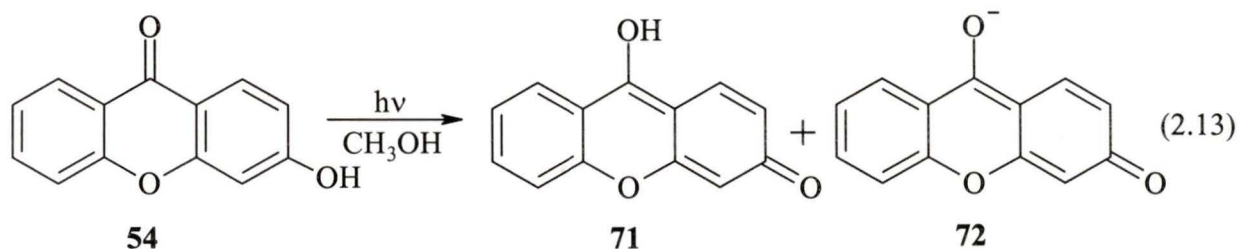
Figure 2.6 Transient absorption observed on LFP of flowing, O₂ purged 1:1 H₂O-CH₃CN solution of **58a**. Decay trace taken at 400 ns intervals [The first trace (■) was centered at ~ 50 ns, the second one (●) was centered at ~ 100 ns, the third one (▲) was centered at ~ 250 ns, and the last one (▼) was centered at ~ 3 μs].
[Inset: biexponential decay of transients at 330 nm with $k_d = 6.3 \times 10^6 \text{ s}^{-1}$ and $k_d = 1.8 \times 10^5 \text{ s}^{-1}$.]

Decay traces of the 330 nm transient at pH 7 showed that it is composed of two first order decays, a major component (~ 70%) with $k_d = 6.3 \times 10^6 \text{ s}^{-1}$, and a minor (~ 30%) component with $k_d = 1.8 \times 10^5 \text{ s}^{-1}$, assignable to two species with very similar UV absorptions. The proportion is calculated assuming identical extinction coefficients for the two species at this wavelength. Kinetic studies at other pHs showed that the proportion of the longer-lived species increases with increasing pH and that it is not observed below pH 6. Correspondingly, the proportion of the short-lived species decreases with increasing pH. This indicates that these two species are related by a prototropic equilibrium. LFP of **58a** in 1:1 D₂O-CH₃CN solution revealed that the decay rates for both of those two species were about 2-fold slower, further substantiating that there is a prototropic equilibrium between the two species.

The shorter-lived component is attributed to *p*-QM **67a** and the longer-lived component to its conjugate base, enolate/phenolate **70** (eq. 2.12). The UV-Vis spectrum of authentic **70** (generated via deprotonation of **58a** at high pH) has $\lambda_{\text{max}} = 330 \text{ nm}$ in 1:1 H₂O-CH₃CN further verifying the assignment of the LFP signal observed at this wavelength (at lower pH).



The assignment of two species undergoing prototropic equilibrium is consistent with literature LFP studies on 7-hydroxyflavone (**51**) and 3-hydroxyxanthone (**54**) by Itoh and coworkers.⁶² They showed (by LFP) that these "p-hydroxy-substituted" ketones undergo an excited state intramolecular proton transfer (ESIrPT), assisted by solvent CH₃OH, to form the corresponding *p*-QMs (e.g., **71**) and their conjugate bases (e.g., **72**) (eq. 2.13).



Our spectral assignment of the 330 nm band as due to simple *p*-QM **67a** and **70** is also consistent with earlier studies on simple *p*-QMs.⁷⁷ Filar and Winstein^{77a} reported the UV spectra of several simple *p*-QMs which are summarized in Table 2.1. It shows that the λ_{max} of the simplest of the series (in CH₃OH) is at 290 nm, and the effect of electron-donating substituents on the methylene group changes the position of the UV band in the expected direction (to longer wavelength). Leary and coworkers^{77b,c} reported that the λ_{max} of *p*-QM **74** in water is at 350 nm, and *p*-QM **75** in 7:1 (v/v) *t*-butyl alcohol-heptane could be monitored at 310 nm. In addition, the α -phenyl-*p*-QM **76a** has been photogenerated by Wan and coworkers⁷⁹ and shown to have $\lambda_{\text{max}} = 360$ nm in water with

a rate of decay not affected by O₂ (Figure 2.7)

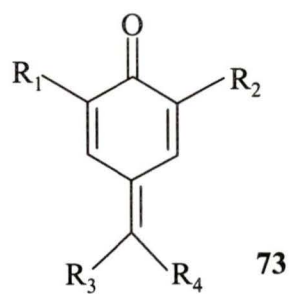


Table 2.1 Data for UV spectra of some p-QMs (73)

R ₁	R ₂	R ₃	R ₄	λ _{max} (nm, in CH ₃ OH)
CH ₃	CH ₃	H	H	290
CH ₃	CH ₃	H	CH ₃	312
CH ₃	CH ₃	H	CH ₂ =CH ₂	338
t-Bu	CH ₃	H	H	290
t-Bu	t-Bu	H	H	289
t-Bu	t-Bu	H	CH ₃	303
t-Bu	t-Bu	CH ₃	CH ₃	322

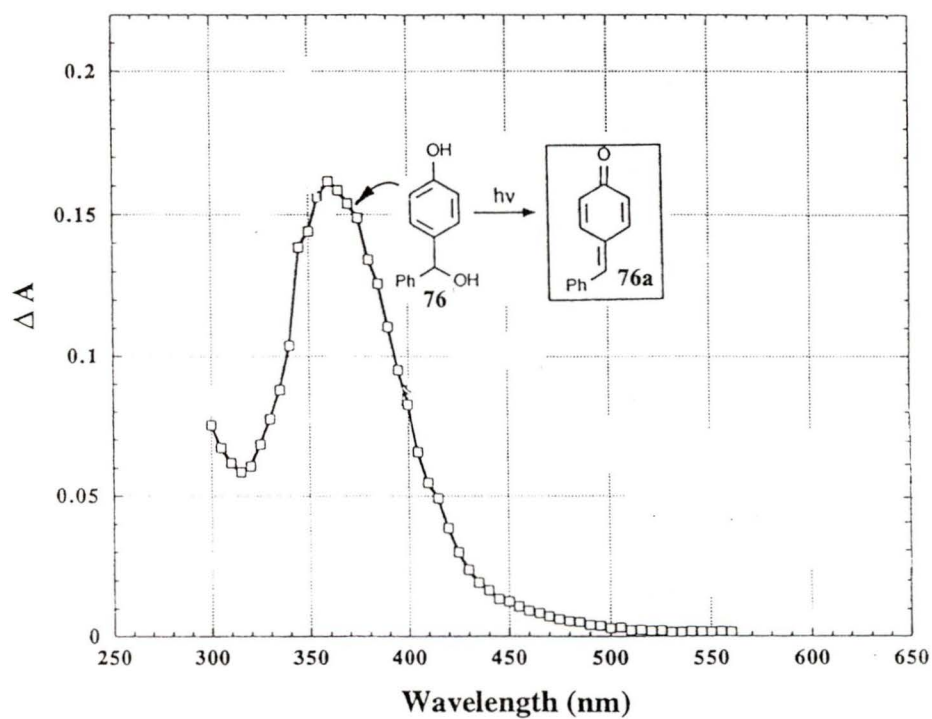
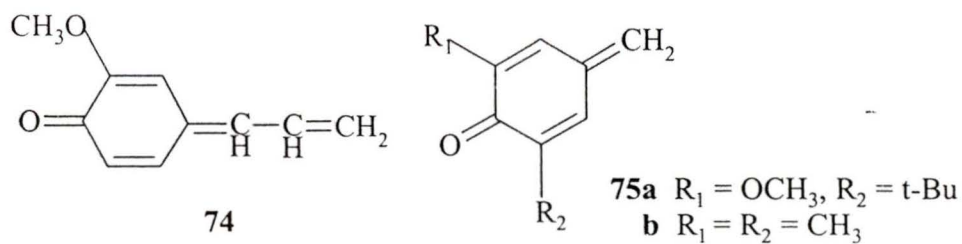
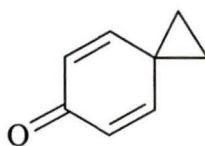


Figure 2.7 Spectrum observed on LFP of hydroxybenzyl alcohol **76** in 1:1 $\text{H}_2\text{O}-\text{CH}_3\text{CN}$ (taken from reference 79).

Moreover, the absorption at 330 nm is unlikely to be spiroketone **66**. Winstein and Baird⁷⁸ reported that spiro[2,5]octa-1,4-diene-3-one (**77**) has absorption maxima at 261 nm in ether, 271 nm in *t*-butyl alcohol, 274 nm in methanol, and 282 nm in water. Since **66** has a very similar structure to **77**, its UV absorption in 1:1 H₂O-CH₃CN should be around this region, i.e., below 300 nm.



77

Examination of the plot of transient absorption intensity (ΔA) at 330 nm for **58a** vs pH in 1:1 H₂O-CH₃CN also strongly indicates the involvement of an ESIRaPT process (Figure 2.8). Significant permanent bleaching of the ground state phenolate was observed above pH 10 making ΔA measurements problematic above this pH. This is presumably due to irreversible photoionization of the phenolate ion which is only significant under laser photolysis and not in product studies where low intensity lamps were used. The sigmoid behavior in the plot in the pH 8-10 region is due to deprotonation of photogenerated **67a** (via ESIPPT) to form **70** which has a larger extinction coefficient, with an estimated $pK_a \approx 9-10$, which is fully consistent with enolic protons of this kind. Moreover, the rapid increase in ΔA in the pH 8-10 region indicates that the phenol and not the phenolate is responsible for generation of *p*-QM **67a** and its conjugate base, enolate/phenolate **70**. This is consistent with an ESIRaPT mechanism for initial formation

of *p*-QM and subsequently its conjugate base, by deprotonation. This mechanism is presumably operative throughout the plateau region (pH 4-9) observed in these plots. That the plot of ΔA vs pH is qualitatively similar (in the pH4-9 region) to that observed for Φ_p vs pH (Figure 2.2) strongly support the notion that the species responsible for the laser transient at 330 nm is involved in the mechanism of reaction.

The intensity of transient signals observed for **58a** increases on increasing the acidity, beginning at pH 2 as shown by Figure 2.8. The decays of these transients at low pH are single exponential with $k_d \approx 10^7 \text{ s}^{-1}$, consistent with a single and more reactive species than the proposed *p*-QMs **67a** and **70**, observed at high pH. This new species at

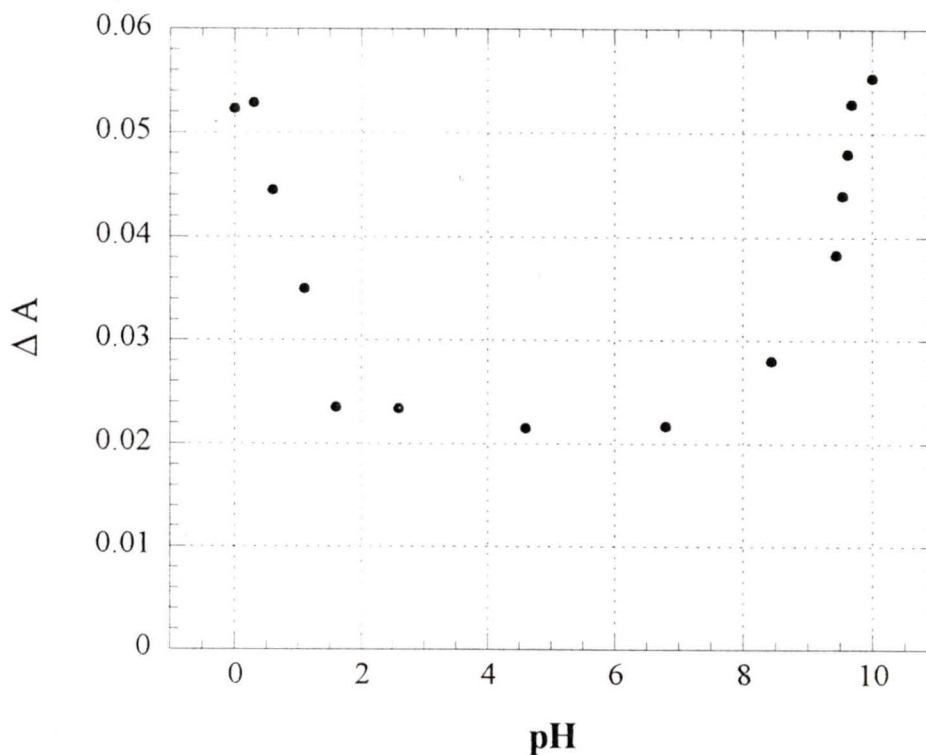
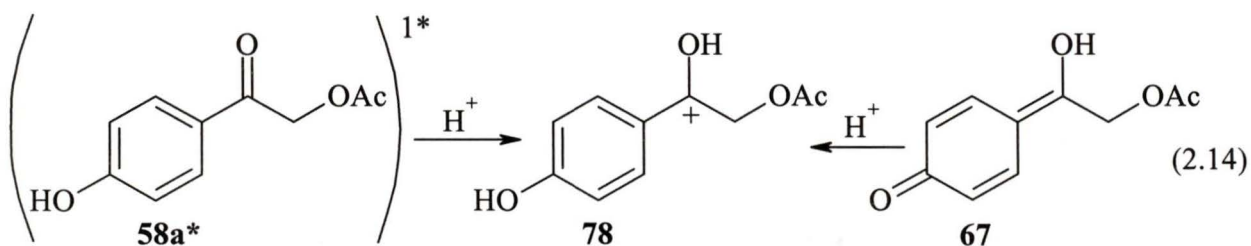


Figure 2.8 ΔA at 330 nm vs pH observed on LFP of **58a** in 1:1 $\text{H}_2\text{O}-\text{CH}_3\text{CN}$

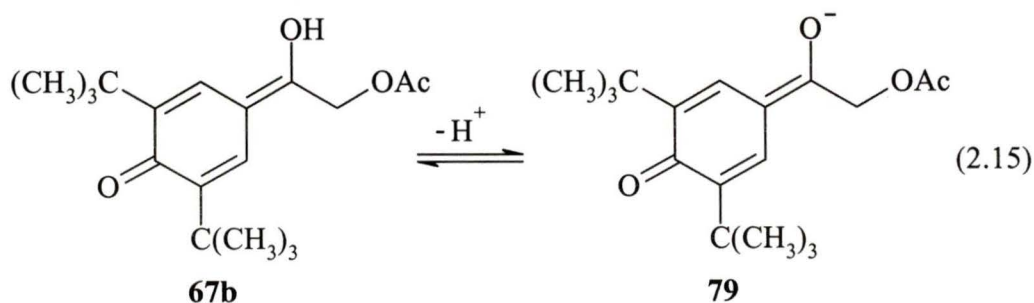
low pH is assigned to carbocation **78**. Similar benzylic carbocations have been photogenerated by McClelland and coworkers⁸⁰ who showed that they have absorption maxima at $\sim 320\text{-}360\text{ nm}$ with $k_d \approx 10^7\text{ s}^{-1}$ (in water). Two possible pathways are envisioned to account for its formation: (i) protonation of singlet excited **58a*** and (ii) protonation of *p*-QM **67a** (eq. 2.14)



In order to verify how carbocation **78** was produced, LFP studies on **60**, the *p*-methoxy analog of **58a**, were taken under oxygen at pHs from 0 to 7 in 1:1 $\text{H}_2\text{O-CH}_3\text{CN}$. No transient was observed between 300 nm and 400 nm for any of these samples thereby ruling out pathway (i) above. Therefore, the most likely pathway for formation of carbocation **78** is protonation of the carbonyl oxygen of the photogenerated *p*-QM **67a**. This is not unreasonable as the carboxyl oxygen of this *p*-QM is expected to be sufficiently basic for protonation at low pH.

2.5.2 Di-*tert*-Butyl-*p*-Hydroxyphenacyl Acetate (**59a**) and *p*-Hydroxyacetophenone (**69**)

LFP of **59a** was also performed for comparison with of **58a**. Results showed that **59a** behaved similarly under the same conditions. The λ_{\max} for excited triplet state of **59a** is at 380 nm. A new transient at 360 nm was observed for **59a** in 1:1 H₂O-CH₃CN besides the 380 nm transient, and it was also unaffected by O₂. Decay traces at 360 nm are best fitted to the sum of two single exponential decays, the major component with $k_d = 5.9 \times 10^6 \text{ s}^{-1}$ and the minor component with $k_d = 2.8 \times 10^5 \text{ s}^{-1}$. Kinetic studies at other pHs revealed that these two species are related by a prototropic equilibrium, just like that for **58a**. Therefore, the shorter-lived species is assigned to *p*-QM **67b**, and the longer-lived species to its conjugate base, enolate /phenolate **79** (eq. 2.15). Further confirmation comes from a UV absorption of authentic **79** (generated from **59a** in high pH) which shows a $\lambda_{\max} = 360 \text{ nm}$.

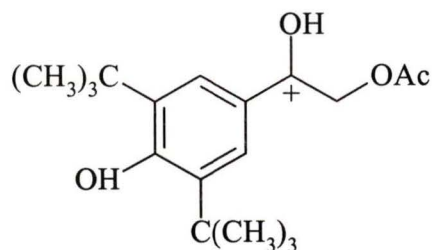


A plot of transient absorption intensity (ΔA) at 360 nm for **59a** vs pH (Figure 2.9) is similar to that for **58a**. Significant permanent bleaching was observed on excitation of the phenolate **79** above pH 10. Transient signal increases sharply between pHs 8 and 10 because of the formation of more and more **79** from the deprotonation of **67b** (eq. 2.15).

Therefore it is the phenol that is responsible for the generation of *p*-QM **67b** and its conjugate base **79**, and for the formation of photoproduct **61**. The intensity of the 360 nm transient is weaker compared to that of the 330 nm transient from **58a** because of its lower extinction coefficient.

All of the above results indicate that a parallel mechanism (ESIrPT) is operative for the di-*tert*-butyl compound. The 30 nm red shift observed for the corresponding *p*-QM as well as 20 nm red shift for its triplet state are consistent with the presence of two electron donating substituents (*tert*-butyl groups) on the molecule.

As was the case observed for **58a**, the intensity of transient signals observed for **59a** increases on increasing the acidity of the solution below pH 1. The decay of the transient at 360 nm at low pH is single exponential with $k_d \approx 10^7 \text{ s}^{-1}$. This is due to the formation of carbocation **80** which should also come from protonation of the photogenerated *p*-QM **67b**. The pH onset for this pathway is apparently earlier for **67a** than for **67b**, consistent with a kinetically more basic oxygen center for *p*-QM **67a**, since the corresponding carbonyl oxygen of the di-*tert*-butyl derivative **67b** would be much more sterically hindered.

**80**

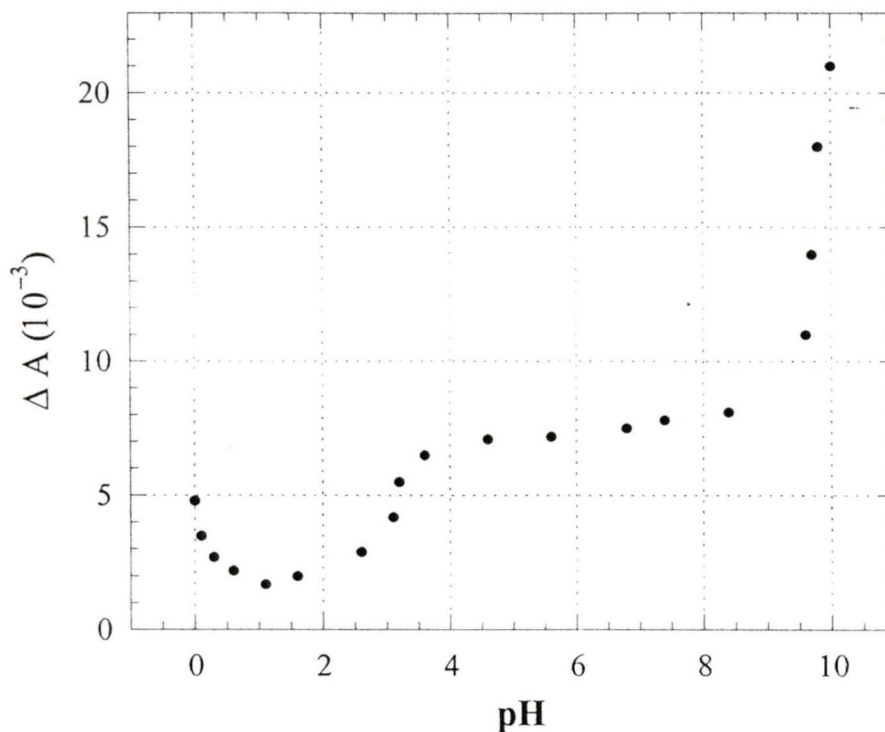
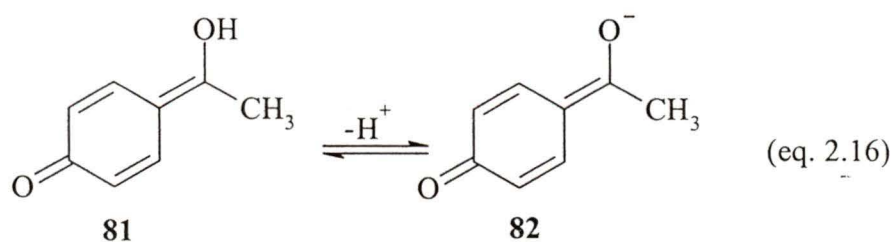


Figure 2.9 ΔA at 360 nm vs pH observed on LFP of **59a** in 1:1 H₂O-CH₃CN.

LFP studies of *p*-hydroxyacetophenone (**69**) gave similar results. The UV absorption of its excited triplet state is at 360 nm. New absorption at 340 nm in 1:1 H₂O-CH₃CN is due to *p*-QM **81** ($k_d \approx 6.4 \times 10^6 \text{ M}^{-1}\text{s}^{-1}$) and its conjugate base **82** ($k_d \approx 3.3 \times 10^5 \text{ M}^{-1}\text{s}^{-1}$), and these two species are also related by prototropic equilibrium (eq. 2.16). The LFP behaviour of **69** in 1:1 H₂O-CH₃CN at different pHs is similar to that observed for **58a** and **59a**, and is shown in Figure 2.10. Here, the onset of the QM protonation pathway (at low pH) is even earlier than observed for **67a** and **67b**. Since **81** lacks an electron withdrawing acetate group at the α -carbon, the carboxyl oxygen of **81** should be the most basic of the series **67a**, **67b**, and **81**.



All these results on *p*-hydroxyphenacyl derivatives, together with the studies of Itoh and coworkers⁶² indicate that ESIRA^{PT} mediated by solvent is a general behavior for *p*-hydroxyaryl ketones. Additional work is required to further substantiate this finding and this is in process by other students in the Wan group.

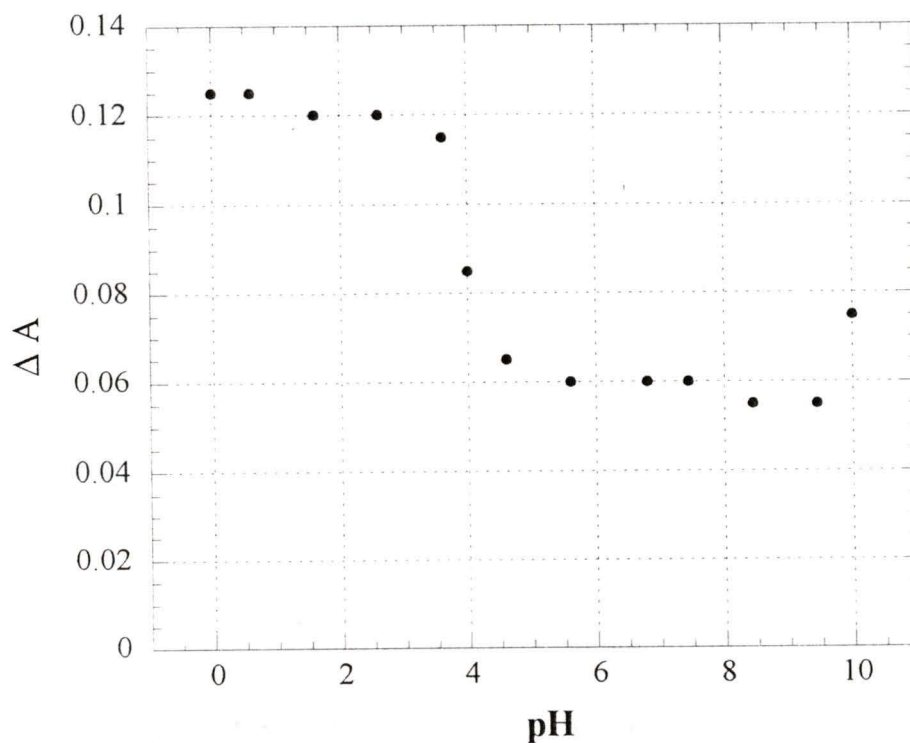


Figure 2.10 ΔA at 340 nm vs pH observed on LFP of **69** in 1:1 H₂O-CH₃CN.

2.6 Mechanism

The results presented above are consistent with a mechanism of reaction of *p*-hydroxyphenacyl esters involving ESIRA_{PT} as a necessary and primary step. The proposed mechanism is shown in Scheme 2.4 for the parent substrate **58a**. Here, the primary photochemical step is water mediated excited state proton transfer (ESIRA_{PT}) from which *p*-QM **67a** is produced. The responsible excited state is singlet (S_1), since triplet quenchers, such as sodium sorbate, trans-piperylene, 1,3-cyclohexadiene, as well as oxygen were unable to reduce the product yield. LFP studies also showed that quenching of triplet did not cause a reduction of *p*-QM signal. The quantum yield for this ESIRA_{PT} process is unknown, but it probably is quite high as it competes well with intersystem crossing which is known to be very fast for aromatic ketones. The fact that the di-*tert*-butyl derivatives reacted with very similar quantum yields as the parent *p*-hydroxyphenacyl system imply that the ESIRA_{PT} process is unhampered by the steric bulk of the two *tert*-butyl groups. Literature precedent for the above type of long-range ESIRA_{PT} are available in Itoh's studies⁶² as well as Fischer and Wan's recently reported examples involving hydroxystyrenes.^{70a}

Deprotonation of the enol proton of **67a** gives rise to the phenolate/enolate **70** which is unreactive with respect to forming **66** and hence product **31** (as confirmed by thermal control experiments). In addition, it is also known that photoexcitation of **70** does not lead to any reaction (Figure 2.2). It appears therefore that formation of spiroketone **66** requires a concerted Favorskii-type rearrangement with loss of neutral acetic acid. The

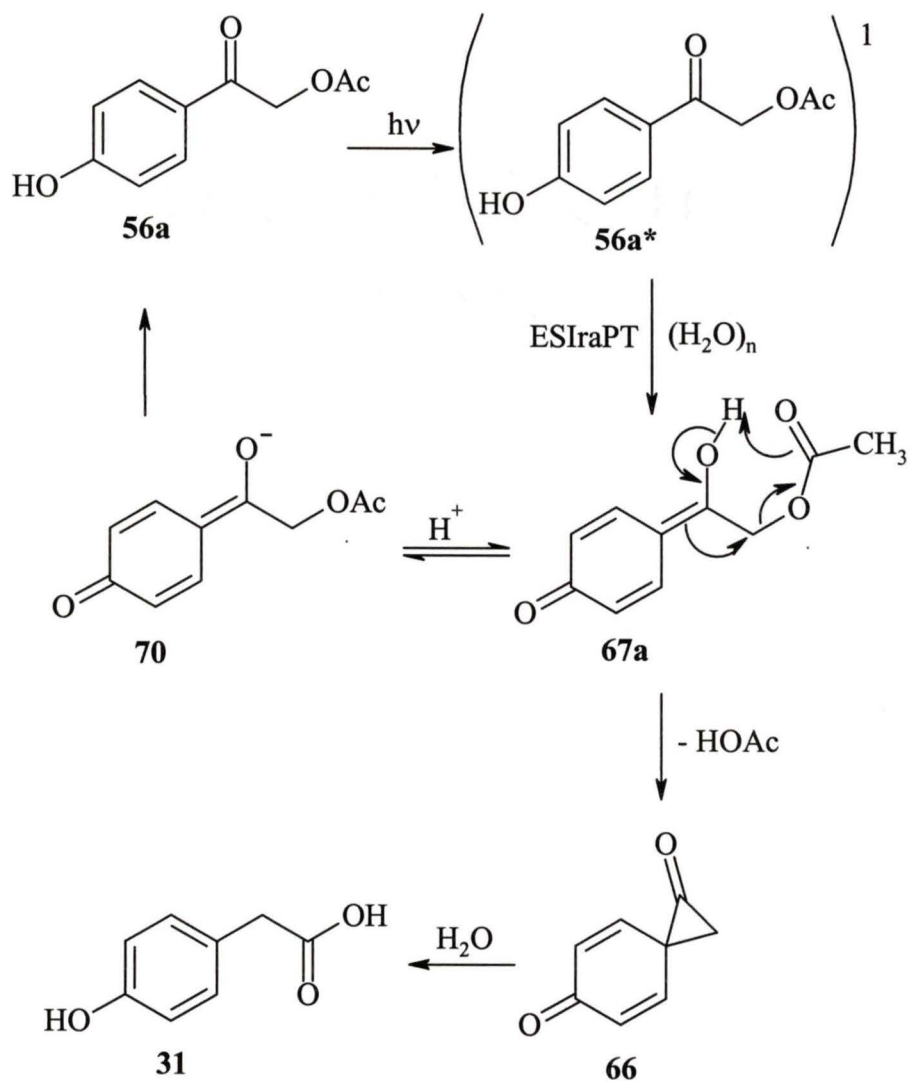
lack of reactivity of **70** is probably due to the fact that the negative charge resides mostly on the phenolic oxygen thereby reducing the propensity for an analogous Favorskii rearrangement. The product determining step **67a** to **66** determines the rate in which acetic acid is released. The upper limit of this rate is governed by the observed rate of decay of **67a** ($k_d = 6.3 \times 10^6 \text{ s}^{-1}$). This is considerably faster than the unsubstituted phenacyl system reported by Bannerjee and Falvey⁶⁹ ($k_{\text{release}} \approx 10^3 \text{ s}^{-1}$) which employs photoinduced electron transfer for activation.

Based on studies by Winstein and Baird⁸⁰ on spiro[2,5]octa-1,4-diene-3-one (**77**), it is inferred that the UV absorption of spiroketone **66** should be below 300 nm. Therefore, the existence of **66** as an intermediate in the mechanism could not be verified using the LFP (technical difficulties in absorption measurements below 300 nm). However, it would be anticipated that **66** would be short-lived, undergoing fast ring opening by H₂O to give the aromatic phenol product **31**.

2.7 Summary

Photochemically-removable protecting groups have been the focus of attention of many biochemists, physiologists, and chemists for several decades as discussed in Chapter 1. The *p*-hydroxyphenacyl group is a new and promising system because it fulfills several of the criteria advanced by Lester¹⁴, especially the requirements of high efficiency, benign photoproduct, good solubility in aqueous solution, and absence of chiral centers. All of these desirable features make the *p*-hydroxyphenacyl group a

suitable candidate for applications in mechanistic biochemistry, physiology, and related fields. Therefore, research into its mechanism of photoreaction is very important as it may allow for improvements in design. Our results show that the primary photochemical step from the singlet excited state is intramolecular proton transfer from the phenolic proton to the carbonyl oxygen of the distal ketone, to generate the corresponding *p*-QM phototautomer, which subsequently expels the ester group with concerted rearrangement to a spiroketone intermediate, subsequently leading to the final observed product, *p*-hydroxyphenylacetic acid. Our research, together with the studies of Itoh and coworkers⁶² imply that ESIRA^{PT} mediated by solvent may be a general process for all aromatic hydroxy ketones. Continuing studies are in progress to further verify this possibility.



Scheme 2.4

Chapter 3

Experimental

3.1 General Instrumentation

^1H NMR spectra were recorded on a Bruker WM-300 (300 MHz) instrument in $(\text{CD}_3)_2\text{CO}$ or $\text{D}_2\text{O}-\text{CD}_3\text{CN}$. UV-Vis spectra were obtained on a Varian Cary 5 spectrophotometer. Low resolution mass spectra (MS) were taken on a Finnigan 3300 (CI) instrument via chemical ionization (CI) with methane while high resolution MS (HRMS) were recorded on a Kratos Concept H (EI) instrument. IR spectra were recorded on a Bruker IFS25 FTIR spectrometer using a KBr pellet. Melting points were determined on a Koeffler hot stage microscope. Measurements of pHs were carried out on a Corning pH meter 140. Preparative thin layer chromatography (TLC) was carried out on 20 cm \times 20 cm silica gel GF Uniplates (Analtech).

3.2 Common Laboratory Reagents

Methylene Chloride was distilled before use. Anhydrous THF used in triplet quenching experiments was obtained by distillation over potassium metal. Anhydrous CH_3CN was obtained by distillation of HPLC grade CH_3CN over CaH_2 and used immediately. Anhydrous CH_3OH used in quantum yield measurements was dried over molecular sieves. Other reagents were purchased from Aldrich Chemical Co. and employed as received without further purification. Deuterated acetone $(\text{CD}_3)_2\text{CO}$ (99.9%) used for ^1H NMR spectroscopy was purchased from Isotec Inc., and CD_3CN (99.8%) used

for product studies (and NMR) was purchased from Isotec Inc.. D₂O (99.9%) used for product studies, solvent isotope effect studies, NMR spectroscopy, and LFP was purchased from Cambridge Isotope Laboratory. Aqueous solutions of various pHs used in preparative experiments were made by diluting aq. H₂SO₄ or aq. NaOH to the desired pH, and used immediately.

3.3 Materials

Triplet quenchers sodium sorbate, trans-piperylene, and 1,3-cyclohexadiene were purchased from Aldrich Chemical Co. and used as received. All of the *p*-hydroxyphenacyl esters and derivatives were synthesized by Dr. J. E. T. Corrie and coworkers at the National Institute for Medical Research, London, U. K., and used as received. The details of their synthesis and spectroscopic characterization will be reported in a forthcoming paper.

3.4 Product Studies

Product studies were carried out using a Rayonet RPR 100 photochemical reactor equipped with 300 nm lamps.

General Procedure for Preparative Runs

A solution was made by dissolving the compound (20 - 100 mg) in the appropriate solvent (40-100 ml), and then was poured into a 100 ml quartz tube. The solution was cooled by a cold finger (with tap water) and purged with a stream of argon via a stainless

steel syringe needle for approximately 15 minutes before and continuously during irradiation. Photolysis times ranged from 3 to 30 min, depending on the number of lamps used, the conversion desired, the efficiency of the reaction, and the size of the sample.

General Procedure for Analytical Runs

A solution was made by dissolving ~ 3 mg substrate in ~ 2 mL 1:1 D₂O-CD₃CN. The solution was then purged by argon for 10 minutes, and transferred to an NMR tube. This NMR tube was subsequently placed in the middle of a Rayonet RPR 100 photochemical reactor and irradiated. An internal fan in the reactor was used to cool the sample during the photolysis. Photolysis times ranged from 1 to 10 min, depending on the number of lamps used, the conversion desired, the efficiency of the reaction, and the size of the sample. ¹H NMR was taken directly after the photolysis without further treatment.

General Work-up Procedure for Preparatory Photolysis Runs

After photolysis, the solution was first acidified with 10% HCl to pH 2, and then saturated with sodium chloride followed by extraction with CH₂Cl₂. The combined organic extracts were dried with magnesium sulfate and the solvent evaporated on the rotary evaporator. The same procedure was followed for the control experiments, except the argon purge and the irradiation step were omitted. ¹H NMR was used to calculate percentage conversion. Preparative TLC was used to isolate products.

3.4.1 Photolysis of *p*-Hydroxyphenacyl Alcohol 56

In neat CH₃CN

Using the general procedure for preparative runs, solutions made by dissolving 20 mg of compound in 40 mL neat CH₃CN were irradiated by 16 lamps for 30 minutes. ¹H NMR ((CD₃)₂CO) showed that only starting material **56** was present after photolysis.

In 1:1 H₂O-CH₃CN

Using the general procedure for preparative runs, solutions with 20 mg of sample dissolved in 40 mL 1:1 H₂O-CH₃CN were irradiated by 16 lamps for 30 minutes. The conversion to the photoproduct **31** was 20% measured by ¹H NMR. The conversion was taken to 80% when photolyzed for 60 minutes. Preparative TLC with 10:1 CH₂Cl₂-EtOAc was used to isolate **31**. ¹H NMR ((CD₃)₂CO): δ 3.48 (2H, s), 5.5 (2H, broad, exchangeable with D₂O), 6.76 (2H, d, *J* = 9 Hz), 7.10 (2H, d, *J* = 9 Hz); mp 148-150 °C (lit.⁸² 149-151 °C); MS (CI) *m/z* 153 (M⁺+1). The ¹H NMR was identical to that of an authentic sample.

3.4.2 Photolysis of Di-*tert*-Butyl *p*-Hydroxyphenacyl alcohol **57****In neat CH₃CN**

Using the general procedure for preparative runs, solutions of 30 mg of sample dissolved in 40 mL CH₃CN were irradiated by 16 lamps for 30 minutes. ¹H NMR ((CD₃)₂CO) showed that only the starting material **57** was present after photolysis.

In 1:1 H₂O-CH₃CN

Using the general procedure for preparative runs, solutions of 30 mg of sample

dissolved in 40 mL 1:1 H₂O-CH₃CN were irradiated by 16 lamps for 30 minutes. Conversion to the photoproduct **61** was 16% as calculated by ¹H NMR. Preparative TLC with 10:1 CH₂Cl₂-EtOAc was used to isolate the photoproduct **61**. ¹H NMR ((CD₃)₂CO): δ 1.40 (18H, s), 3.48 (2H, s), 6.0 (1H, s, exchangeable with D₂O), 7.10 (2H, s). Carboxylic acid proton exchanged with residual H₂O and therefore not identified on the spectrum. mp 151-153 °C (lit.⁸³ 154-156 °C); IR (cm⁻¹) 3630, 2958, 1698, 1432, 1309, 1233; MS (CI) m/z 265 (M⁺+1); HRMS (EI), Calcd for C₁₆H₂₄O₃: 264.1725. Found: 264.1726.

3.4.3 Photolysis of *p*-Hydroxyphenacyl Acetate (**58a**)

In neat CH₃CN

Using the general procedure for preparative runs, solutions of 20 mg of sample dissolved in 40 mL CH₃CN were irradiated by 8 lamps for 3 minutes. ¹H NMR ((CD₃)₂CO) showed the presence of only the starting material **58a** after photolysis.

In 1:1 H₂O-CH₃CN

Substrate **58a** (20 mg) was dissolved in 40 ml 1:1 H₂O-CH₃CN, and the solution was irradiated for 3 min by 8 lamps using the general procedure for preparative runs. After work up and evaporation of the solvent, the photolysate was checked by ¹H NMR which showed the conversion to photoproduct **31** was 40%. Separation by preparative TLC (silica, 10:1 CH₂Cl₂-EtOAc) gave the pure photoproduct *p*-hydroxyphenyl acetic acid (**31**). The conversion was 90-95% when sample was photolyzed for 10 minutes.

In Neat CH₃OH

Using the general procedure for preparative runs, solutions of substrate **58a** (20 mg) dissolved in 40 mL neat CH₃OH were irradiated by 8 lamps for 15 min. Conversion to the photoproduct **65** was 40%, which was separated by preparative TLC (silica, 2:1 hexanes-EtOAc). ¹H NMR ((CD₃)₂CO): δ 3.48 (2H, s), 3.61 (3H, s), 6.0 (1H, s, exchangeable with D₂O), 6.76 (2H, d, *J* = 9 Hz), 7.10 (2H, d, *J* = 9 Hz). This spectrum is identical to that reported for the authentic sample.⁸² mp 55-56 °C (lit.⁸² 59 °C); MS (CI) *m/z* 167 (M⁺+1).

In 1:1 CH₃OH-CH₃CN

Using the general procedure for preparative runs, a solution of substrate **58a** (20 mg) dissolved in 40 mL 1:1 CH₃OH-CH₃CN was irradiated by 8 lamps for 30 min. Conversion to the photoproduct **65** was 40%.

3.4.4 Photolysis of *p*-Hydroxyphenacyl Esters **58b-d**

Using the general procedure of analytical runs, solutions of 2.5 mg of substrate pivalate ester **58b** dissolved in 1.6 mL 1:1 D₂O-CD₃CN were irradiated by 16 bulbs for 10 minutes. Conversion to photoproduct **31** was ≈ 95%. The ¹H NMR of photolysate is made up of 1:1 mixture of **31** and pivalic acid (δ 1.52, D₂O-CD₃CN). The latter was confirmed by addition of an authentic sample of pivalic acid, which results in enhancement of the δ 1.52 peak.

Substrate **58c** was studied in the same way as that for **58b**. The conversion to the

photoproduct **31** was $\approx 95\%$. The ^1H NMR ($\text{D}_2\text{O}-\text{CD}_3\text{CN}$) of photolysate is made up of 1:1 mixture of **31** and phenylacetic acid which has peaks at δ 3.95 (2H, s), 7.60 (5H, m). The carboxylic acid proton exchanged with residual H_2O and therefore not identified on the spectrum. Addition of an authentic sample of phenylacetic acid results in enhancement of all of the peaks quoted above for phenylacetic acid.

Substrate **58d** was also studied in the same way as that for **58b** and **58c**. The conversion to the photoproduct **31** was $\approx 95\%$. The ^1H NMR of photolysate is made up of 1:1 mixture of **31** and benzilic acid (δ 7.78, 10H, m, $\text{D}_2\text{O}-\text{CD}_3\text{CN}$). Due to presence of residual H_2O , the OH protons of benzilic acid were not identifiable. The latter was confirmed by addition of an authentic sample, which resulted in enhancement of the δ 7.78 peak.

3.4.5 Photolysis of Di-*tert*-Butyl *p*-Hydroxyphenacyl Acetate (**59a**) in 1:1 $\text{H}_2\text{O}-\text{CH}_3\text{CN}$

Using the general procedure for preparative runs, solutions of compound **59a** (30 mg) dissolved in 40 mL 1:1 $\text{H}_2\text{O}-\text{CH}_3\text{CN}$ were photolyzed by 8 lamps for 3 min. Conversion to pure photoproduct **61** was 36%. Photolysis for 10 minutes gave photoproduct **61** with $\approx 95\%$ conversion. Pure **61** was obtained by preparative TLC (silica, 10:1 $\text{CH}_2\text{Cl}_2-\text{EtOAc}$). ^1H NMR ($(\text{CD}_3)_2\text{CO}$): δ 1.40 (18H, s), 3.48 (2H, s), 6.0 (1H, s, exchangeable with D_2O), 7.10 (2H, s). Carboxylic acid proton exchanged with residual H_2O and therefore not identified on the spectrum.

3.4.6 Photolysis of Di-*tert*-Butyl *p*-Hydroxyphenacyl Esters **59b-d**

Using the general procedure of preparative runs, solutions of 100 mg of substrate **58b** dissolved in 100 mL 1:1 H₂O-CH₃CN were irradiated by 16 bulbs for 10 minutes. Conversion to photoproduct **61** was \approx 95%. Pure **61** was obtained by extraction of the photolysate with 1M NaOH. Substrates **59c** and **59d** were also studied under the same conditions as that for **59b**, and the conversions to photoproduct **61** were 90-95% for both of them. In all cases, the corresponding released carboxylic acid was also observed in a 1:1 ratio with **61**.

3.5 Quantum Yield Measurements

Absolute product quantum yields (Φ_p) were measured on an optical bench utilizing an Oriel 200 W Hg-arc lamp in conjunction with an Applied Physics monochromator set for 254 nm with 4 nm slits. A chemical actinometer was used to measure the light intensity⁶⁶: 3 mL of 0.006 M K₃Fe(C₂O₄)₃ in 0.05 M H₂SO₄ was irradiated for 5 minutes (Fe³⁺ is reduced to Fe²⁺) after which 1 mL was diluted to 10 mL with 2 mL of 0.2% by weight of 1,10-phenanthroline in water, 0.5 mL buffer (0.6 M NaOAc·3H₂O in 0.2 M H₂SO₄) and water. The mixture was left for one hour in the dark to allow complete reaction of the Fe²⁺ with 1,10-phenanthroline to form a complex whose absorption can be subsequently measured. The same procedure was followed for the blank, except the irradiation step was omitted. The absorption difference (ΔA) at 510 nm between the above solution and that of the blank reflects the amount of Fe²⁺ produced.

$$I = (\Delta A V_2 V_3 \times 10^{-3}) / (\epsilon \phi_\lambda t V_1) \quad (3.1)$$

The light intensity (I) in einsteins/min can be calculated (1 einstein = 1 mole of photons) using eq. 3.1. Here V_1 , V_2 and V_3 are the volume of the actinometer solution diluted (1 mL), the volume of the irradiated actinometer solution (3 mL), and the final volume of the diluted solution (10 mL), respectively, t is the irradiation time in minutes, ϵ is the molar extinction coefficient of the ferrous phenanthroline complex at 510 nm ($\sim 1.11 \times 10^4 \text{ cm}^{-1}\text{M}^{-1}$), and ϕ_λ is the quantum yield of ferrous production at λ_{ex} (1.25 at 254 nm).

Solutions of **58a** and **59a** ($\sim 0.1 \text{ mM}$) in $\text{H}_2\text{O}-\text{CH}_3\text{CN}$ were irradiated for 5 minutes in UV-Vis cuvettes (conversion $\sim 15\%$). Both the standard and sample solutions were purged with argon 10 minutes before and during irradiation in order to eliminate oxygen and ensure a mixed solution. Φ_p can be calculated from eq. 3.2 where ΔA_λ (at a

$$\Phi_p = \Delta A_\lambda / (\epsilon_\lambda I t \times 10^3) \quad (3.2)$$

specific wavelength where only starting material and not the product absorbs) is the change in absorption upon irradiation (corresponds to loss of starting material forming the product), ϵ_λ is the molar extinction coefficient ($\sim 15,700 \text{ M}^{-1}\text{cm}^{-1}$ for **58a** at 279 nm, and $\sim 8,400 \text{ M}^{-1}\text{cm}^{-1}$ for **59a** at 284nm), and t is the irradiation time in minutes. Here I is the light intensity calculated above, except converted to the units einsteins/min. The corresponding photoproduct quantum yield of **58a** and **59a** in 1:1 $\text{H}_2\text{O}-\text{CH}_3\text{CN}$ at pH 7

was (0.41 ± 0.04) and (0.36 ± 0.04), respectively.

To determine the molar absorptivity (ϵ) of **58a** at 279 nm and **59a** at 284 nm, respectively, various amounts of stock solution of sample in 1:1 H₂O-CH₃CN were diluted with 1:1 H₂O-CH₃CN. Concentrations ranged from $0.5\text{-}1.2 \times 10^{-4}$ M with an absorption range of 0.7 - 1.9 for **58a**, and 0.4 - 1.0 for **59a**, measured with a Varian Cary 5 spectrophotometer. The ϵ was calculated according to the Beer-Lambert law ($A = \epsilon bc$), where the pathlength of the cuvette (b) was 1 cm. The values for ϵ are $15,700 \text{ cm}^{-1}\text{M}^{-1}$ and $8,400 \text{ cm}^{-1}\text{M}^{-1}$ for **58a** and **59a**, respectively.

Product quantum yields (Φ_p) at other pHs for **58b-d** and **59b-d** were determined by a relative method, using Φ_p of **58a** and **59a** at pH 7 as standard, respectively. All of these compounds were irradiated under the same conditions (same number of moles and irradiation time) and the relative amounts were determined by ¹H NMR where the conversion to product was kept below 40%.

In studying the effect of H₂O concentration on conversion to photoproduct **31**, solutions of 0.1 mM **58a** were prepared in H₂O-CH₃CN with varied H₂O concentrations (0 - 100%, v/v). Conversion was measured by UV-Vis. The irradiation time was 1 minute for all of these samples. The change of absorption was monitored at 279 nm, since any small amount of photoproduct **31** formed would not absorb significantly at this wavelength. Similarly, solutions of 0.1 mM **58a** were prepared in CH₃OH-CH₃CN with varied CH₃OH concentrations (0 - 100%), and the absorbance loss was monitored at 279 nm with irradiation for 1 minutes.

3.6 Solvent Isotope Effect

Solutions of 0.1 mM **58a** were prepared in 1:1 H₂O-CH₃CN and 1:1 D₂O-CH₃CN, respectively. The change of absorption was monitored for both at 279 nm with irradiation for 1 minute. The conversion to **31** in 1:1 H₂O-CH₃CN was almost the same as that to deuterated **31** in 1:1 D₂O-CH₃CN ($\Delta A(\text{H}_2\text{O}) / \Delta A(\text{D}_2\text{O}) = 0.95 \pm 0.05$).

Using the general procedure for preparative runs, solutions of 20 mg **58a** dissolved in 40 mL 1:1 H₂O-CH₃CN and 1:1 D₂O-CH₃CN, respectively, were irradiated at 300 nm by 8 lamps for 3 minutes. Quantum yields were measured by ¹H NMR ((CD₃)₂CO) which showed no solvent isotope effect ($\Phi(\text{H}_2\text{O}) / \Phi(\text{D}_2\text{O}) = 0.95 \pm 0.05$).

3.7 Triplet Quenching Experiments

Using the general procedure for preparative runs, solutions of 20 mg of **58a** dissolved in suitable solvent were irradiated by 8 lamps for 3 minutes with triplet quencher in solutions. For sodium sorbate or trans - piperylene 1:1 H₂O-CH₃CN was used, and 1:1 H₂O-THF was employed when the triplet quencher was 1,3-cyclohexadiene because of its poor solubility in 1:1 H₂O-CH₃CN. The concentration used for all these triplet quenchers was 0.01 M - 0.1 M. Conversions to **31** were measured by ¹H NMR and compared to runs without triplet quencher. Only a marginal decrease in conversion was observed even with 0.1 M triplet quencher in solution (i.e., from 40% to 35% for sorbate acid, from 40% to 36% for trans - piperylene, and 40% to 32% for 1,3-cyclohexadiene). The marginal drop in conversion yield can be attributed to the slight cloudiness of these

solutions at such high quencher concentrations.

3.8 Laser Flash Photolysis (LFP)

Nanosecond laser flash photolysis (LFP) experiments were carried out at the University of Victoria LFP Facility at $20 \pm 2^\circ\text{C}$.⁸⁵ A Spectra-Physics excimer laser (308 nm, ~ 10 ns, < 30 mJ/pulse) was used as excitation source, which is directly aligned on to the sample holder. The laser pulse energies are typically attenuated to less than 30 mJ/pulse by adjusting the high voltage for the flash lamp to avoid multiple photon process. The analysing beam employed consists of a pulsed 150 W xenon lamp (Oriel housing Model 66057, PTI power supply Model LPS-220) 90° angled with the excitation source (laser). The output of the Xe lamp is increased significantly for 4 ms in a wavelength-dependent manner by using a custom-made pulser. Light intensities at fixed wavelength are detected using a photomultiplier (PMT, Hamamatsu R446, five dynodes)/monochromator (CVI Digikrom 240) system. The high voltage for the PMT tube is set by a custom built programmable power supply interfaced to the computer. Signals from the PMT are fed into a base line compensation circuit that incorporates a sample and hold amplifier with digital memory based on a published circuit. This unit offsets the background intensity of the Xe lamp. On receiving a trigger pulse, it holds the value of the background intensity (V_0) constant and provides a dc output proportional to its magnitude. The remained transient signal (V_t) can then be measured with high precision using a Tecktronix TDS 520 digital oscilloscope (50Ω input impedance for

transmission experiments). Spectrally resolved data are recorded with an intensified dual diode array system from Princeton Instruments (DIDA 700/RG, detector controller ST 116, high-voltage gating pulse generator PG200 and ISA spectrometer HR-320). The transient absorption signals were corrected for fluorescence from the sample or for slope in the base line when a total data collection time is equal or longer than 20 μ s, depending on the experimental conditions. The correction shot was performed after each signal shot, i.e., for fluorescence correction the lamp shutter remained closed, whereas for base line correction the laser shutter remained closed. The system is fully integrated to a Macintosh IIfx computer with a program written using Labview 3.1.1, which could transform the data collected (V_t) into absorbance values ($\Delta A = -\log(1 - \text{corrected } V_t/V_0)$).

Generally, a solution of $OD \leq 0.3$ at 308 nm was prepared by dilution from a stock solution, followed by 10-min prepurge of nitrogen or oxygen. Experiments for obtaining spectra were carried out in a flow system (7mm \times 7mm quartz cell) with continuous purge of oxygen or nitrogen, to ensure that a fresh solution was irradiated each time in order to avoid complications from long-lived intermediates and/or photoproducts. The flow rate was set from 2-3 for spectra recording and 5-8 for sample decays. Static cells were used for kinetic studies.

The absorption spectra of a transient were collected within four time windows, specified according to the signal decay trace obtained at the maximum absorption of the transient. Therefore, the determined ΔA at fixed wavelength was the average of the absorbance within each time frame, while the first trace has the shortest delay and the

forth one recorded after the longest delay among the four. When data collecting during one continuous period was not possible, i.e., laser system has to be turned off between experiments, one or two conditions were repeated in the second period under exactly same conditions, including the ground state absorption, flow rate etc.. Thus, the laser power difference could be compensated and a set of comparable results obtained.

Decay traces of the 330 nm transient from **58a** in 1:1 H₂O-CH₃CN at pH 7 showed that it is composed of two first order decays with $R = 0.997$, a major (~ 70%) component with $k_d = 6.3 \times 10^6 \text{ s}^{-1}$, and a minor (~ 30%) component with $k_d = 1.8 \times 10^5 \text{ s}^{-1}$ (Figure 3.1). Kinetic studies at other pHs showed that the proportion of the longer-lived species increased with increasing pH and that it was not observed below pH 6. Correspondingly, the proportion of the shorter-lived species decreased with increasing pH. Kaleidagraph was used to fit the decay traces, and summarized in Table 3.1.

Similar results were obtained when **59a** or **69** in 1:1 H₂O-CH₃CN was studied. Decay traces of the 360 nm transient from **59a**, and the 340 nm transient from **69** were also studied in the same way as that for 58a. All of these traces were analyzed using the Kaleidagraph fitting program and all of the kinetic data are summarized in Tables 3.2 and 3.3.

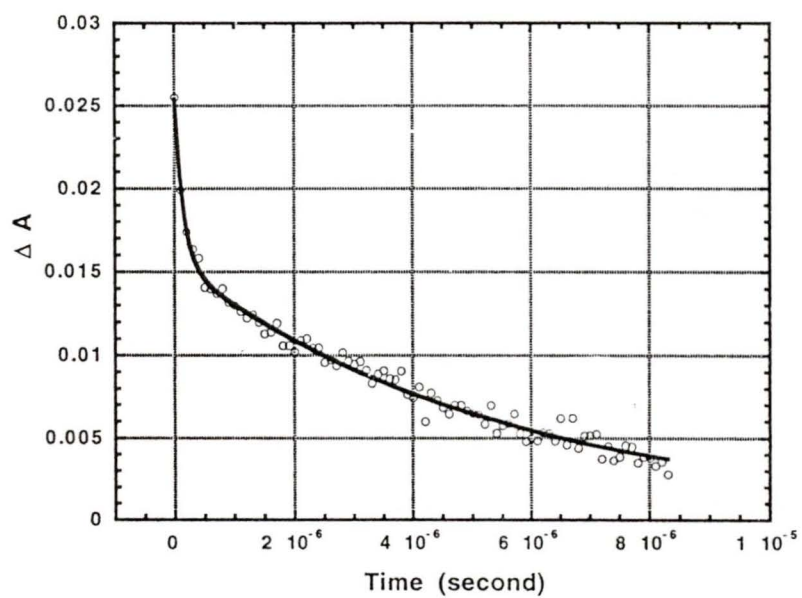


Figure 3.1 Decay trace of the 330 nm transient from **58a** in 1:1 H₂O-CH₃CN at pH 6.8 fitted to biexponential decay with R = 0.997.

Table 3.1 Data for the fitting of decay traces of the 330 nm transient obtained by LFP on **58a** in 1:1 H₂O-CH₃CN at various pHs.

pH	Longer-lived Species [k _d ^a (s ⁻¹) (proportion) ^c] ^d	Shorter-lived species [k _d ^a (s ⁻¹) (proportion) ^c] ^d	R ^b
0		1.16 × 10 ⁷ (100%)	
0.6		1.17 × 10 ⁷ (100%)	
1.6		1.12 × 10 ⁷ (100%)	
2.6		9.21 × 10 ⁶ (100%)	
4.6		4.93 × 10 ⁶ (100%)	
6.8	1.80 × 10 ⁵ (30%)	6.31 × 10 ⁶ (70%)	0.997
8.4	1.73 × 10 ⁵ (80%)	5.79 × 10 ⁶ (20%)	0.999
9.4	1.70 × 10 ⁵ (>95%)	6.49 × 10 ⁶ (< 5%)	0.999
9.7	2.42 × 10 ⁵ (100%)		0.993
above 10.0	significant bleaching of phenolate observed		

^a First order decay rate constant

^b Pearson's r (General curve fit)

^c Where there are two components, the proportion was calculated assuming identical extinction coefficient for the two species

^d Data from LFP has ±10% error

Table 3.2 Data for the fitting of decay traces of the 360 nm transient obtained by LFP on **59a** in 1:1 H₂O-CH₃CN at various pHs.

pH	Longer-lived Species [k _d ^a (s ⁻¹) (proportion) ^c] ^d	Shorter-lived species [k _d ^a (s ⁻¹) (proportion) ^c] ^d	R ^b
0		9.04 × 10 ⁶ (100%)	
0.6		1.03 × 10 ⁷ (100%)	
1.1		2.76 × 10 ⁶ (100%)	
2.6		2.57 × 10 ⁶ (100%)	
4.6	2.37 × 10 ⁵ (34%)	3.47 × 10 ⁶ (66%)	0.989
6.8	2.76 × 10 ⁵ (33%)	5.93 × 10 ⁶ (67%)	0.997
9.4	2.16 × 10 ⁵ (>95%)	5.49 × 10 ⁶ (< 5%)	0.960
above 10.0	significant bleaching of phenolate observed		

^a First order decay rate constant

^b Pearson's r (General curve fit)

^c Where there are two components, the proportion was calculated assuming identical extinction coefficient for the two species.

^d Data from LFP has ±10% error

Table 3.3 Data for the fitting of decay traces of the 340 nm transient obtained by LFP on **69** in 1:1 H₂O-CH₃CN at various pHs.

pH	Longer-lived Species [k _d ^a (s ⁻¹) (proportion) ^c]	Shorter-lived species [k _d ^a (s ⁻¹) (proportion) ^c]	R ^b
0		1.56 × 10 ⁷ (100%)	
0.6		1.68 × 10 ⁷ (100%)	
1.6		1.44 × 10 ⁷ (100%)	
2.6		1.24 × 10 ⁷ (100%)	
4.6		7.51 × 10 ⁶ (100%)	
6.8	3.25 × 10 ⁵ (34%)	6.42 × 10 ⁶ (66%)	0.999
7.4	3.98 × 10 ⁵ (34%)	5.02 × 10 ⁶ (66%)	0.998
9.4	3.68 × 10 ⁵ (60%)	6.49 × 10 ⁶ (40%)	0.999
above 10.0	significant bleaching of phenolate observed		

^a First order decay rate constant

^b Pearson's r (General curve fit)

^c Where there are two components, the proportion was calculated assuming identical extinction coefficient for the two species.

^d Data from LFP has ±10% error

References

1. (a) Pillai, V. N. R., *Organic Photochemistry*, M. Dekker: New York, **1987**, Vol. 9, 225. (b) Pillai, V. N. R., *Synthesis*, **1980**, 1.
2. Amit, B., Zehavi, U., Patchornik, A., *Isr. J. Chem.*, **1974**, 12, 103.
3. Sheehan, J. C., Wilson, R. M., Oxford, A. W., *J. Am. Chem. Soc.*, **1971**, 93, 7222.
4. Barltrop, J. A., Schofield, P., *Tetrahedron Lett.*, **1962**, 3, 697.
5. Brinkly, R. W., Flechtner, T. W., *Synthetic Organic Photochemistry*, Plenum Press: New York, **1984**, Chapter 7.
6. Fordor, S. P. A., Read, J. L., Pirrung, M. C., Stryer, L., Liu, A. T., Solas, D., *Science*, **1991**, 251.
7. Pease, A. C., Solas, D., Sullivan, E. J., Cronin, M. T., Holmes, C. P., Fodor, S. P. A., *Proc. Natl. Acad. Sci. USA*, **1994**, 91, 5022.
8. (a) Cameron, J. F., Wilson, C. G., Frechet, J. M. J., *J. Am. Chem. Soc.*, **1996**, 118, 12925. (b) Cameron, J. F., Frechet, J. M. J., *J. Am. Chem. Soc.*, **1991**, 113, 4303. (c) Pirrung, M. C., Huang, C.-Y., *Tetrahedron Lett.*, **1995**, 36, 5883.
9. Kaplan, J. H., *Annu. R. Physiol.*, **1990**, 52, 897.
10. Adams, S. R., Kao, J. P. Y., Tsien, R. Y., *J. Am. Chem. Soc.*, **1989**, 111, 7957.
11. Schlichting, I., Rapp, G., John, J., Wittinghoffer, A., Pai, E. F., Goody, R. S., *Proc. Natl. Acad. Sci. USA*, **1989**, 86, 7687.
12. Adams, S. R., Tsien, R. Y., *Annu. R. Physiol.*, **1993**, 55, 755.
13. Kaplan, J. H., Somlyo, A. P., *Trends Neurosci.*, **1989**, 12, 54.
14. (a) Gurney, A. M., Lester, H. A., *Physiol. Rev.*, **1987**, 67, 58. (b) Lester, H. A., Nerbonne, J. M., *Annu. R. Biophys. Bioeng.*, **1982**, 11, 151.

15. Engels, J., Schlaeger, E. J., *J. Med. Chem.*, **1977**, *20*, 907.
16. (a) Wootton, J. F., Trentham, D. R., *Photochemical Probes in Biochemistry*, Kluwer Academic: Dordrecht, **1989**, 277. (b) McCray, J. A., Trentham, D. R., *Annu. R. Biophys. Biophys. Chem.*, **1989**, *18*, 239. (c) Corrie, J. E. T.; Trentham, D. R., *Bioorganic Photochemistry*, New York, John Wiley, **1993**, Vol 2, 243. (d) Gurney, A.M., Lester, H.A., *Physio. Rev.*, **1987**, Vol. 67, No.2, 583.
17. DeMayo, P., *Adv. Org. Chem.*, **1960**, *2*, 367.
18. DeMayo, P., Reid, S. T., *Quart. R. Chem. Soc.*, **1961**, 393.
19. Morrison, H. A., *The Chemistry of the Nitro and Nitroso Groups*, Wiley, New York, **1970**, Part I, 185.
20. Ciamician, G, Silber, P., *Chem. Ber.*, **1901**, *34*, 2040.
21. Barltrop, T. A., Plant, P. J., Schofield, P., *J. Chem. Soc. Chem. Commun.*, **1966**, 822.
22. Patchornik, A., Amit, B., Woodward, R.B., *J. Am. Chem. Soc.*, **1970**, *92*, 6333.
23. Kaplan, J. H., Forbush, G., Hoffman, J. F., *Biochemistry*, **1978**, *17*, 1929.
24. Nerbonne, J. M., *Opt. Methods Cell Physiol*, **1986**, *40*, 418.
25. Homsher, E., Millar, N. C., *Annu. R. Physiol*, **1990**, *52*, 857.
26. Corrie, J. E. T., Katayama, Y., Reid, G. P., Anson, M., Trentham, D. R., *Philos. Trans. R. Soc. London, Ser. A.*, **1992**, *340*, 233.
27. Corrie, J. E. T., Trentham, D. R., *biological Applications of Photochemical Switchers*, J. Wiley and Sons: New York, **1994**, 243.
28. Walker, J. W., Lu, Z., Moss, R. L., *J. Biol. Chem.*, **1992**, *267*, 2459.
29. Ostap, E. M., Thomas, D. D., *Biophys. J.*, **1991**, *59*, 1235.

30. Lewis, S. M., Thomas, D. D., *Biochemistry*, **1991**, *30*, 8331.
31. Barth, A., Hauser, K., Mantele, W., Corrie, J. E. T., Trentham, D. R., *J. Am. Chem. Soc.*, **1995**, *117*, 10311.
32. Hajdu, J., Andersson, I., *Annu. R. Biophys. Biomol. Struct.*, **1993**, *22*, 467.
33. Park, C. H., Givens, R. S., *J. Am. Chem. Soc.*, **1997**, *119*, 2453.
34. (a) Corrie, J. E. T.; Trentham, D. R., *J. Chem. Soc., Perkin Trans 1*, **1992**, 2409. (b) Thirlwell, H., Corrie, J. E. T., Reid, G., Trentham, D. R., Ferenczi, M. A., *Biophys. J.*, **1994**, *67*, 2436.
35. (a) Sheehan, J. C., Wilson, R. M., *J. Am. Chem. Soc.*, **1964**, *86*, 5277. (b) Sheehan, J. C., Wilson, R. M., Oxford, A. W., *J. Am. Chem. Soc.*, **1971**, *93*, 7222.
36. Pirrung, M. C., Shuey, S. W., *J. Org. Chem.*, **1994**, *59*, 3890.
37. (a) Gees, K. R., Keuper, III, L. W., Barnes, J., Dudley, G., Givens, R. S., *J. Org. Chem.*, **1996**, *61*, 1228. (b) Givens, R. S., Athey, P. S., Matuszewski, B., Kueper, III, L. W., Xue, J.-Y., Fister, T., *J. Am. Chem. Soc.*, **1993**, *115*, 6001. (c) Givens, R. S., Keuper, III, L. W., *Chem. Rev.*, **1993**, *93*, 55. (d) Givens, R. S., Athey, P. S., Matuszewski, B., Kueper, III, L. W., Xue, J.-Y., *J. Am. Chem. Soc.*, **1992**, *114*, 8708. (e) Givens, R. S., Matuszewski, B. J., *J. AM. Chem. Soc.*, **1984**, *106*, 6860.
38. (a) Cameron, J. F., Wilson, C. G., Frechet, J. M. J., *J. Am. Chem. Soc.*, **1996**, *118*, 12925. (b) Cameron, J. F., Frechet, J. M. J., *J. Am. Chem. Soc.*, **1991**, *113*, 4303.
39. Shi, Y.-J., Corrie, J.E.T., Wan, P., *J. Org. Chem.*, **1997**, *62*, 8278.
40. (a) Corrie, J. E. T., Trentham, D. R., *J. Chem. Soc., Perkin Trans. 1*, **1992**, 2409. (b) Thirlwell, H., Corrie, J. E. T., Reid, G., Trentham, D. R., Ferenczi, M. A., *Biophysio. J.*, **1994**, *67*, 2436.
41. Baldwin, J. E., McConnaughie, A. W., Moloney, M. G., Pratt, J., Shim, S. B., *Tetrahedron*, **1990**, *46*, 6879.
42. (a) Futura, T., Torigai, H., Sugimoto, M., Iwamura, M., *J. Org. Chem.*, **1995**, *60*,

3953. (b) Futura, T., Torigai, H., Osawa, T., Iwamura, M., *Chem. Lett.*, **1993**, 1179.
43. Cameron, J. F., Wilson, C. G., Frechet, J. M. J., *J. Chem. Soc., Chem. Commun.*, **1995**, 923.
44. Anderson, J. D., Reese, C. B., *Tetrahedron Lett.*, **1962**, 1.
45. Sheehan, J. C., Umezawa, K. J., *J. Org. Chem.*, **1973**, 38, 3711.
46. (a) Serebryakov, E. P., Kucherov, V. F., *Izv. Akad. Nauk. SSR, Ser. Khim.*, **1974**, 2872; *Chem. Abstr.*, **1975**, 82, 171233a. (b) Serebryakov, E. P., Suslova, L. M., Kucherov, V. F., *Tetrahedron*, **1978**, 34, 345.
47. Epstein, W. M., Garrossian, M. J., *J. Chem. Soc., Chem. Commun.*, **1987**, 532.
48. (a) Givens, R. S., Kueper, III, L. W., *Chem. Rev.*, **1993**, 93, 55. (b) Gives, R. S., Athey, P. S., Matuszewski, B., Kueper, III, L. W., Xue, J.-Y., Fister, T., *J. Am. Chem. Soc.*, **1993**, 115, 6001.
49. (a) Arnold, B., Donald, L., Jurgens, A., Pincock, J. A., *Can. J. Chem.*, **1985**, 63, 3140. (b) De Costa, D. P., Pindodk, J. A., *J. Am. Chem. Soc.*, **1989**, 111, 8948. (c) Hilborn, J. W., Pincock, J. A., *J. Am. Chem. Soc.*, **1991**, 113, 2683.
50. (a) Givens, R. S., Park, C.-H., *Tetrahedron Lett.*, **1996**, 37, 6259. (b) Park, C.-H., Givens, R. S., *J. Am. Chem. Soc.*, **1997**, 119, 2453. (c) Givens, R. S., Jung, A., Park, C.-H., *J. Am. Chem. Soc.*, **1997**, 119, 8376.
51. (a) Zimmerman, H. E., Sandel, V. R., *J. Am. Chem. Soc.*, **1963**, 85, 915. (b) Zimmerman, H. E., Somasekhara. S., *J. Am. Chem. Soc.*, **1963**, 85, 922.
52. Chamberlin, J. W., *J. Org. Chem.*, **1966**, 31, 1658.
53. Birr, C., Flor, F., Fleckenstein, P., Lochinger, W., Wieland, T., *Peptides, Proc. 11th Eur. Pept. Symp.*, Vienna, 1971, North Holland Publishing Company, Amsterdam, 1972.
54. Hibbert, F., *Adv. Phys. Org. Chem.*, **1986**, 22, 113.

55. (a) Kasha, M., *J. Chem. Soc., Faraday Trans. 2*, **1986**, 82, 2379. (b) Kasha, M., *Acta Phesica Polonica*, **1987**, 71A, 717.
56. (a) Arnaut, L. G., Formosinho, S. J., *Photochem. Photobio. A: Chem.*, **1993**, 75, 1. (b) Formosinho, S. J., Arnaut, L. G., *Photochem. Photobio. A: Chem.*, **1993**, 75, 21.
57. Kasha, M., McMorrow, D., Parthenopoulos, D. A., *J. Phys. Chem.*, **1991**, 95, 2668.
58. Lee, J., Robinson, G. W., Webb, S. P., Philips, L. A., Clark, J. H., *J. Am. Chem. Soc.*, **1986**, 108, 6538.
59. Bridges, J., Creaven, P., Williams, R., *Biochem. J.*, **1965**, 96, 872.
60. Schwartz, B. J., Peteanu, L. A., Harris, C. B., *J. Phys. Chem.*, **1992**, 96, 3591.
61. Itoh, M., Adachi, T., *J. Am. Chem. Soc.*, **1984**, 106, 4320.
62. Mukaihata, H., Nakagawa, T., Kohtani, S., Itoh, M., *J. Am. Chem. Soc.*, **1994**, 116, 10612.
63. Collins, S. T., *J. Phys. Chem.*, **1983**, 87, 3202.
64. Konijnenberg, J., Ekelmans, G. B., Huizer, A. H., Varma, C. A. G. O., *J. Chem. Soc., Faraday Trans. 2*, 1989, 85(1), 39.
65. (a) Barltrop, J. A., Coyle, J. D., *Excited states in organic chemistry*, 1975, John Wiley & Sons, Ltd. (b) Gilbert, A., Baggott, J., *Essentials of molecular photochemistry*, 1991, Blackwell Scientific Publications. (c) Turro, N. J., *Modern molecular photochemistry*, 1978, The Benjamin/Cummings Publishing Company, Inc.
66. Murov, S. L., Carmichael, I., Hug, G. L., *Handbook of photochemistry*, 2nd ed.; Dekker, New York, 1993.
67. Wan, P., Barker, B., Diao, L., Fisher, M., Shi, Y., Yang, C., *Can. J. Chem.*, **1996**,

- 74, 465.
68. (a) Vandenberg, G. M., Henrich, C., Berg, S. G., V., *Anal. Chem.*, **1954**, 26, 726. (b) Bordwell, F. G., Cooper, G. D., *J. Am. Chem. Soc.*, **1952**, 74, 1058.
69. Banerjee, A., Falvey, D., *J. Am. Chem. Soc.*, **1998**, 120, 2965.
70. (a) Fischer, M., Wan, P., *J. Am. Chem. Soc.*, **1998**, 120, 2680. (b) Diao, L., Yang, C., Wan, P., *J. Am. Chem. Soc.*, **1995**, 117, 5369. (c) Shi, Y., Wan, P., *J. Chem. Soc., Chem. Commun.*, **1997**, 273.
71. (a) Pincock, J. A., *Acc. Chem. Res.* **1997**, 30, 43. (b) Pincock, J. A., *CRC Handbook of Organic Photochemistry and Photobiology*; Horspol, W. M., Song, P.-S., Eds.; CRC press: Boca Raton, FL, 1995; Chapter 32. (c) Hillborn, J. W., Pincock, J. A., *J. Am. Chem. Soc.* **1991**, 113, 2683. (d) Hilborn, J. W., MacKnight, E., Pincock, J. A., *J. Am. Chem. Soc.* **1994**, 116, 3337.
72. Bockman, T. M., Hubig, S. M., Kochi, J. K., *J. Org. Chem.* **1997**, 62, 2210.
73. (a) Ireland, J. F., Wyatt, P. A. H., *Adv. Phys. Org. Chem.* **1976**, 12, 131. (b) Vander Donckt, E. *Prog. React. Kinet.* **1970**, 5, 273. (c) Lahiri, S. C., *J. Sci. Ind. Res. (India)* **1979**, 38, 492.
74. (a) Carmeli, I., Huppert, D., Tolbert, L. M., Haubrich, J. E., *Chem. Phys. Lett.* **1996**, 260, 109. (b) Tolbert, L. M., Haubrich, J. E., *J. Am. Chem. Soc.* **1994**, 116, 10539. (c) Yao, S. H., Lee, J., Robbison, G. W., *J. Am. Chem. Soc.* **1990**, 112, 5698. (d) Lee, J., Robinson, G. W., Webb, S. P., Philips, L. A., Clark, J. H., *J. Am. Chem. Soc.* **1986**, 108, 6538.
75. (a) Schwartz, B. J., Peteanu, L. A., Harris, C. B., *J. Phys. Chem.* **1992**, 96, 3591. (b) Frey, W., Laermer, F., Elsaesser, T., *J. Phys. Chem.* **1991**, 95, 10391. (c) Moog, R. S., Maroncelli, M., *J. Phys. Chem.* **1991**, 95, 10359.
76. Das, P. K., Encinas, M. V., Scaiano, J. C., *J. Am. Chem. Soc.*, **1981**, 103, 4151.
77. (a) Filar, L., Winstein, S., *Tetrahedron Lett.* **1960**, 25, 9. (b) Leary, G., *J. Chem. Soc., Perkin II* **1972**, 640. (c) Leary, G., Miller, I., Thoms, W., Woolhouse, A.,

- J. Chem. Soc., Perkin II* **1977**, 1737.
78. Baird, R., Winstein, S., *J. Am. Chem. Soc.*, **1975**, *79*, 4238.
79. Sheehan, J. C., Umezawa, K. J., *J. Org. Chem.* **1973**, *38*, 3771.
80. McClelland, R. A., Chan, C., Cozens, F., Modro, A., Steenken, S., *Angew. Chem. Int. Ed. Engl.* **1991**, *30*, 1337.
81. Pavia, D. L., Lampman, G. M., Kriz, G. S., *Introduction to Spectroscopy*, Saunders College Publishing, Philadelphia, 1979.
82. Pouchert, C. J., Behnke, J., *The Aldrich Library of ¹³C and ¹H FTNMR Spectra*, vol. 2, Edition I, Aldrich Chemical Company, 1993.
83. Reiker, A.; Kaufmann, H.; Bruck, D.; Workman, R.; Muller, E., *Tetrahedron* **1968**, *24*, 103.
84. (a) Taylor, A., *Chemistry 346 laboratory Manual*, University of Victoria, British Columbia, 1994. (b) Devore, J. L., *Probability and Statistics for Engineering and the Sciences*, Brooks/Cole Publishing Company, California, 1987.
85. Liao, Y.; Bohne, C. *J. Phys. Chem.* **1996**, *100*, 734.

VITA

Surname: Zhang

Given name: Kai

Place of Birth: Weihai, Shangdong, P. R. China

Educational Institutions Attended:

University of Victoria	1996-1998
Peking University	1992-1995
Nanjing University	1985-1989

Degrees Awarded:

M.Sc.	Peking University	1995
B.Sc.	Nanjing University	1989

Publications and Presentations:

Kai Zhang, J. E. T. Corrie, V. R. N. Munasinghe, P. Wan, Mechanism of Photosolvolytic Rearrangement of *p*-Hydroxyphenacyl Esters: Evidence for Excited State Intramolecular Proton Transfer as the Primary Photochemical Step, submitted.

Kai Zhang, P. Wan, Mechanism of Photorelease of Protected Esters from the *p*-Hydroxyphenacyl System: Intramolecular Proton Transfer Occurs in the First Step, 81st Canadian Society for Chemistry Conference, Whistler, B. C., May 31 – June 4, 1998.

D. Brousmiche, Kai Zhang, Z. Chen, P. Wan, Long Range Excited State Intramolecular Proton Transfer in *p*-Hydroxyphenyl Ketones, 81st Canadian Society for Chemistry Conference, Whistler, B. C., May 31 – June 4, 1998.


PARTIAL COPYRIGHT LICENSE

I hereby grant the right to lend my thesis (or dissertation) to users of the University of Victoria Library, and to make single copies only for such users or in response to a request from the Library of any university, or similar institution, on its behalf or for one of its users. I further agree that permission for extensive copying of this thesis for scholarly purposes may be granted by me or a member of the University designated by me. It is understood that copying or publication of this thesis for financial gain shall not be allowed without my written permission.

Title of thesis/Dissertation:

Mechanism of Photosolvolytic Rearrangement of *p*-Hydroxyphenacyl Esters: Evidence for Excited State Intramolecular Proton Transfer as the Primary Photochemical Step

Author:


Kai Zhang

December, 1998